Imaging luminescence using focussed stimulation: a potential solution to problems of heterogeneity in dating sedimentary systems

Iain James Houston

BSc (Hons) Physics, University of Strathclyde 1999

Presented as a thesis submitted for the degree of Master of Science by research

School of Physical Sciences, Department of Geography and Topographic Science

University of Glasgow

April 2001

Abstract

In this thesis the potential of using scanning instrumentation coupled to focussed lasers to measure luminescence from single grains was explored. An original concept was used to build an instrument capable of conducting single grain measurements. The thesis focusses on the evaluation of this instrument through experiments using F1 feldspar which were subsequently reinforced by numerical modelling.

Development of the scanning instrument was initially prompted through measurements on samples from the NE Thailand "cover sands" for which competing aeolian and bioturbation origins have been proposed. In the case of aeolian deposition the doses found within the grains should be relatively homogeneous. If mixing has occurred within the layer then there is likely to be a large grain to grain variation in stored dose at some depths. In problems of this nature single grain luminescence analysis should be capable of identifying which of these models is more appropriate.

Initial experiments produced images of F1 feldspar grains on conventional discs revealing that the IR laser, which was widely used for the single grain measurements, operated with a visible spot size of around 100 μm. This spot size was small enough to produce meaningful images and individual grains could be imaged if they were separated widely enough. A single scan was found to remove the bulk of the measurable signal from the grains. It was also shown that the system had the potential to measure doses as small as 2 Grays.

Further investigations were conducted on the effect of scattered light within the sample chamber. Numerical modelling showed this effect should result in an initial peak in the results as well as a gradient throughout the measurement. This effect was observed in some results. Numerical modelling also showed that on more sparsely covered discs the effect of laser scatter would not be as marked. Attempts were made, using several different approaches, to reduce the effect of this scatter when measuring evenly covered discs. Although it was not possible to reduce the effect of such scatter it was found that presenting the grains in pits within the discs appeared to eliminate the problem.

Finally, measurements on evenly covered discs of irradiated and unirradiated feldspar blends of known concentration tested the potential of the system for measuring samples of mixed grains with different luminescence characteristics. The results produced by these analyses were found to be consistent with those produced by numerical modelling.

To conclude, results using F1 feldspar suggest that the performance of the system is sufficient to determine whether mixing has occurred. Improvements are suggested which would further refine the instrument to allow the detection of mixing in samples from natural environments.

Declaration

I hereby declare that this submission is my own work and that, to the best of my knowledge and belief, it contains no material previously published or written by another person nor material which to a substantial extent has been accepted for the award of any other degree or diploma of the university or other institute of higher learning, except where due acknowledgement has been made in the text.

Acknowledgements

There are several people who I would like to thank for taking the time to support and encourage me throughout this project. I would especially like to thank Dr Alan Cresswell and Dr Von Whitley for sharing their knowledge of programming with me and for the many stimulating conversations which took place in chinese restaurants. I would also like to thank Simon Murphy for his invaluable technical support during this project which prevented disaster on several occasions.

The support provided by my colleagues at the Scottish Universities Research and Reactor Centre has been invaluable throughout the course of this project and I would like to thank Dr Lorna Carmichael, Iona Anthony, Ann Somerville and Davina White as their presence within the group made this project more enjoyable.

I would also like to thank Professor Tony Fallick, Dr Finn Stewart, and my supervisors Professor Paul Bishop and Dr David Sanderson for their guidance during this project.

Finally, I must thank my family who have helped me in support in so many ways over the course of this project.

List of Figures

Chapter 1: Introduction

The problem of determining the origin of the cover sands of North East Thailand initially prompted this investigation into the feasibility of single grain luminescence dating. A conspicuous feature of the surficial geology of continental and insular Southeast Asia is a surface mantle or cover layer of generally sandy material which may be up to 5 m or more in thickness (Sanderson et al., 2000). The layer is reported to be extensively distributed throughout the region, including throughout Vietnam and Cambodia, in NE and N Thailand, from the uplands of Malaysia and Myanmar, and even from the Punjab in India (Hoang Ngoc Ky, 1989, 1994). Over the last decade, the characteristics and genesis of the cover layer, particularly in Vietnam and NE Thailand, have received significant attention in the local Quaternary geological literature, being generally interpreted as an aeolian (loess-like) mantle of Late Pleistocene to Holocene age. The cover layer has most recently been interpreted as a Late Tertiary "biomantle", emplaced as a result of termite activity and subsequent degradation of termite mounds (Loffler and Kubiniok, 1991, 1996). It has been argued (Sibrava, 1993) that the age and mode of emplacement of the cover layer is a significant issue as it has far ranging implications for the origin of loessic sediments across the entire region. For this reason, it is important that the origin of the cover layer is clarified.

One method of analysis which could be applied to this type of problem is luminescence dating. Luminescence analysis involves estimating the cumulative radioactive dose received by a sample in its natural environment by measuring the

amount of light emitted by the sample when subjected to heat (thermoluminescence) or light (optically stimulated luminescence). The amount of light emitted is related to the number of electrons trapped in lattice defects within the material (usually quartz or feldspar) which is in turn related to the amount of radiation received by the material in its natural environment. The Thai cover sands contain quartz and are ideally suited to luminescence analysis, responding well to optical stimulation (Houston, 1999).

Dose profiles produced using thermoluminescence (TL) and optically stimulated luminescence dating (OSL) on bulk samples from the same section of the sediment (Figures 1.1 and 1.2) suggest two possible explanations for the origin of the cover layer. The increasing dose with depth is consistent with aeolian origin, although Sanderson et al. (2000) suggests there may be heterogeneity near to the surface. An alternative explanation is that the dose levels are a result of gross heterogeneity throughout the sediment which has an increased effect closer to the surface. In the case of aeolian deposition the doses found within the grains should be relatively homogeneous. If mixing has occurred within the layer then there is likely to be a large grain to grain variation in stored dose at some depths. In principle, single grain measurements could quantify the heterogeneity throughout the layer and help identify which of these models is more appropriate. Single grain luminescence analysis should be capable of determining whether distinct populations of grains with varying dose histories are present. For this reason the development of a single grain instrument capable of dose quantification is now timely.

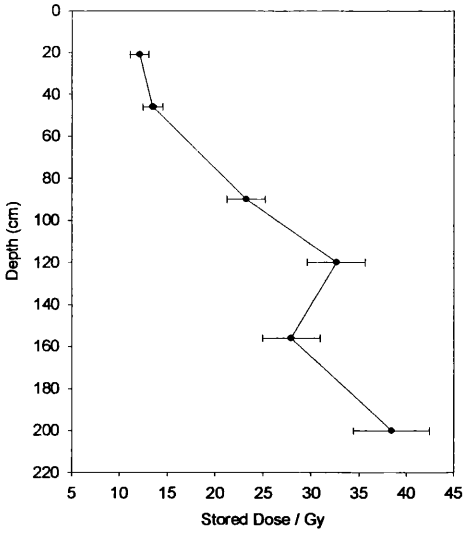

Figure 1.1: *TL dose profile from Thai quartz*

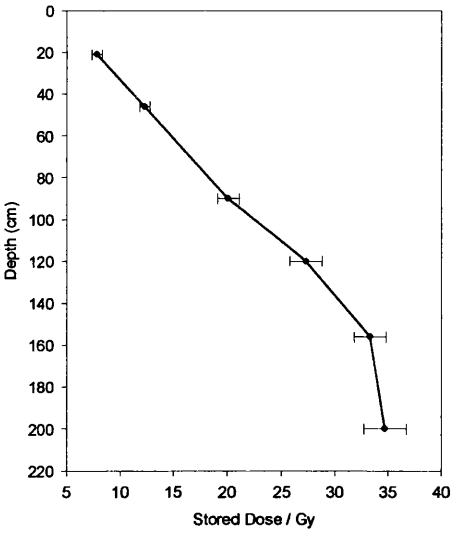

Figure 1.2: *OSL dose profile from Thai quartz*

The aims of this project are to use an original concept to build an instrument capable of conducting single grain measurements and to assess the feasibility of using the instrument to solve problems such as the origin of the Thai cover sands. After construction, the performance of the system is evaluated and its usefulness in analysing samples from natural environments is assessed.

The following chapter outlines the principles behind luminescence analysis and describes existing approaches to single grain measurements. In chapter three the design and use of the instrumentation used to conduct both bulk and single grain measurements is described. In chapter four preliminary results obtained using the single grain reader are presented. The efficiency with which the available signal is measured and the minimum dose measurable using the system is determined. In

chapter five numerical modelling is used to predict and identify the effects of laser scatter and methods of reducing this scatter are investigated. In chapter six irradiated and unirradiated grains are mixed in known concentrations and analysed and the results are compared with predictions from numerical modelling. The implications of these results, the potential for further research and the conclusions which were reached are discussed in chapters seven and eight.

Chapter 2: Background

2.1 Principles of luminescence

When radiation is incident on a material some of the radiation may be absorbed and re-emitted as light of a different wavelength. This is the process known as luminescence. A useful way of illustrating the mechanism underlying this phenomenon is the energy level diagram (Figure 2.1). The luminescence model originally proposed by Jablonski (1935) requires metastable bands within the "forbidden" energy gap between the ground and excited energy states. An electron excited from the ground state to the excited state can become trapped in the metastable level. In this way the "memory" of the accumulated exposure to nuclear radiation is carried by trapped electrons (or other charge carriers). As the material is heated (as in thermoluminescence), these electrons can be released from their traps by vibrations within the lattice or, alternatively, the absorption of a photon of light (as in optically stimulated luminescence). Recombination with certain centres, which are known as "luminescence centres", leads to the emission of light. The amount of light emitted depends upon the number of trapped electrons, which, in turn, depends upon the previous exposure to radiation (also known as the stored dose).

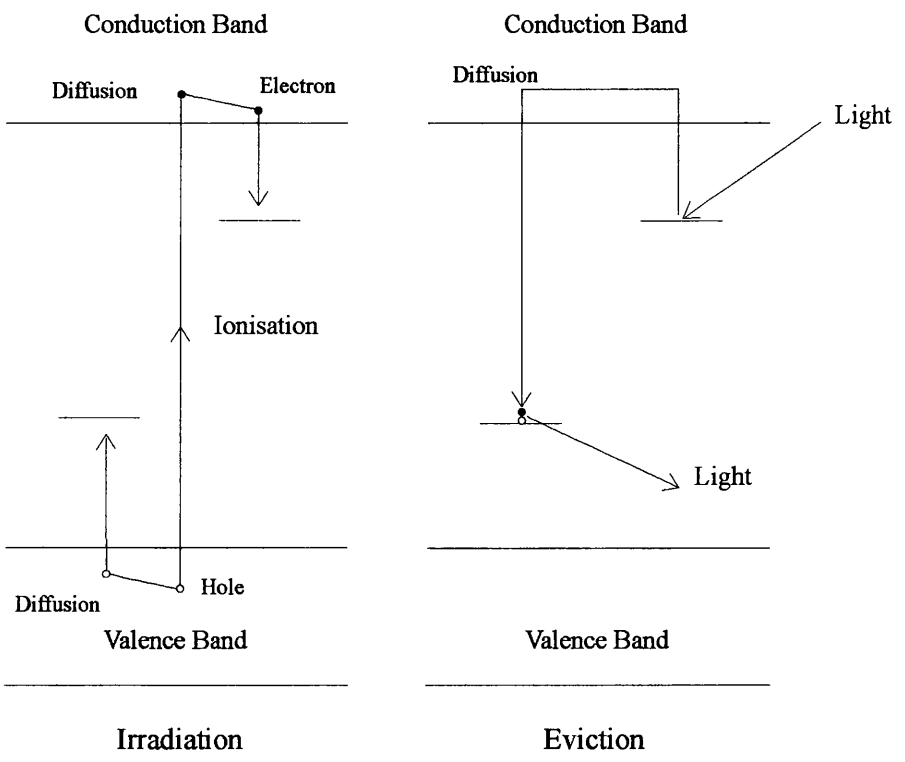

Figure 2.1: *Transition between energy bands resulting in luminescence*

Optically stimulated luminescence (OSL) dating was developed in order to provide an improved method of dating sediments (Huntley et al., 1985). The principles behind optical dating are similar to those involved in thermoluminescence (TL) dating and rely on the fact that when subjected to light, quartz or feldspar grains may emit a small quantity of light. The amount of light emitted can be used to determine the time since the grains were subjected to a "zeroing event".

Quartz and feldspar are the minerals which are most frequently used in luminescence dating. Quartz is one of the most commonly chosen materials for luminescence dating as it is one of the most abundant minerals found on the earth's surface and it is relatively uncommon to find sedimentary deposits that do not contain a quartz fraction

(Aitken, 1998). Quartz emits most strongly at 365 nm, in the near UV. OSL emission was first observed using green laser light at 514 nm by Huntley et al. (1985). Quartz does not respond to infrared stimulation but is sensitive to stimulation by blue or green light. Figure 2.2 shows a typical OSL decay curve.

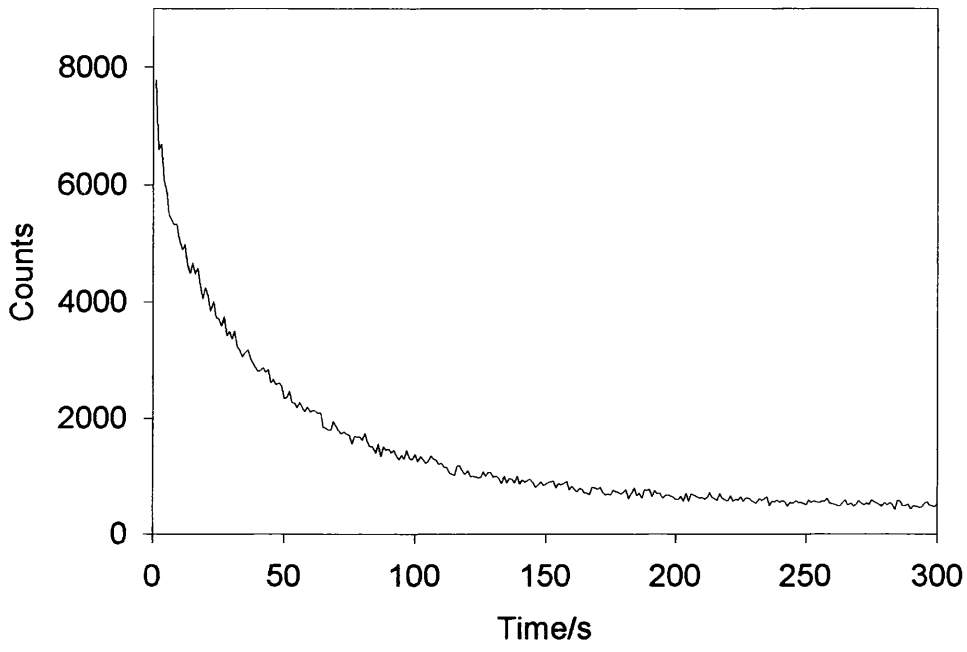

Figure 2.2: *Quartz OSL decay curve*

The sensitivity of feldspar to stimulation by infrared light was first noticed by Hutt et al., (1988). The excitation spectrum of F1 feldspar contains three main excitation regions, at 500-540 nm, 550-650 nm and 800-1000 nm (Figure 2.3).

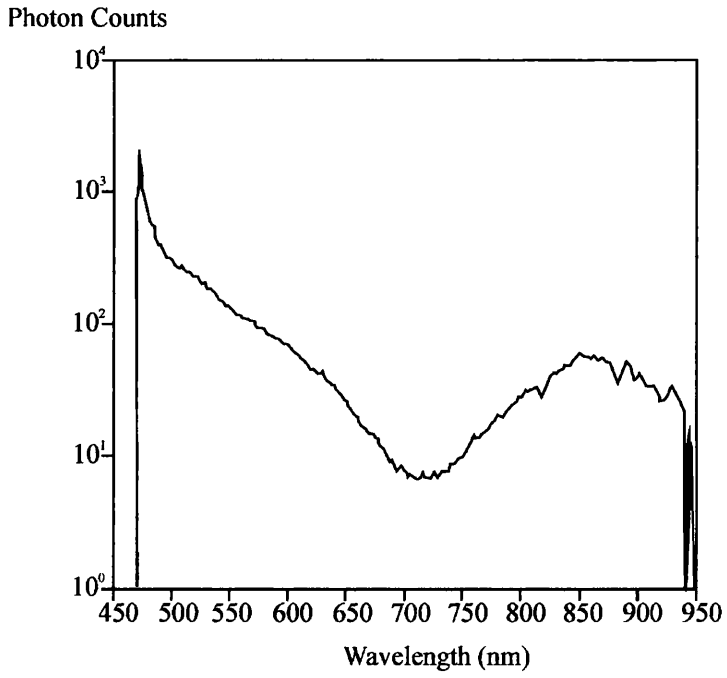

Figure 2.3: *Excitation spectrum of F1 feldspar (from Clark and Sanderson, 1994)*

A model which accounts for this is described by Clark and Sanderson (1994) and this model suggests that the excitation spectrum is generated by at least two traps (Figure 2.4). One of these traps has a ground state which can be evicted directly to the conduction band by 500 nm photons, and two excited states which can be reached by 625 and 910 nm photons. This trap generates the 550-650 nm and 500-540 nm components of the excitation spectrum. The other trap contributes to the 500-540 nm component in the spectrum. As well as infrared stimulation feldspar also responds to stimulation using blue or green light. Figure 2.5 shows a typical OSL decay curve.

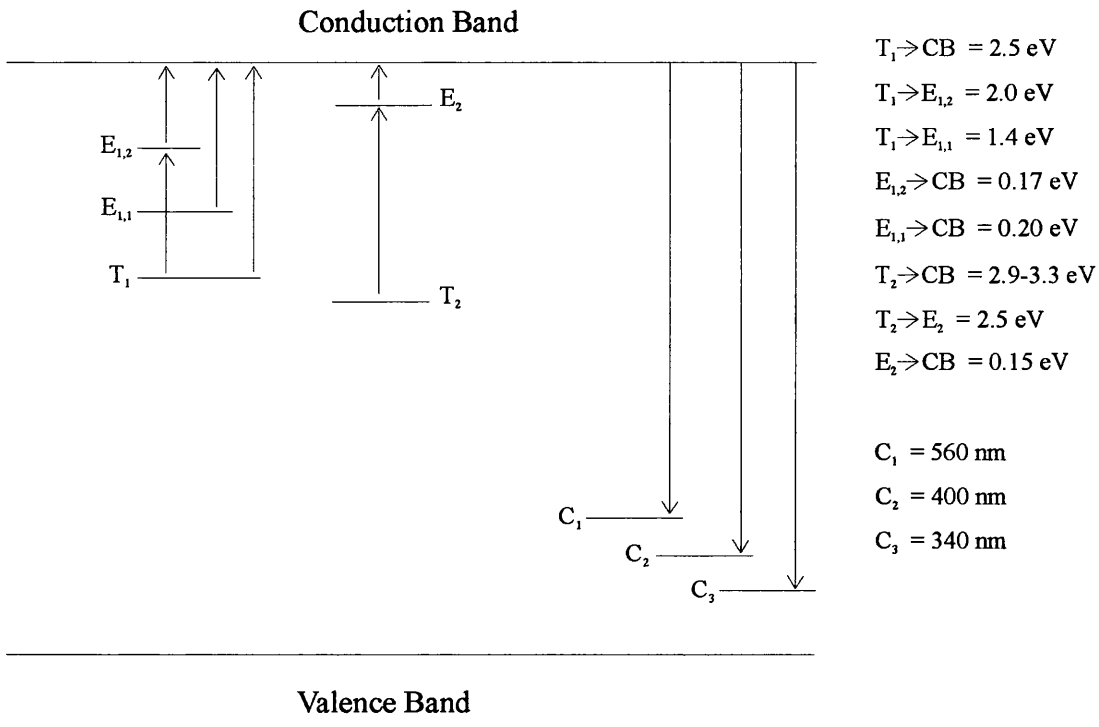

Figure 2.4: *Energy model for F1 feldspar (from Clark et al., 1994)*

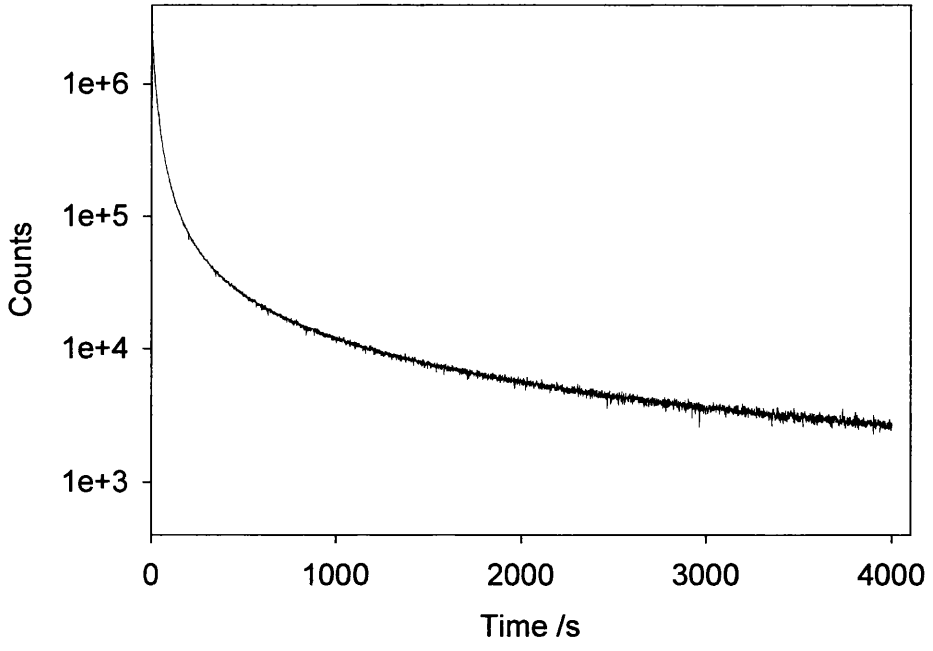

Figure 2.5: *F1 feldspar OSL decay curve*

2.2 Luminescence dating

Luminescence dating involves the estimation of a sample's stored dose (the amount of energy absorbed per unit mass due to incident radiation) by measuring the amount of light emitted by the sample when subjected to heat or light. Electrons which have been ionised from their parent nuclei in the host lattice by radiation and have become trapped within defects, which are known as "traps", carry the "memory" of accumulated exposure to nuclear radiation. If the amount of radiation received by the sample per year can be measured then it is possible to produce an estimate for the time since the sample experienced the last "zeroing event". This is commonly referred to as the "age" of the sample. For this method to be accurate an efficient zeroing event which removes all trapped electrons and restores them to their ground states is required. The zeroing event can occur as a result of the "bleaching" of sediments by sunlight prior to deposition or, in the case of fired materials, by heating. In this way the time elapsed since the deposition of sediment or since the firing of pottery can be determined, if the dose rate is known.

Stored dose can be measured using either the additive or regenerative methods. The additive method involves giving different doses to several samples and extrapolating to obtain the value for the natural stored dose (Aitken, 1998). The regenerative method involves only a single sample which is repeatedly dosed and analysed to construct a master curve as described by Murray and Roberts (1997) from which the natural dose within a sample is determined by interpolation (Figure 2.6). Care should always be taken to prevent, or compensate for, variations in response due to

sensitivity changes within the samples during the measurement or irradiation cycles. In the regenerative method the effects of any sensitivity changes should be minimised as each result is normalised with respect to a small test dose (Murray and Roberts, 1997). Regenerative OSL determinations involve using an OSL test dose to monitor sensitivity changes while samples are subjected to different cycles of heating, measurement, bleaching and irradiation. All signals are normalised to the response from the test dose and stored doses are determined by interpolating the natural luminescence intensity onto the resultant regenerative OSL dose response plot (Murray and Roberts, 1997).

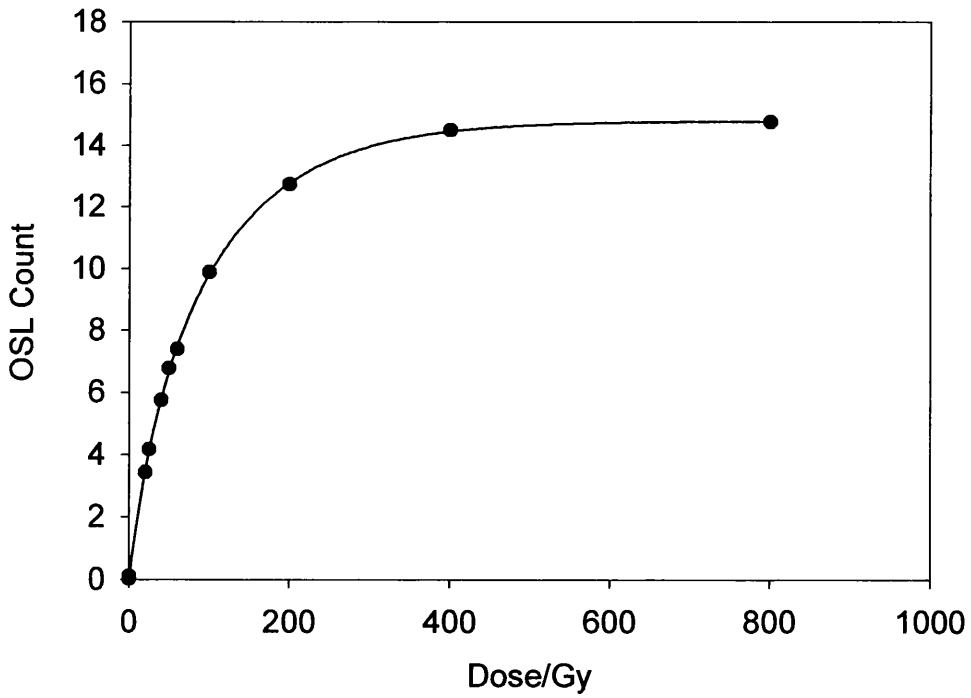

Figure 2.6: *OSL dose response plot produced using regenerative method*

Mineralogical heterogeneity may also present problems (Huntley and Berger, 1995) and for this reason samples are sieved and separated by density to provide samples which are as homogeneous as possible.

To produce accurate estimates of stored dose a detectable luminescence signal is required. A knowledge of the dose levels that the sample has been subjected to in its natural environment is also required and this is usually derived from measurements taken during sample collection together with laboratory measurements of the internal concentrations of U, Th and K (Aitken, 1985). This information is vital if estimates of stored dose are to be used to produce age estimates. A reproducible dose response is also required and although it is very difficult to say how well laboratory dose imitates natural dose, the response of a sample to laboratory dose should at least be consistent. This means the signal from the sample must be stable with time and the nature of the sample itself must not change with repeated heating and measurement. Most importantly, a distinct event that zeroes any pre-existing luminescence is required. Sediment samples must be adequately bleached at the time of deposition and the comparison between the TL and OSL results may show whether adequate bleaching has taken place given that OSL is more rapidly and easily bleached than TL (Godfrey-Smith et al., 1988).

The bleaching of quartz shows a strong wavelength dependence. The bleaching efficiency decreases by a factor of 10 between 400 and 500 nm and by 50 between 500 and 600 nm (Spooner, 1994). This is significant for subaqueous samples as the

green part of the spectrum becomes dominant when sunlight is attenuated by water (Berger, 1990). This means that quartz which is transported underwater is unlikely to be well bleached.

There is also a wavelength dependence in the bleaching of feldspar. As is the case with quartz, short wavelength light is most effective at bleaching the OSL signal. However, there is also an infrared resonance centred on 850 nm which will significantly contribute to bleaching (Clark et al., 1994). For this reason long wavelength light will make a significant contribution to bleaching and this must be taken into account when providing illumination during sample preparation.

2.3 Heterogeneous bleaching

The principal advantage that optical dating has over thermoluminescence dating is that in the former any residual signal due to incomplete bleaching is at least an order of magnitude lower (Rhodes, 1990). In using the TL method it is often necessary to consider the possibility that not all TL was removed during bleaching at the time of deposition. In OSL this does not present as great a problem, as the OSL is associated with traps which are generally easy to bleach (Smith et al., 1986).

Conventional bulk luminescence measurements require samples which have a homogeneous stored dose, a requirement that is not always satisfied. In some systems, where mixing and/or inadequate bleaching of the sediment has occurred, the sample may contain incompletely bleached grains. In situations where material has not been well bleached prior to deposition it may be necessary to distinguish between stored doses which have been accumulated prior to and after deposition. Fluvially deposited material is unlikely to be completely bleached since water strongly attenuates sunlight as shown by Berger (1990). In this case single grain measurements may provide an improved technique for accurately dating sediment. Post depositional processes that expose some of the sediments to light, such as bioturbation processes that bring sediments to the surface, may also result in heterogeneously bleached materials. In situations where mixing or partial bleaching has occurred, single grain measurements are ideally suited to separating two or more populations of grains which have different luminescence characteristics.

2.4 Single grain analysis

Early single grain measurements were conducted to investigate the possibility of grain-to-grain variation in luminescence response. The results showed that even in apparently homogeneous samples the luminescence response from individual grains was not identical. Recently, as the use of automatic readers has become more widespread, it is now possible to apply single grain analysis to samples in which mixing or partial bleaching has occurred in an attempt to identify the processes involved or to produce more accurate dates.

Several techniques, which are all variations on two basic ideas, have been used to measure both OSL and TL from single grains. One approach is to measure all grains simultaneously using a detector capable of spatial resolution on the single grain scale so that the signals from individual grains can be identified. The second approach measures the luminescence of individual grains.

2.4.1 Simultaneous multi-grain measurement techniques

Solid state imaging photon detectors have been used to measure OSL from single grains (Duller, 1997) although the sensitivity of these detectors is not as high as that of photomultiplier tubes. This approach has been used to detect zoning within zircon grains using an image intensifier (Templer and Walton, 1983).

Imaging photon detectors have been used to investigate the relationship between the physical properties and response of individual grains (McFee and Tite, 1994; McFee 1998). It was found that 5% of quartz grains were responsible for more than 20% of the luminescence signal. However, no correspondence could be found between the signal and grain characteristics such as volume, angularity, sphericity or transparency. It was assumed that most grain-to-grain variation in luminescence characteristics was due to differences in the populations of traps and luminescence centres. The populations of traps and luminescence centres are determined by differences in the concentrations of elemental impurities or lattice defects within the grains, but as the concentrations of these traps are at the level of parts per million, it is unlikely that their concentrations can be accurately determined. It is possible that feldspar inclusions have an effect on the signal from quartz grains but no evidence was found for this in McFee and Tite's (1994) study.

The advantage of using an imaging photon detector is that the grains do not have to be hand picked, which reduces the amount of time that the grains have to spend under

red light, resulting in less signal degradation. However, the detection equipment required to conduct these measurements is relatively expensive when compared to other single grain approaches and the sensitivity of imaging photon detectors is not as great as that of photomultiplier tubes. Photomultiplier tubes detecting one grain at a time utilise a far greater detection area and the high rate of charge release resulting from focussed stimulation leads to a high signal to background ratio.

2.4.2 Single grain measurement techniques

Single grain measurements have also been carried out by measuring the luminescence of individual grains. This is done by selecting grains by hand and measuring them individually and through the use of specially constructed or adapted single grain readers.

Benko (1983) conducted thermoluminescence measurements on individual quartz grains in an attempt to establish a relationship between the signal, grain size and appearance. Grains were separated on the basis of their appearance (clear or frosty). Although no relationship was found between the signal from the grains and their appearance, these experiments established that it was possible to measure the signal from individual grains.

Grun et al. (1989) conducted single grain measurements on feldspars, finding that 5% of the grains produced 5-10 times the intensities of the majority of grains. Berger (1994) suggested that although the TL properties of individual grains are highly variable there are likely to be regional consistencies, and recommended that the micro-properties of samples from various regions should be characterised. This information could be used to form a database which may help in the choice of sample pre-heat procedures and measurement techniques.

More recently several groups have used the approach of measuring individual grains using automatic readers. Single grain measurements have been conducted using a Daybreak 1100 automatic reader (Lamothe et al., 1994; Lamothe, 1996; Lamothe and Auclair, 1999). The variation in the measured stored doses was attributed to the variability of bleaching during transport as well as fading.

An alternative is to use commercially available automatic OSL/TL readers, such as the Risø TL/OSL-DA-15 reader, which is widely used to conduct bulk luminescence measurements for dating work. By using one grain per disc the Risø reader can carry out single grain measurements on up to 48 discs and can conduct TL measurements as well as OSL measurements using blue LEDs or a red laser. The reader also incorporates a radioactive source to irradiate samples between measurements. Murray and Roberts (1997) carried out single grain measurements using this equipment. Their analyses of sediment from Southern Australia showed a wide range of stored doses which they attributed to heterogeneity in beta dosimetry, and also identified a peak in the dose distribution which they suggested may be due to bioturbation. Roberts et al. (1998) applied similar measurements to the optical dating of sediment from the Jinmium rock shelter in Northern Australia. These measurements successfully showed that some deposits were considerably younger than first thought and brought the luminescence dates into agreement with radiocarbon dates. Although impossible using conventional optical dating techniques, the single grain measurements successfully identified grains which had not been fully "zeroed" (bleached) prior to burial and, by excluding these, improved the dating accuracy.

Risø readers currently have no specific single grain capability. However, the recent interest in single grain measurements has led the Risø laboratory in Denmark to convert one of their instruments to conduct single grain measurements using a green laser. The disc is held in a fixed position while the laser is directed onto each grain in turn. The laser scans a matrix of 81 pits (each containing one grain) on each disc which results in a large throughput. However, the close proximity of the grains to each other means the measurement of each grain also affects neighbouring grains. This "cross talk" reduces the accuracy of results and limits the effectiveness of the system. Also, as the grains are presented within a matrix of pits on the discs there is no possibility of imaging individual grains. Spatial resolution is lost as the laser light reflects around each pit. Also, the reader has no way to conduct TL on single grains.

It is clear that the present approaches to single grain measurement have produced valuable results and, using automated readers, it has been possible to apply single grain techniques to mixed populations to address the problems presented by heterogeneous dose distributions. However, none of the available approaches is perfect. An imaging photon detector would image grains quickly but does not have a high sensitivity and is expensive relative to alternative approaches. Existing automatic readers may provide data on the distribution of stored doses within the samples but no existing system can easily change the type of laser used for stimulation and no system has ever been built which uses a red laser, allowing for the measurement of feldspar. For these reasons a reader was constructed using an entirely different approach. The construction of this reader used a conceptually simple and versatile design which would accommodate all of the features necessary to analyse

samples from mixed systems. In the next chapter the design and operation of this reader is discussed.

Chapter 3: Instrumentation

This single grain system is a prototype and is being used to conduct exploratory measurements to test and refine the procedures for making single grain measurements. The apparatus used in this project already existed at SUERC although alterations were made and new control programs were written.

Most measurements to date have been made using an infrared RLD-83N30 laser diode with an operating power of 20 mW, a wavelength of 830 nm and a spot size of 25 μm at 25 mm (Figure 3.1). Some measurements were also carried out using green and blue lasers (Figure 3.2). The green laser used was a LCM-LL-O1CCS250 frequency doubled Nd:YAG laser operating at 532 nm with a power of 0.3 mW and a beam diameter of less than 2 mm. The blue laser was a LCM-F-6M frequency doubled Nd:YAG laser operating at 473 nm with a power of 3 mW with a beam diameter of less than 0.8 mm.

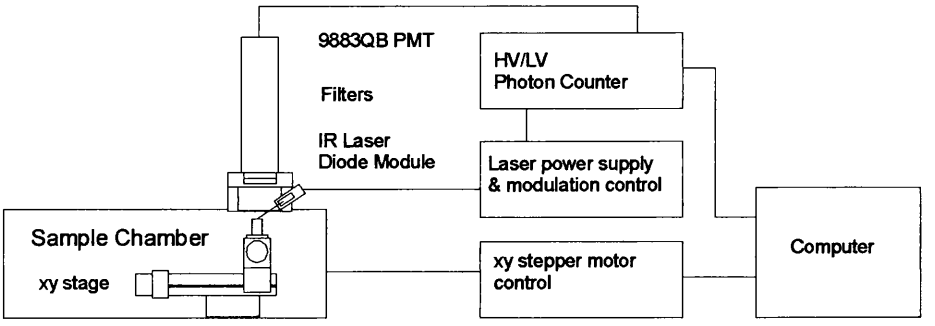

Figure 3.1: *Schematic of single grain system*

The single grain system is based on an x-y stage (Figure 3.1). The stage is moved under computer control using a TURBO BASIC program written at SUERC. The two motor-driven slides which move the stage have a resolution of 2.5 μm and the motors are controlled using pulses from a control board. A 9883QB photo multiplier tube is used in the system and is filtered using a 5 mm Schott UG11 light filter. This prevents scattered laser light from entering the photomultiplier tube. This arrangement is also suitable for use with blue or green lasers. For red laser light BG39 filters would be more appropriate as they allow detection in the blue region of the spectrum.

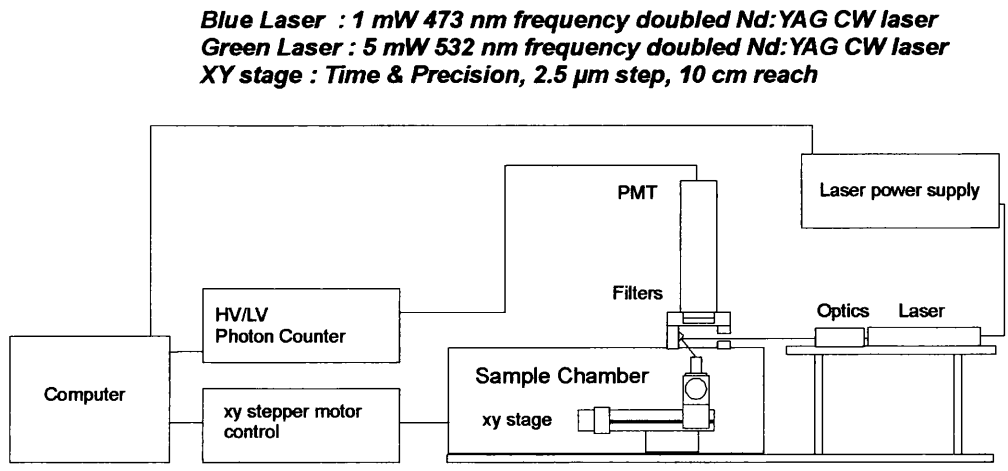

Figure 3.2: *Schematic of blue/green laser system*

The disc is mounted on a holder on the slides within the sample chamber. A small, fixed laser spot is directed onto the sample which is moved so that the sample "rasters" underneath the laser beam (Figure 3.3). The laser is held within a custom made collar which can accommodate several different lasers. The instrument can scan in two different ways. Scanning can be conducted by continuous laser operation, stepping across the entire disc and pausing after each step to record counts. This approach is appropriate where grains are scattered across the entire surface of the disc. If the grains are contained in pits within the disc the laser could be directed to each position on the disc before scanning.

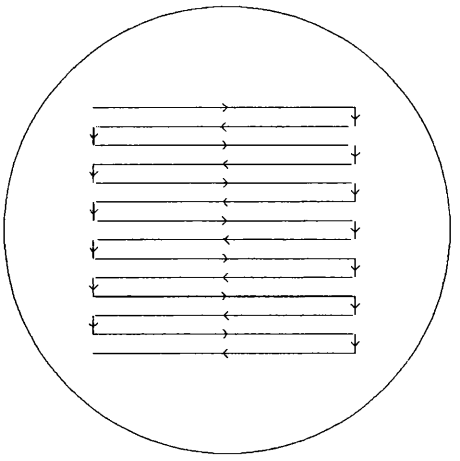

Figure 3.3: *Example of raster pattern used by instrument*

The fact that the sample moves instead of the laser beam allows for high precision in the positioning of the sample. The slides which move the sample have a resolution of 2.5 μm. This compares with the Risø single grain system which has a resolution of 50-100 μm (Duller et al., 1999). The increased resolution achievable with the instrument under development at SUERC should result in a significant advantage over the Risø system which also has no imaging capability. The Risø instrument does not require high resolution as it does not attempt to produce images and the only requirement is that the laser beam enters the 300 μm pit. The Risø system has a higher throughput compared to this instrument, although an improved single grain system using discs larger than the 10 mm discs which are currently used would address this problem.

Although a system based on an imaging photon detector would be able to make measurements quickly, as all grains would be measured simultaneously, imaging photon detectors are expensive and have much lower sensitivity than a photomultiplier tube in combination with high power stimulation. The x-y stage is relatively inexpensive and easy to use.

The instrument under development is intended to provide a highly adaptable research tool which is capable of conducting routine single grain measurements. In particular, it is hoped that the instrument will ultimately prove suitable for conducting single grain measurements on samples from the cover sands of North East Thailand.

The next chapter describes the initial measurements which were carried out to assess the performance of the instrument.

Chapter 4: Initial experiments

4.1 Experimental procedure

The necessary first step in developing a single grain instrument, which can ultimately be used for samples from environments where mixing or partial bleaching has occurred, is to evaluate the performance of the instrument using a standard material containing known doses. The instrument must first be capable of producing clear, reproducible results from standard material containing large doses before it can be used to measure the small doses which are accumulated in the natural environment. A standard material, International Atomic Energy Agency (IAEA) F1 feldspar, was used to test and characterise the imaging equipment. This standard material is used for calibration because of its strong luminescence response and reproducible behaviour (Clark and Sanderson, 1994, Spencer, 1996, Sanderson and Clark, 1994). Most measurements were conducted using the IR diode laser as feldspar responds well to stimulation in the infrared and this system was available at the start of the study.

The feldspar was dispensed onto 0.25 mm thick, 10 mm diameter, stainless steel discs sprayed with Electrolube SCO200D silicone grease. Most measurements were carried out using feldspar already containing a stored dose of 1 kGy, administered over a year before any measurements were carried out. Any further irradiation of samples was carried out using a ^{90}Sr beta source at a rate of 33.3 Gy/min. After irradiation samples were preheated to 160°C for several minutes to remove the effects of phosphorescence. High doses were used to ensure that the luminescence signal was well above the minimum detection limits of the instrument so that unambiguous

results could be obtained. It is unlikely, of course, that stored doses of this magnitude would be accumulated in the natural environment. But, as already stated, instrumental development requires large luminescence signals which can only be obtained using large stored doses.

A key issue when considering the method of measurement is alignment. The ease with which multiple images of the same sample can be compared is dependent upon the reproducibility of disc positioning between measurements. Two 1 mm squares on the sample holder (Figure 4.1) were used to align the laser spot. This provided a method whereby the laser was aligned in relation to the disc which was placed in the 10 mm diameter circle drawn on the sample holder. The laser spot was aligned with the square closest to the sample. With the laser in this position a scan over an area of 12 mm by 12 mm covers the entire sample.

Scanning was conducted in a raster pattern beginning from this position. During the scan, the disc is moved under the laser beam, pausing to take one second measurements at the end of each step. Various step sizes were used but 90 μm steps were used in most cases as this is comparable to the diameter of individual grains. This produces around 18000 data points over a measurement area of 12 mm by 12 mm with measurement times in the order of five or six hours.

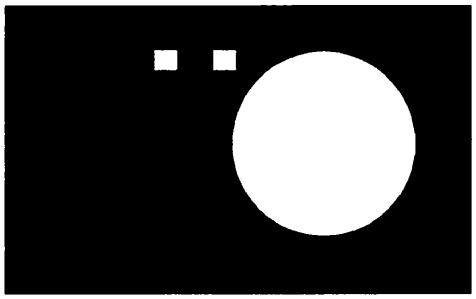

Figure 4.1: *Pattern used to align sample holder with laser*

There are two possible modes in which scanning can be conducted, down counting mode and up/down counting mode. In down counting mode the control board totals all of the counts detected by the photomultiplier. In up/down counting mode the light source is modulated and the measured counts are added together when the light source is on and subtracted when the light source is off (Sanderson et al., 1995). In this way the system is continually subtracting its own background. This mode requires a light source which is precisely modulated. The existing control program for the x-y stage, previously only capable of counting in up/down mode, was modified to allow down counting as well as up/down counting. As a continuous light source was to be used for several measurements it was necessary to use down counting mode.

The software was also modified to write an image to the screen during measurement allowing the operator to view the image being constructed as the data were collected. This image provides an early indication of whether the measurement is proceeding as expected. As the measurements can take several hours, early identification of unsuccessful measurements is valuable. The latest version of the program, SCAN4 (Appendix A), was used to conduct all measurements.

Two methods have been used to analyse the results from the single grain system. An existing TURBO BASIC program, Aerovga3, was initially used to produce 16-colour images of the disc. Aerovga3 is a SUERC program originally used to analyse data from aerial surveys. The program was easily adapted to analyse results from the single grain instrument but is limited to a maximum of 16000 data points per analysis.

Sigmaplot 5.0 for Windows was also used to analyse the results, producing images which can be rotated and viewed in 3 dimensions and can be shown using many different colour schemes. The number of data points which can be analysed is limited only by the processing time required by the program. This program is now used to analyse all results as it is capable of analysing data sets containing more than 16000 data points and can present the results in a variety of formats.

Any single-grain system must be capable of detecting the signal from individual grains and resolving small doses before it can be used to analyse samples from environments where mixing or partial bleaching has occurred. The preliminary measurements to evaluate the single grain system against these requirements are described in the remainder of this chapter. Experiments were also carried out to ensure that the system can quantify the dose within a sample. The problem of laser scatter is investigated as this has limited previous single grain measurement systems to using small numbers of grains within pits in the disc (Duller et al., 1999). Particular consideration is given to the method of sample presentation which minimises laser scatter during measurement. It is also important that mixtures of

irradiated and unirradiated grains can be identified and so irradiated and unirradiated F1 feldspar was mixed in known quantities and analysed. These experiments are described in chapters five and six.

4.2 Imaging

For some measurements it may be desirable that the single grain instrument should be able to produce images of individual grains within samples. The resolution of the system is limited by the laser spot size and so the size of the spot is determined using a single grain of known dimension. A disc containing a sample with an easily identifiable reference mark is also analysed to ensure that the system is capable of resolving single grains within a large sample and producing a representative image of the grains on the disc. This is important as in dose determination measurements multiple scans of the same sample must be compared by matching individual grains (or areas on the image) in one measurement with the same grains, (or areas) in later measurements.

In order to determine the laser spot size, an easily identifiable grain containing a stored dose of 1 kGy was placed on a disc and analysed using the IR laser and a step size of 50 μm. By comparing the size of the image with the size of the grain it is possible to set an upper limit on the effective size of the laser spot. The size of the grain was measured using a microscope and a nylon mesh of known dimension. The grain dimensions were 200 ± 50 μm by 300 ± 50 μm. The maximum extent of the resultant image (Figures 4.2 and 4.3) is 270 ± 50 μm by 320 ± 50 μm. The size of the measured image should be equal to the size of the grain added to the size of the laser spot and this suggests that the maximum effective spot size of the laser is 50-100 μm. This is broadly consistent with the specification of the diode. Moreover, as the grains

used in measurements typically have a diameter of 100 µm this is adequate for measuring single grains.

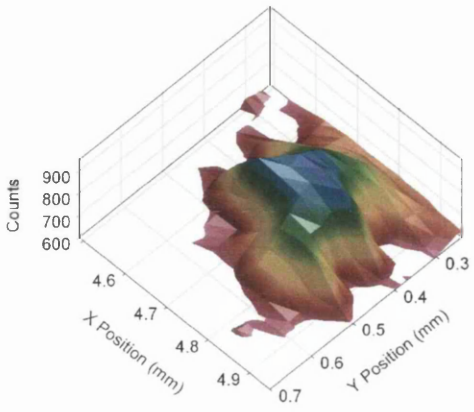

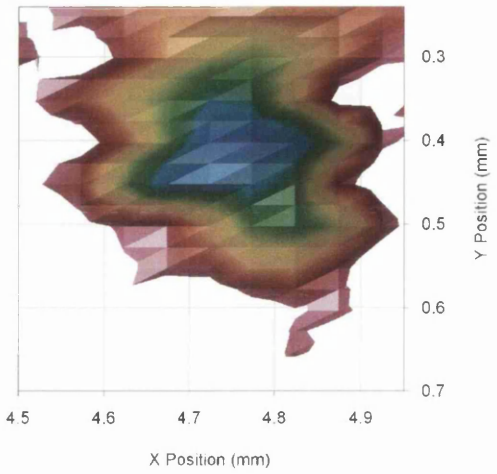

Figure 4.2: *Rotated image of single grain*

Figure 4.3: *Image of single grain*

A disc covered in F1 feldspar with a stored dose of 1 kGy was analysed. A T-shaped reference mark, approximately 5 mm by 4mm, on the disc provided an easily identifiable feature. The measurement was conducted using the IR laser with the sample moving in 125 µm steps over an area of 11mm by 11mm. Analysis of the 6000 data points using Aerovga3 shows the "T shaped" feature which was scratched into the sample (Figure 4.4). Analysis was also carried out using Sigmaplot 5 to assess whether it was more effective than Aerovga3. The feature is also visible when the results are analysed using Sigmaplot 5 (Figures 4.5 and 4.6). The three dimensional plots available within Sigmaplot 5 show several peaks and these more versatile plots can be viewed in three dimensions and from various angles.

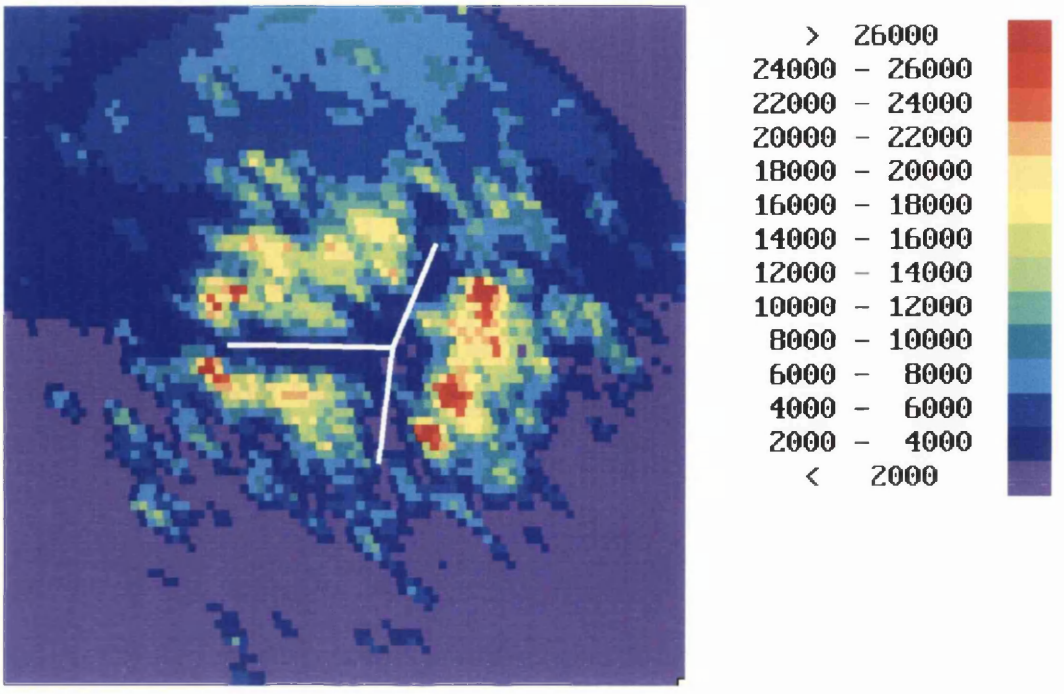

Figure 4.4: *Image produced by Aerovga3 ("T" shaped reference mark shown in white)*

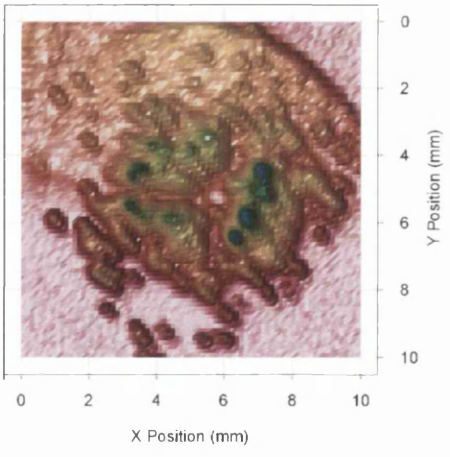

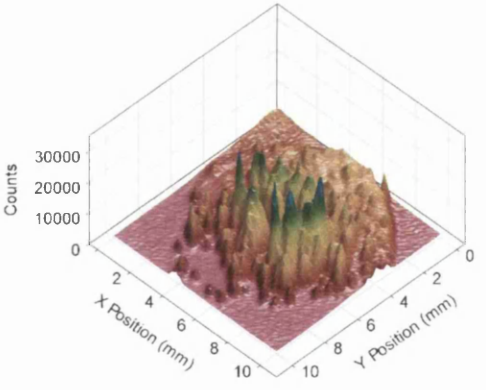

Figure 4.5: *Image produced using Sigmaplot 5*

Figure 4.6: *Rotated image*

These results show that the system is capable of imaging individual grains which are widely spaced. It is impossible to distinguish between single grains in the centre of

the disc as they are too close together. However, where the grains are more widely spaced, there are small peaks due to single grains. The outline of the disc itself is also clearly visible in the top half of the image. The background count is high initially, gradually decreasing during measurement. This may be due to laser light reflecting within the chamber or the disc may have been tilted slightly. This effect is discussed in more detail in chapter 5.

The system's laser spot size, at 50-100 μm, is sufficient to resolve single grains. Imaging a sample of F1 feldspar showed that single grains can be resolved if they are widely spaced. The next section investigates the efficiency with which the available signal is measured. The minimum dose detectable using the system is also determined.

4.3 Bleaching

The accuracy of the results obtained with the single grain system and the range of applications for which it is suitable are likely to be dependent upon the minimum dose that can be detected by the system. In situations where mixing has occurred, doses of around 0.5 Gy may have to be measured (Roberts et al., 1998).

An issue closely related to the sensitivity of the single grain instrument is bleaching during measurement. If the sample is entirely bleached during measurement, removing the entire available signal, then the sensitivity of the system will be maximised. This is investigated by conducting multiple scans on the same samples.

The issue of bleaching during measurement is important for two reasons. Bleaching would be required between measurements if the signal were not entirely removed during measurement. It is also important that the sample is bleached during measurement so that all of the available signal can be measured. Three experiments were conducted to determine the extent of bleaching during measurement. In the first experiment a small area on a disc was analysed before the entire disc was analysed. In the following two experiments sparsely covered discs were analysed twice to show the size of any remaining signal.

A small area of an irradiated sample (1 kGy F1 feldspar) was scanned and read out (Figure 4.7). In a second measurement the entire disc was read out (Figure 4.8). The small area which has been measured twice displays a greatly reduced luminescence signal.

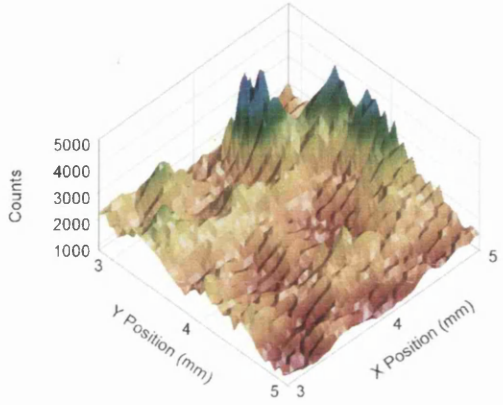

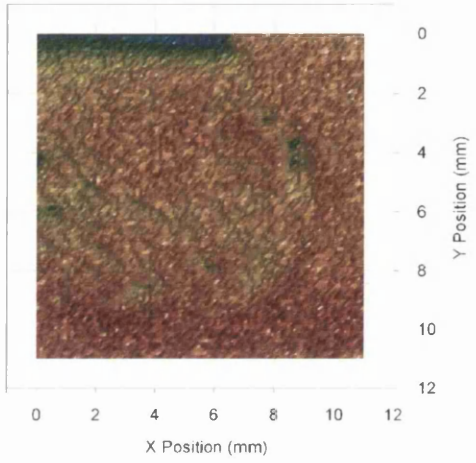

Figure 4.7: *Scan of small area of disc*

Figure 4.8: *Scan of entire disc*

Bleaching during measurement was also investigated by arranging feldspar grains on a disc to form an easily recognisable shape. The disc was given a dose of 1 kGy and two measurements were carried out. The results show that most of the luminescence signal is removed (Figures 4.9 – 4.12).

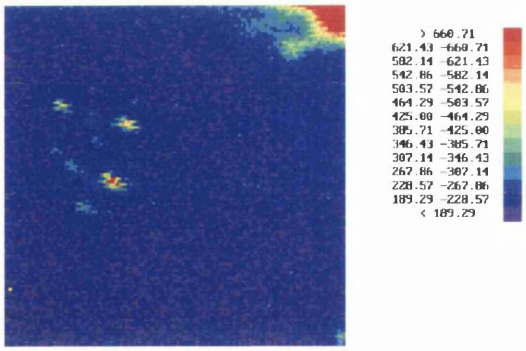

Figure 4.9: *Image after first measurement (produced using Aerovga3)*

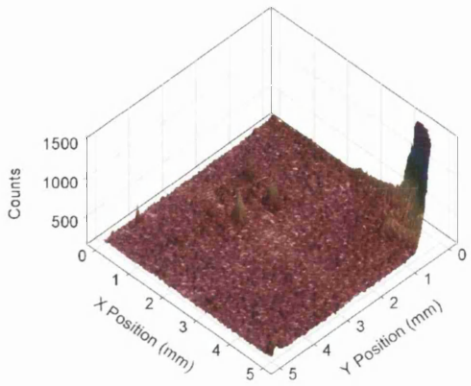

Figure 4.10: *Image after first measurement (produced using Sigmaplot 5)*

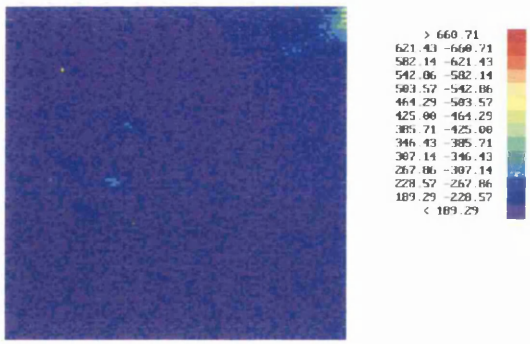

Figure 4.11: *Image after second measurement (produced using Aerovga3)*

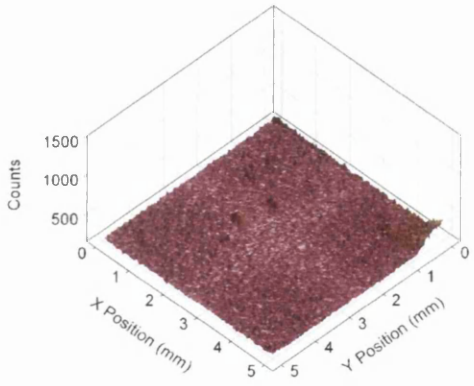

Figure 4.12: *Image after second measurement (produced using Sigmaplot 5)*

A disc was sparsely covered in F1 feldspar grains containing a 1 kGy stored dose and analysed. The resultant image (Figure 4.13) shows several peaks. Visual inspection of the disc confirmed that these peaks corresponded to individual grains. This confirms the earlier result that the signals from individual grains can be detected at

high doses. The peaks are of variable size, which suggests that even F1 feldspar exhibits grain-to-grain variation in luminescence response. One half of the same disc was re-analysed and this shows that there is very little signal left in the grains after measurement (Figure 4.14).

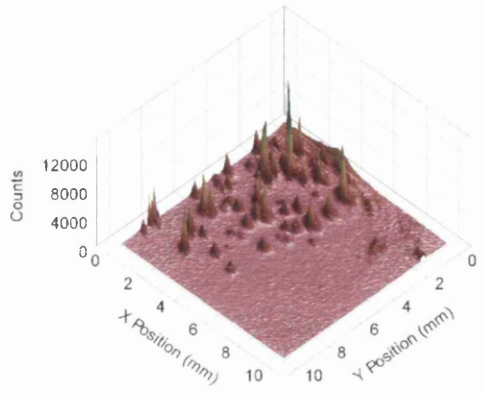

Figure 4.13: *Image produced after first measurement*

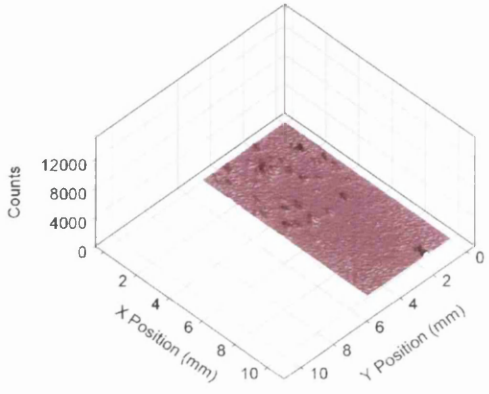

Figure 4.14: *Image produced after second measurement*

These results show that one measurement removes most of the signal from the grains, leaving only a small residual signal. These experiments used stored doses which are far larger than those which would be found in any sample from a natural environment where mixing or partial bleaching has occurred. It is possible that smaller doses would be removed after one measurement which would mean that the maximum possible signal would be obtained. A more powerful laser would be expected to reduce any remaining signal still further, removing the need for bleaching between measurements. However, it should also be noted that in some cases the signal from feldspar does not reduce to background even after long periods of illumination (see

Figure 2.5). For this reason it is likely that the signal from the grains cannot be entirely removed.

Some results (Figures 4.9-4.12) show a signal at the edge of the disc in the top right of the image. The disc has a raised rim around its edge and it is likely that the laser light has reflected off this raised edge to stimulate the grains in the middle of the disc. This effect is examined more thoroughly in chapter 5.

In the next section the minimum detectable dose is determined by examining the background of the system and the measured response from several known doses.

4.4 Minimum detectable limits

In order to measure stored doses, it is essential that the single grain system can measure small doses accurately. The minimum dose which can be measured using the system is determined using measurements on samples containing known doses. These are compared to the background of the system and the minimum measurable dose is calculated. The background signal of the system is examined and the threshold above which a signal can be considered present is calculated. This is then compared to the signal detected from samples containing stored doses of 45, 90, 150, 300, 600 and 1200 Gy.

Six discs were irradiated with doses of 1200, 600, 300, 150, 90 and 45 Grays and analysed (Figures 4.15–4.20). The results show that the system measured a signal at all of these doses and suggests that doses below 45 Grays should also be measurable.

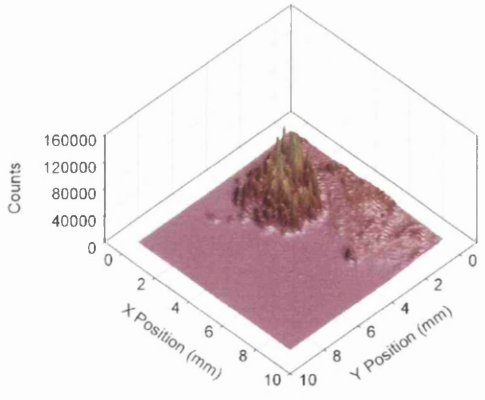

Figure 4.15: *Image from grains with stored dose of 1200 Gy*

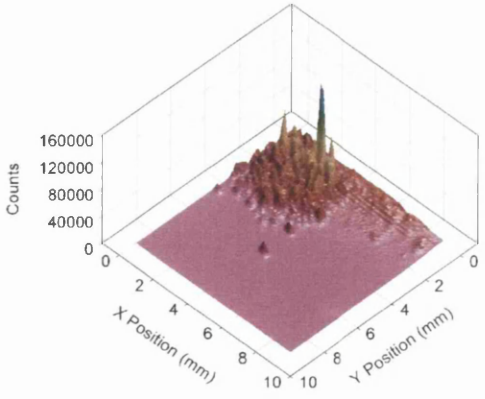

Figure 4.16: *Image from grains with stored dose of 600 Gy*

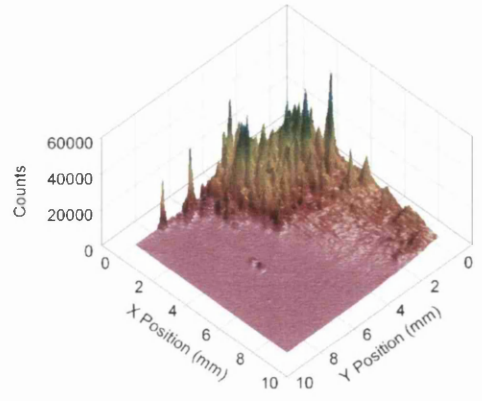

Figure 4.17: *Image from grains with stored dose of 300 Gy*

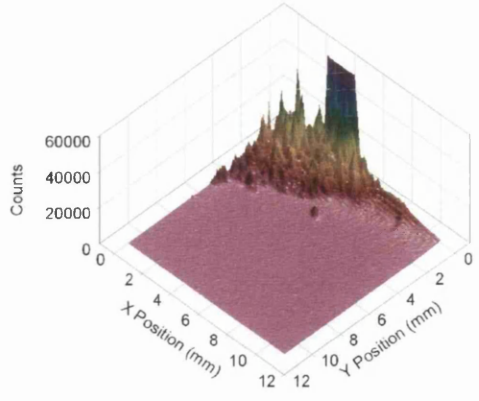

Figure 4.18: *Image from grains with stored dose of 150 Gy*

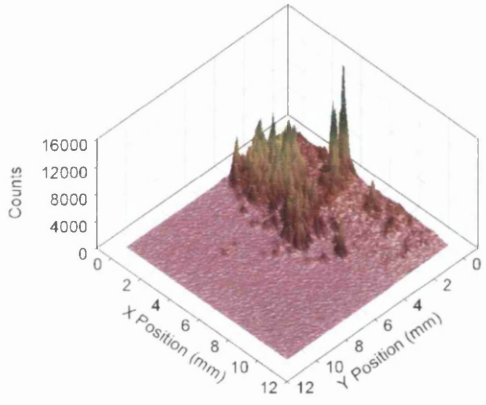

Figure 4.19: *Image from grains with stored dose of 90 Gy*

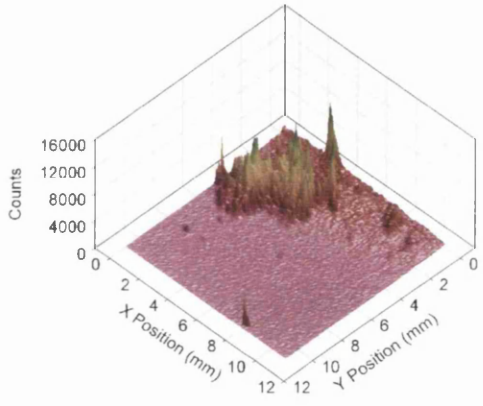

Figure 4.20: *Image from grains with stored dose of 45 Gy*

A second issue concerning minimum detectable limits is for a signal to be detectable it must be higher than the background of the instrument. The mean background of the single grain instrument is typically 120 ±15 counts per second (Figure 4.21).

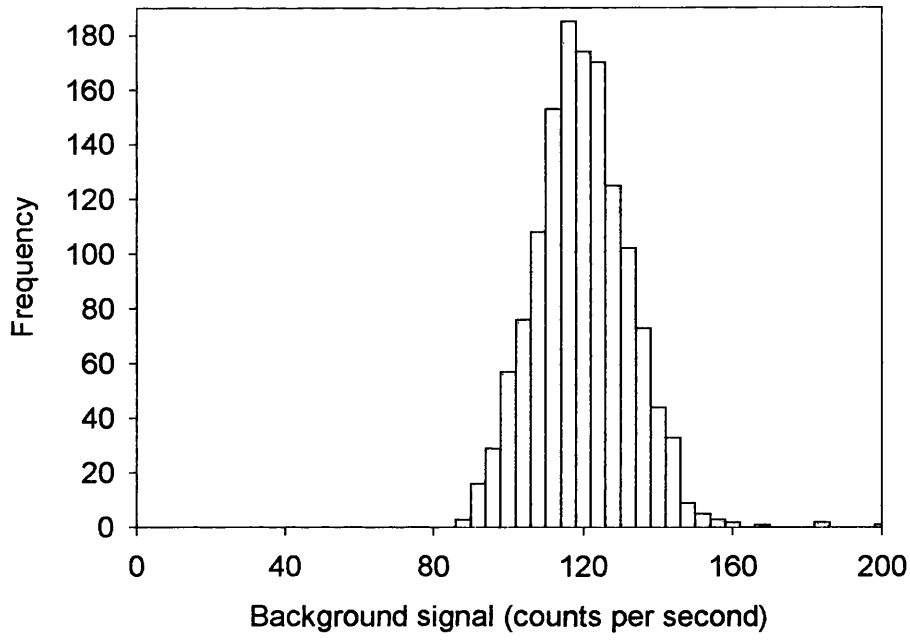

Figure 4.21: *Histogram showing background signal of single grain instrument*

Signals which are more than three standard deviations larger than the background signal can be considered as clear results (with a certainty of 99.7%). For this reason signals above 165 counts per second can be distinguished from background and are measurable. The average count obtained from grains irradiated with 1200 Gy was found to be approximately 30000. This corresponds to 25 counts Gy^{-1} which means 165 counts per second, 45 counts per second above background, would correspond to a dose of approximately 2 Gy. This means the single grain system is capable of measuring doses as small as 2 Grays from materials which are at least as responsive as F1 feldspar. To accurately analyse samples from natural environments where mixing or partial bleaching has occurred it may be necessary to measure doses of around 0.5 Gy (Roberts et al., 1998). This suggests that the system may not be ready to analyse natural samples without further improvement or modification.

Modulation of the laser would improve the performance of the system. By switching the laser on and off at a known frequency and ensuring that the photon counting is switched at the same time then the system could operate with a greatly reduced background count. This technique has already been developed at SUERC (Sanderson et al., 1995). By subtracting the counts measured while the laser is off and adding the counts while the laser is on the system is effectively subtracting its own background several times a second. It may also be possible to improve the sensitivity of the system by reducing the duration of each measurement to less than one second. If most of the available signal could be removed in a much shorter time then the signal to background ratio would be increased and the sensitivity of the system would be improved.

Before natural samples can be measured using the single grain system further experiments must be conducted using the single grain system to characterise, and improve, its performance. By addressing the problem of laser scatter during measurement it should be possible to improve the performance of the instrument.

Chapter 5: Effect of laser scatter

One solution to the problem of laser scatter, where the laser light which stimulates grains is scattered into other grains by external and internal reflection and refraction in grains that are being directly illuminated/stimulated, is to place the grains in pits on the discs (Duller et al., 1999). At present the single grain system constructed at SUERC does not use this method of sample presentation, as this would remove the imaging capability of the instrument and may result in longer sample preparation times. By using pits in discs to present grains the number of grains on each disc is reduced from approximately 10000 to around 100. A system which could avoid or limit the effects of laser scatter when analysing evenly covered discs would have the advantage of short sample preparation times as well as the ability to image individual grains.

In this chapter the presence and nature of scatter is shown using a stationary laser spot to bleach evenly covered discs. Laser scatter during measurement has been modelled using a specially written computer program which predicts the effect scatter has on the measured results. Various methods of sample presentation are considered in an attempt to limit the effect of scatter.

5.1 Bleaching of samples by stationary laser

The time taken to bleach individual grains is important as ideally they should be well bleached within the one second that the laser illuminates each point. This would ensure that the maximum possible signal was obtained from each grain (as discussed earlier in section 4.3, pp 36). However, if scatter occurs a luminescence signal will still be measured after the individual grain that is directly illuminated by the laser has been entirely bleached. This will result in a slowly decreasing shine-down curve in which the signal takes a very long time to reduce to background. Hence, the form of bleaching can be used to identify whether scatter occurs.

In this section evenly and sparsely covered discs were bleached using a stationary laser spot. Discs of F1 feldspar were bleached using an IR laser. The first measurement was conducted using an evenly covered disc. Other measurements were conducted using more sparsely covered discs as this should result in less scatter. Measurements were also carried out using green and blue lasers on quartz and F1 feldspar. Blue and green lasers were also used in the experiments as one of the first steps in broadening the capabilities of the system would be to add lasers of lower wavelength. Feldspar responds well to infrared illumination (Hutt et al., 1988) but quartz generally has a very poor response to stimulation by red or infra–red light (Huntley et al., 1985) and so any measurements on quartz would require a blue or green laser.

The IR laser was directed onto a sample of 1 kGy irradiated F1 feldspar for several seconds without the disc being moved. The resultant measurement forms the shine down curve for the feldspar sample. The results (Figure 5.1) show that the signal drops significantly during the first few seconds but does not drop to below 10% of its initial value until after more than 600 seconds of measurement.

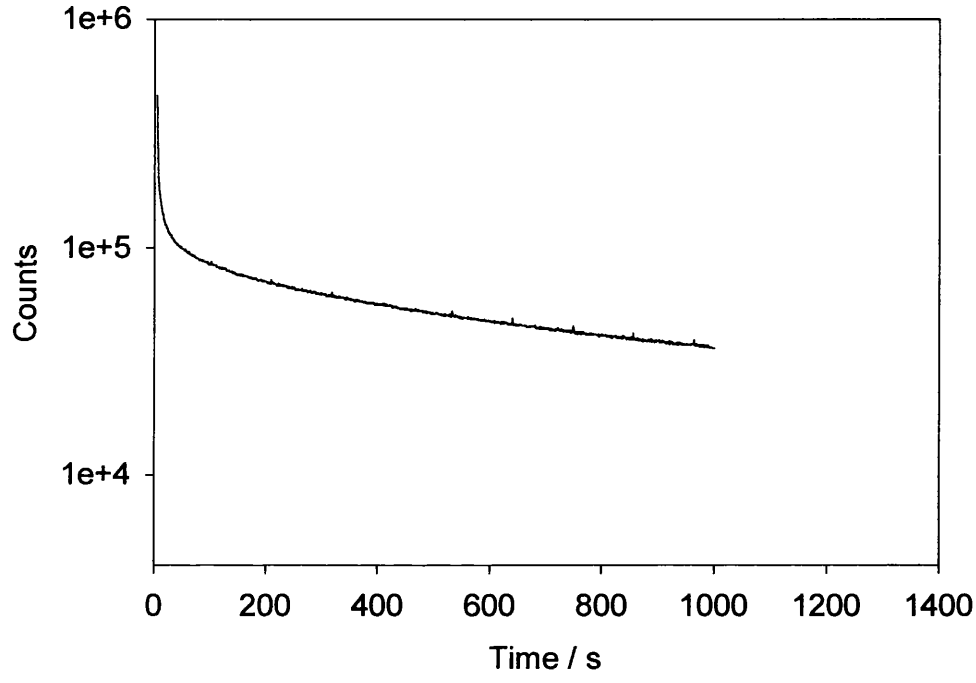

Figure 5.1: *Bleaching of feldspar using IR laser*

Three scans were conducted on more sparsely coated discs (Figures 5.2-5.4). The signal is depleted more rapidly but is not reduced to the background level, typically 200 – 300 counts, even after several minutes of illumination. This may suggest that the effect of scatter has been reduced, but is still significant.

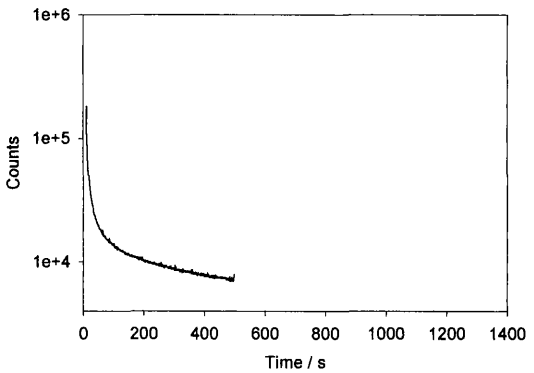

Figure 5.2: *Bleaching of feldspar using IR laser, disc 1*

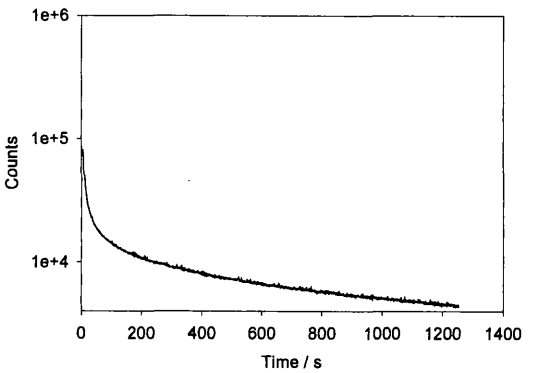

Figure 5.3: *Bleaching of feldspar using IR laser, disc 2*

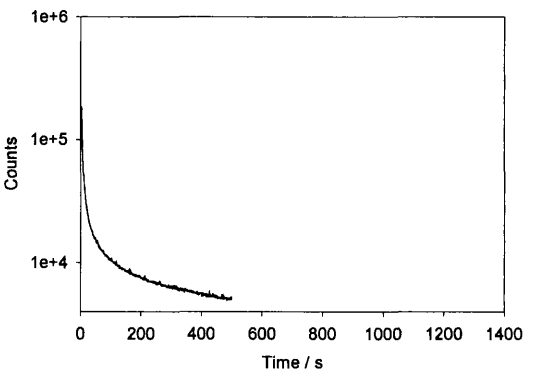

Figure 5.4: *Bleaching of feldspar using IR laser, disc 3*

The bleaching results on feldspar and quartz using the blue laser (Figure 5.5 and 5.6) show that scatter is also significant as the shine-down curves do not rapidly decrease to background. During both quartz measurements a peak occurred in the shine down curve at around 250 seconds. The experiment was repeated and the same peak was again observed. The cause of this effect is unknown. The peak could not have been caused by a change in the laser characteristics as the laser was allowed time to stabilise before each measurement.

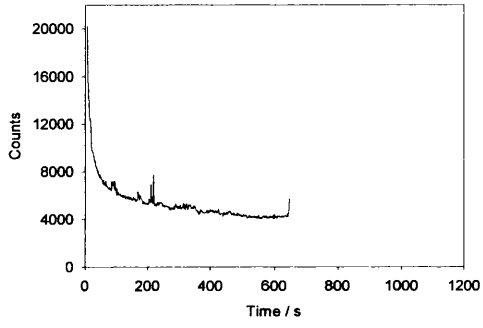

Figure 5.5: *Bleaching of feldspar using blue laser*

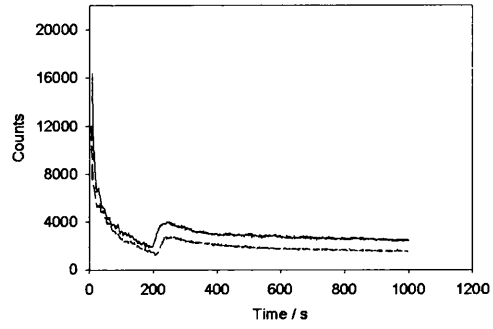

Figure 5.6: *Bleaching of quartz using blue laser*

The results obtained using the green laser (Figure 5.7 and 5.8) on feldspar and quartz also show that the bleaching of the sample has not been completed after several minutes of measurement.

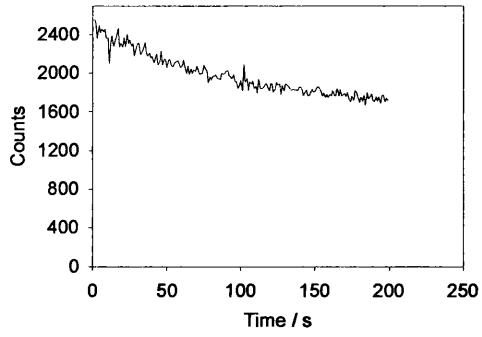

Figure 5.7: *Bleaching of feldspar using green laser*

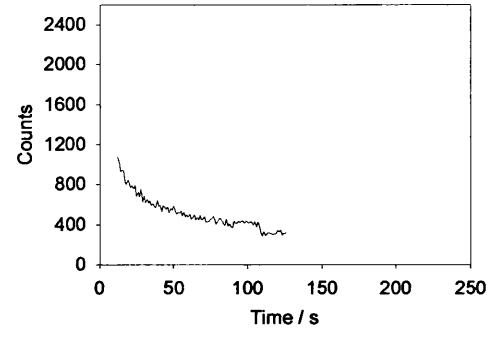

Figure 5.8: *Bleaching of quartz using green laser*

The intensity of the measured signal from feldspar was far smaller using the green and blue lasers than when using the IR laser. This was unexpected, as feldspar should respond more strongly to low wavelength stimulation. However, the experimental set-up for the green and blue lasers was not ideal. The blue and green lasers were not as highly focussed as the IR laser and so the stimulation was not as efficient. The relative measurement capability of the green laser is shown by a scan of quartz irradiated with 1 kGy (Figure 5.9). The result shows individual grains but the amount of measured light is relatively low and is unlikely to be large enough to conduct measurements at lower doses.

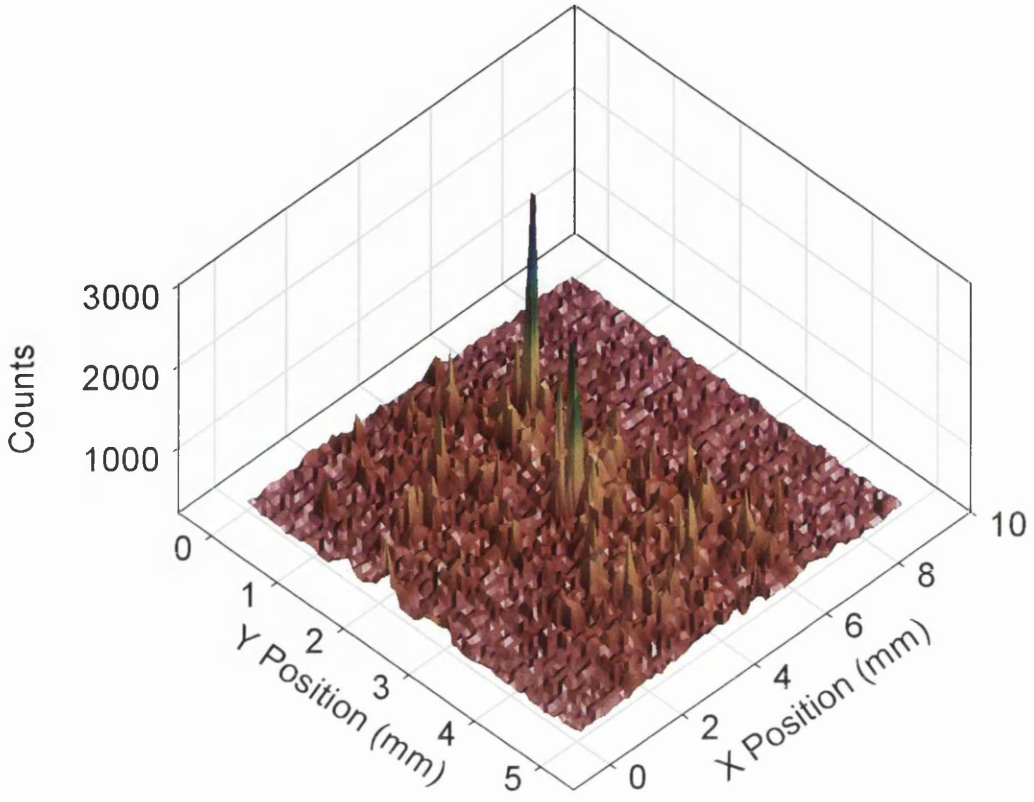

Figure 5.9: *Image of quartz grains produced using green laser*

The above bleaching results suggest that scattering is occurring across the surface of the disc. Although previous results (section 4.3, pp 39) have shown that bleaching is not entirely completed during measurements it would seem unlikely that the signal within one or two grains could persist for 1000 seconds as shown in Figure 5.1. Feldspar can contain a small, unbleachable component (see Figure 2.5) but this is not large enough to account for the observed results. The total number of counts measured during this time is more than sixty million. This number of counts could only have resulted from the stimulation of several grains simultaneously. The likely explanation is that scattering occurs on the disc during measurement.

There are two possible mechanisms which can result in scattering (Figure 5.10). The laser beam may reflect around the chamber during measurement, illuminating several areas of the disc simultaneously, or the beam could have been scattered by the grains themselves. In the latter case light would be scattered across the surface of the disc, illuminating almost every grain in the sample. The degree of illumination would decrease rapidly with distance and a single, stationary laser spot would require an extremely long illumination time to bleach an entire disc, consistent with the observed results (Figures 5.1-5.8). The form of the shine down curves cannot be explained by the direct stimulation of several grains by the laser spot as, although this would result in a larger initial signal, this should result in the same bleaching time as for a single grain. Instead, the observed effect is consistent with a large number of grains receiving a low level of stimulation.

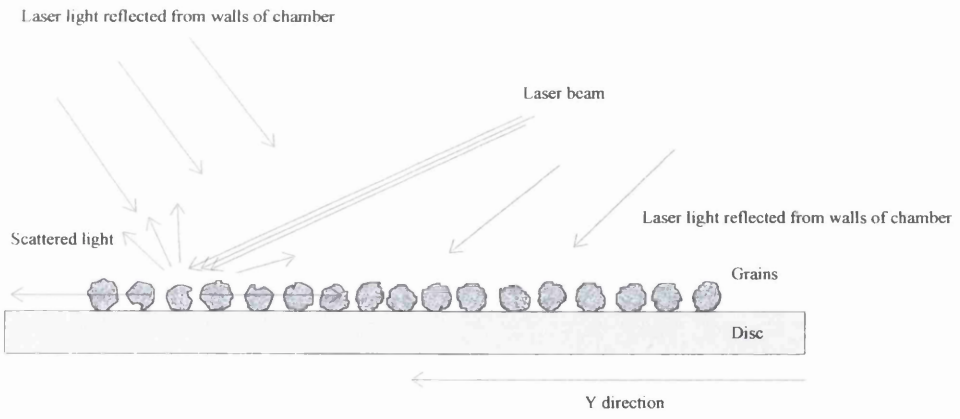

Figure 5.10: *Possible scattering mechanisms*

From the results using IR, green and blue lasers shining on a single spot on the disc it seems likely that light is scattered by grains across the surface of the disc. Of course, it is also possible that laser light is scattered onto the disc from the walls of the chamber.

In the next section scatter across the disc during measurement is modelled using a specially written program. The results of this numerical modelling are used to identify the effects of scatter in subsequent measurements. A number of scans were also conducted under different conditions designed to quantify or eliminate the effect of scatter.

5.2 Modelling of laser scatter

5.2.1 Model description

To predict the expected forms of scatter if laser light were scattered across the surface of the disc a program, Kring6, was written in TURBO BASIC (Appendix B). The earliest version of this program used a one-dimensional array of bins to represent the grains. Each bin was allocated a number representing the grain's luminescence content, initially 100, which decreased during each measurement. The program was expanded into two dimensions to create a more realistic picture. Several arrangements of "grains" are possible. Simulations can be conducted assuming one large circular area, with a diameter of 80 bins, which is covered in grains (Figure 5.11) or up to five small circular areas, with a diameter of 10 bins, of variable size and position (Figure 5.12). The "laser" follows the same raster pattern as the real measurements and the one second measurements conducted by the real laser are simulated. The apparatus is assumed to be counting in "down" counting mode.

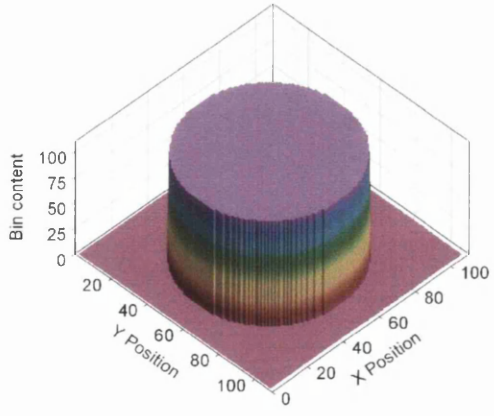

Figure 5.11:-*One large circle*

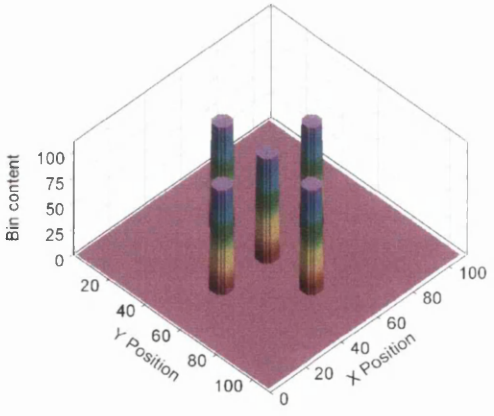

Figure 5.12:-*Five circles*

The effect of scatter is simulated by assuming that stimulation affects more than one grain at a time. As one grain is stimulated the grains around it are affected to varying degrees depending on their distance from the point of stimulation (Figure 5.13). By default the program assumes that the laser removes 70% of the signal from the "grain" being directly illuminated. Grains which are one step away have 60% of their signal removed and this decreases by 10% with each step until grains which are seven steps away are not affected. The depletion caused at each distance can be varied by the user to simulate different scattering regimes.

The size and shape of the area affected during stimulation can be varied by the user before running the program. The model assumes scatter involving the six nearest bins in each direction. If the measurement area in the numerical model is compared to the measurement area in the experimental results this would correspond to a distance of around 1 mm in each direction. This would not affect the entire disc which has a diameter of 10 mm and so this stimulation area may not represent the full extent of the laser scatter. The relative effect of stimulation can also be varied with distance to produce a large, uniform stimulation or one which decreases with distance. The type of scattering is also varied within the program. The expanded stimulation area can be effective throughout the measurement or can be set to appear only when the "laser" is over a point which contains a "grain", even if the grain contains no signal. In this way two possible scattering mechanisms are simulated. Scattering can be assumed to either occur at every point on the measurement area or only when grains are being illuminated.

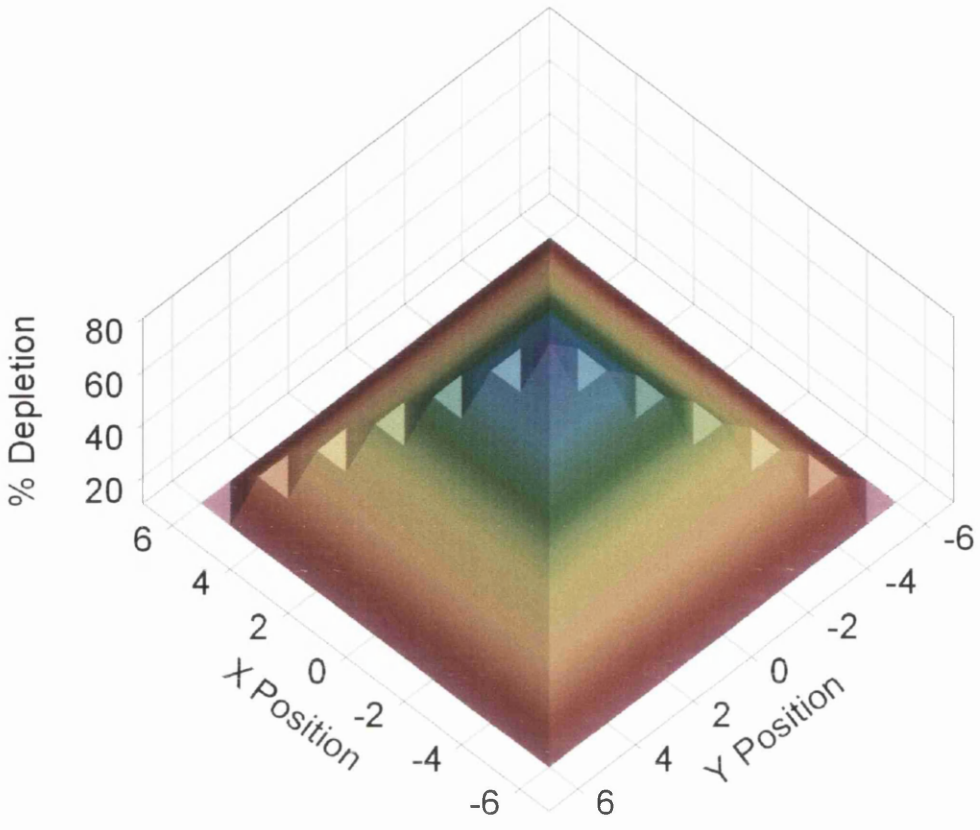

Figure 5.13: *Laser spot*

The output of the program includes the original matrix (which shows the content of each bin in the model), the simulated result and the remaining content in each bin after measurement (Figures 5.14-5.16). The results are analysed using Sigmaplot 5.0.

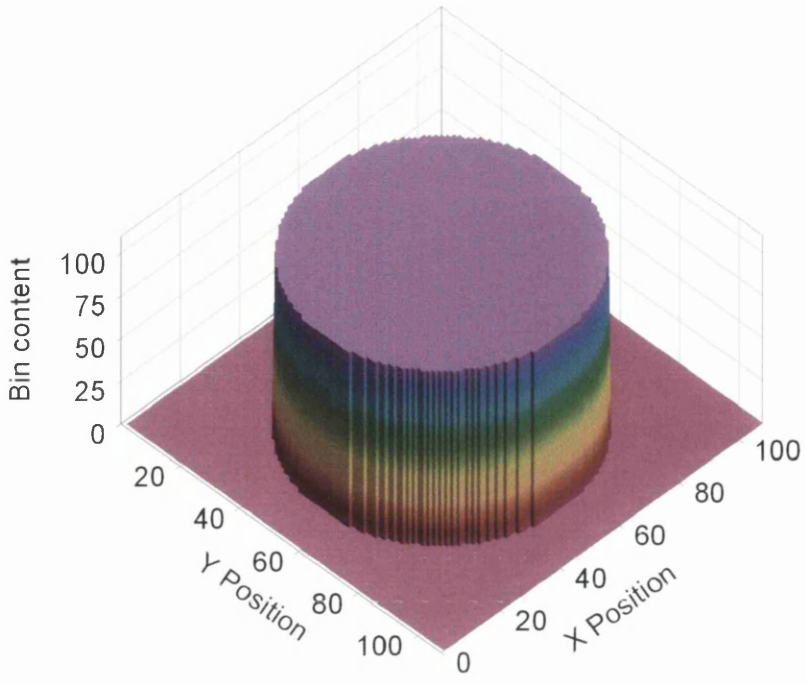

Figure 5.14: *Test matrix*

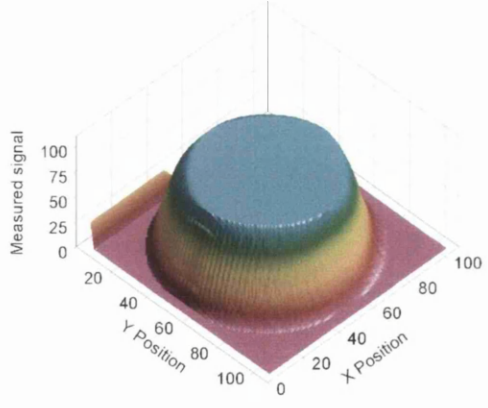

Figure 5.15: *Measured matrix*

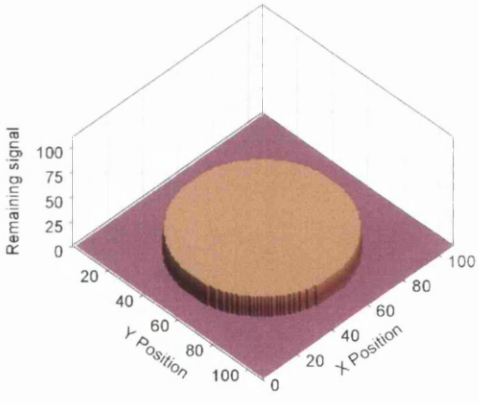

Figure 5.16: *Remaining signal*

The aim of the modelling of the possible effects of laser scatter is to show the type of features which are suggestive of scattering across the face of the disc. These features can be used to identify the presence of scatter in subsequent measurements.

5.2.2 Results

In this section numerical modelling is used to predict the results of laser scatter during measurement. Preliminary results using a one-dimensional array are presented. Results are also generated using a two dimensional array assuming different scattering mechanisms and varied stimulation areas. Results are produced assuming evenly covered discs and more sparsely coated discs with five small areas of grains.

The result produced using a one-dimensional array (Figure 5.17) shows a decreasing exponential. By expanding the model to include some areas which did not include grains (i.e. setting the values in some bins to zero) the results begin to show troughs (Figure 5.18).

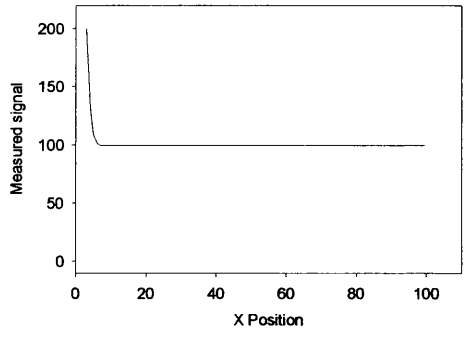

Figure 5.17: *Initial results produced using one dimensional model of laser scattering*

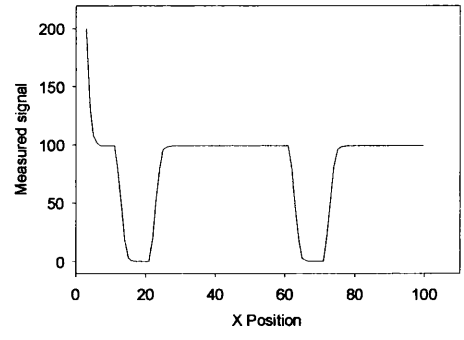

Figure 5.18: *Results produced using one dimensional model in combination with variable grain signal*

Results are produced using the two-dimensional model assuming evenly covered discs and discs with small areas of irradiated grains. Results produced by assuming the disc is evenly covered and scatter occurs from all points on the disc show an initial peak in an area where no grains are present (Figure 5.19). The measured signal also decreases with increasing y position. This gradient through the results indicates that the measured signal is decreasing as the measurement progresses. In similar results produced using a sparsely covered disc neither of these effects is as pronounced (Figure 5.20) By assuming that scatter occurs only when a grain is present a peak does not occur until the first grain is measured (Figures 5.21 and 5.22). The gradient through the results is much more obvious and large peaks are observed as the first grains are measured. This occurs on both the evenly covered and more sparsely covered disc.

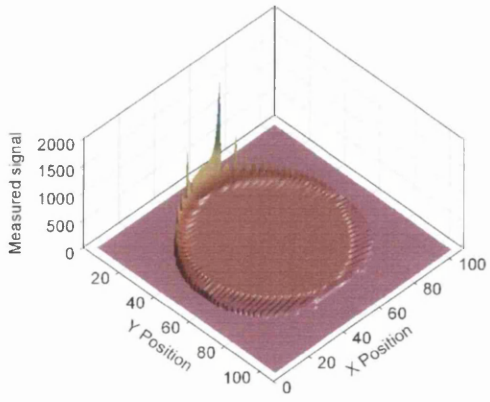

Figure 5.19: *Simulated result from evenly covered disc assuming scatter from all points*

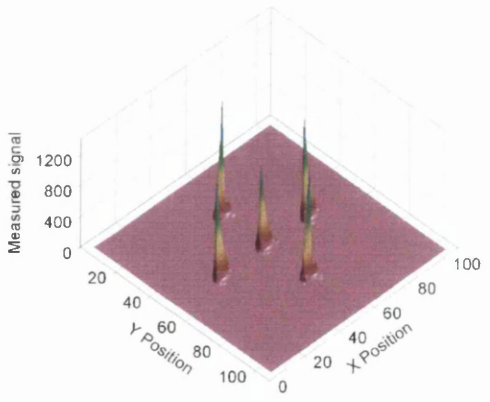

Figure 5.20: *Simulated result from disc containing five patches of grains assuming scatter from all points*

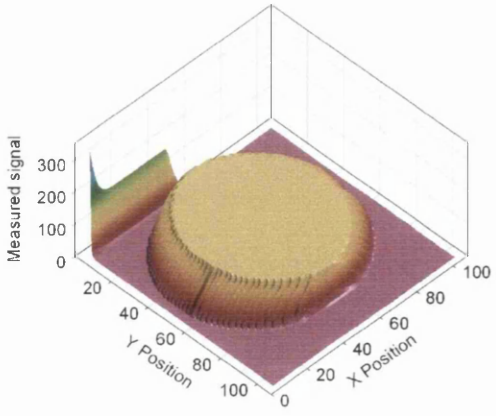

Figure 5.21: *Simulated result from evenly covered disc assuming scatter occurs only from grains*

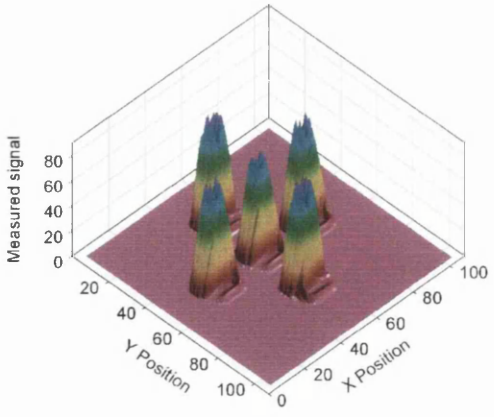

Figure 5.22: *Simulated result from disc containing five patches of grains assuming scatter only from grains*

Results were also generated using rectangular stimulation areas instead of a square stimulation area (Figures 5.23 and 5.24), both with a reduced y dimension (Figures 5.25 and 5.26) and a reduced x dimension (Figures 5.27 and 5.28).

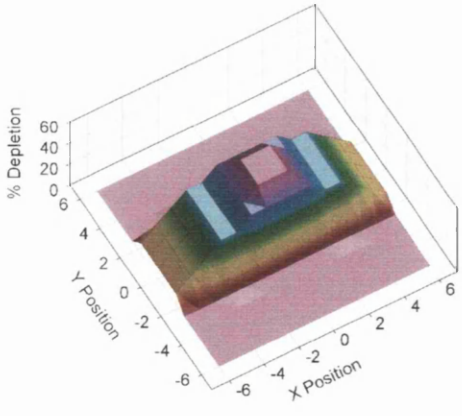

Figure 5.23: *Laser spot with reduced y dimension*

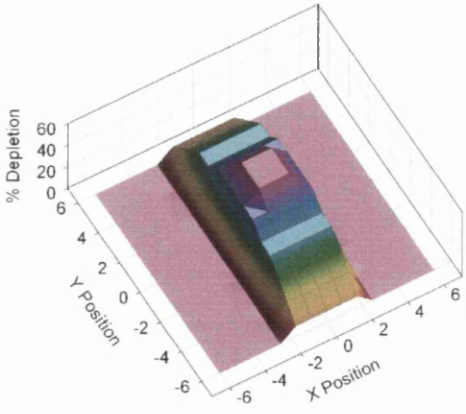

Figure 5.24: *Laser spot with reduced x dimension*

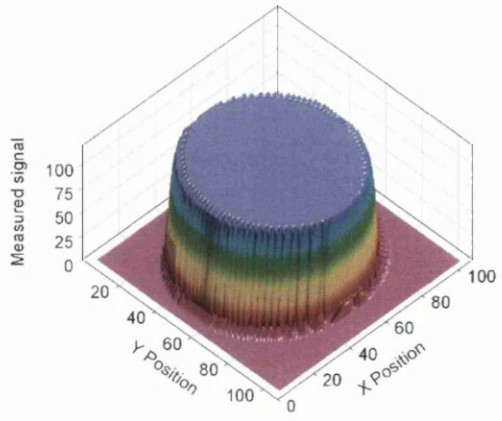

Figure 5.25: *Simulated result from evenly covered disc assuming scatter from all points and stimulation area with reduced y dimension*

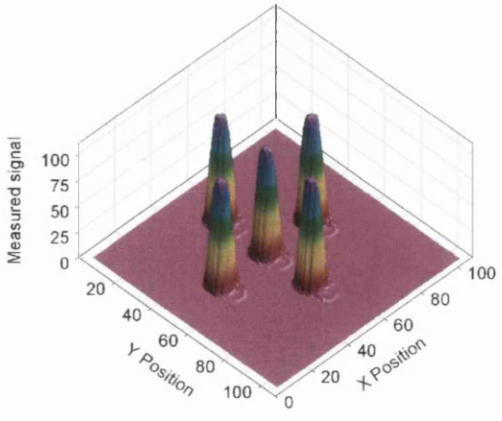

Figure 5.26: *Simulated result from disc containing five patches of grains assuming scatter from all points and stimulation area with reduced y dimension*

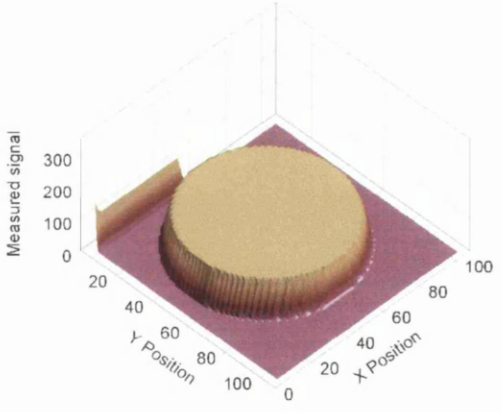

Figure 5.27: *Simulated result from evenly covered disc assuming scatter from all points and stimulation area with reduced x dimension*

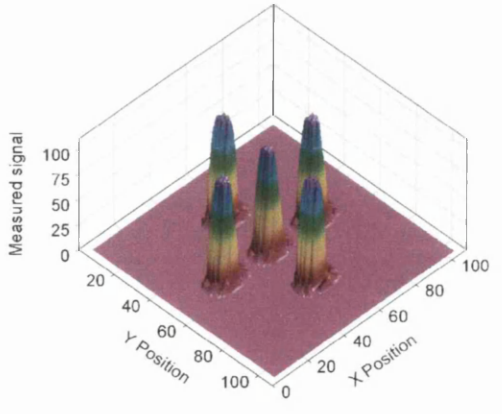

Figure 5.28: *Simulated result from disc containing five patches of grains assuming scatter from all points and stimulation area with reduced x dimension*

Figure 5.25 shows no peak before the laser spot is over any grains. This shows that the peak at the start of the measurement shown in Figure 5.19 was caused by scatter in the y direction. The measured signal decreases during measurement, indicating that the same gradient observed in Figure 5.19 is present. If the x dimension of the beam is reduced a peak (similar to the peak observed in Figure 5.19) is present (Figure 5.27). This shows the initial peak produced by the laser scatter is smaller if the x dimension of the beam is reduced although the peak is still present. A gradient is present through the results as was previously observed in Figures 5.19, 5.21, and 5.25. The results from the more sparsely covered discs show again that the effect of scatter is less significant than when evenly covered discs are used (Figures 5.26 and 5.28).

In the single grain instrument the laser beam illuminates the stimulation area from an angle (as shown in Figure 5.10) and so it is likely that the laser spot will be elliptical with a reduced x dimension. The results predict that the scatter due to a laser spot of this type will produce a peak at the start of the measurement, before the laser spot is shining directly onto any grains, and a gradient through the results (Figure 5.27).

Varying the degree and nature of the scatter around the laser spot has no significant effect on the nature of the results (Figures 5.30-5.32). Reducing the degree of depletion across the laser spot (Figure 5.29) reduces the size of the initial peak but both the initial peak and the gradient through the results are present (Figure 5.30). Results produced assuming uniform depletion across the laser spot (Figures 5.31 and 5.32) show an initial peak as well as a gradient through the results.

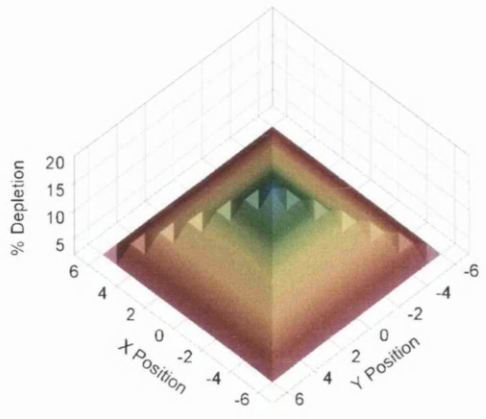

Figure 5.29: *Laser spot with reduced depletion*

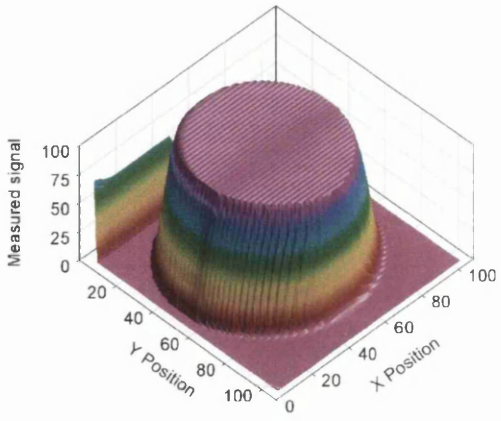

Figure 5.30: *Simulated result from evenly covered disc assuming scatter from all points on disc and reduced depletion*

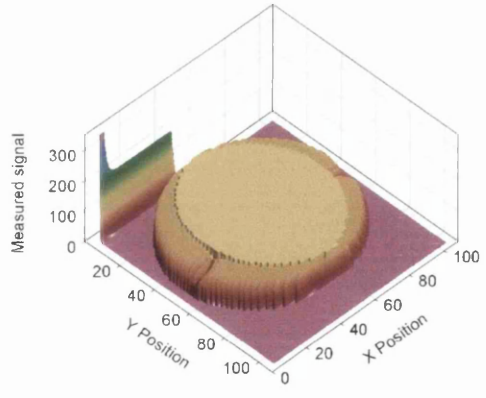

Figure 5.31: *Simulated result from evenly covered disc assuming scatter from all points on disc and uniform depletion of 40% across laser spot*

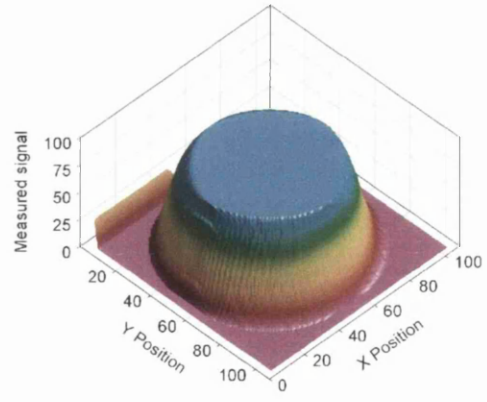

Figure 5.32: *Simulated result from evenly covered disc assuming scatter from all points on disc and uniform depletion of 1% across laser spot*

If laser scatter is occurring within the chamber or across the surface of the disc a peak should occur initially and a gradient should appear through the results. However, the results show that there are two effects which indicate the presence of laser scatter: a peak which appears initially before grains are directly illuminated and a gradient through the results as the measured signal decreases with time. These occur even when the laser scatter takes place over the relatively small scale that is considered here. These two effects have already been observed in previous measurements (Figures 4.8, 4.18). The results also show that the effect of scatter is not as significant if discs are sparsely covered in grains.

The form of the observed scatter can now be investigated and compared to the results from the model. The two features predicted by the model can be used to identify the occurrence of laser scatter during measurement. In the next section various approaches are employed in an attempt to reduce or eliminate the effect of laser scatter and the presence or absence of the two features predicted by numerical modelling is used to determine whether scattering has occurred.

5.3 Experimental investigation into the effect of laser scatter

In this section attempts were made to reduce the effect of laser scatter during measurement. The likelihood of laser light scattering from the walls of the chamber is reduced by altering the chamber and the method of sample presentation is changed to prevent grains scattering light across the surface of the disc. All experiments used 1 kGy irradiated feldspar which was scanned using the IR laser.

Visual inspection using a laser was used to confirm that scattering occurs. The effect of laser scatter was also illustrated through the analysis of two evenly covered discs. Methods of reducing this scatter were then investigated. The walls of the chamber were covered in black opaque plastic to limit the effect of scatter due to laser light reflecting around the chamber during measurement. The problem of scatter from the disc surface was addressed by dispensing the feldspar grains onto a piece of glass instead of a stainless steel disc and blackening the substrate. An attempt was made to limit grain-to-grain scattering by using silicone grease to cover the grains after they were dispensed. This method was tested as it does not compromise the throughput or imaging capability of the system. Finally, grains were dispensed into pits within a disc to limit grain-to-grain scatter. This method has been used in other single grain instruments (Duller et al., 1999) but would decrease the throughput and remove the imaging capability of the system being developed at SUERC.

Metal discs covered in feldspar grains were examined using a 532 nm green laser to assess evidence of reflection or refraction. The laser was directed onto the disc and the reflected light was observed. While shining the laser onto the disc and visually observing the reflected light, small points of light were visible within the reflected laser light. These small, bright points of light were clearly the result of reflection or refraction from individual grains and were visible at angles of 40° to 50° from the plane of the disc. Even at distances of several centimetres these points were still bright and well defined. These cannot be due to luminescence from grains as this would be far too weak to be visible to the naked eye. These beams of scattered light have implications for both scattering mechanisms. Multiple reflections scattering within the chamber will result in signal degradation and the effect of these beams of reflected laser light travelling across the surface of the disc and stimulating neighbouring grains is likely to be significant.

The analysis of two evenly covered feldspar discs shows the effect of scattering during measurement. Evenly covered discs were used as the results from numerical modelling show that the analysis of evenly covered discs should result in more scatter than the analysis of sparsely covered discs. Both images show an initial peak as well as a gradient through the results (Figures 5.33 and 5.34). These features are consistent with the predictions from numerical modelling and for this reason the presence of these features is assumed to be a reliable indicator for the presence of scatter during measurement.

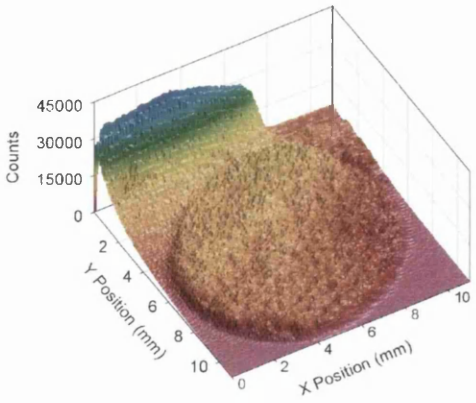

Figure 5.33: *Scan of evenly covered disc, disc 1*

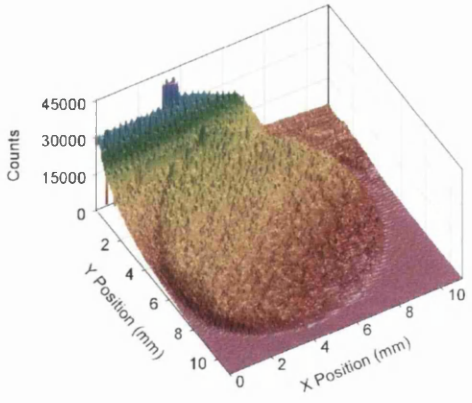

Figure 5.34: *Scan of evenly covered disc, disc 2*

Black opaque plastic was used to cover the interior of the chamber to reduce the possibility of specular reflection. The results of the analysis of an evenly covered feldspar disc, conducted with the black opaque plastic covering the surfaces of the chamber, are shown in Figure 5.35. The scan begins with the laser already on the disc and so only part of the disc is shown in the result. In the early stages of the measurement a large signal is detected which is consistent with scattering. The large initial signal results as signal is drained from all parts of the disc through scattering. This results in the depletion observed nearer the end of the measurement. The measured signal decreases during the measurement, leading to a gradient through the results. Both of these effects were predicted by numerical modelling and indicate that scattering occurs during measurement. This means that blackening the walls of the chamber does not eliminate the effects of scatter. Grain-to-grain scatter, of the type considered during numerical modelling, still occurs and appears to be the dominant scattering mechanism. The reduction in reflections around the chamber does not significantly decrease the effects of scatter.

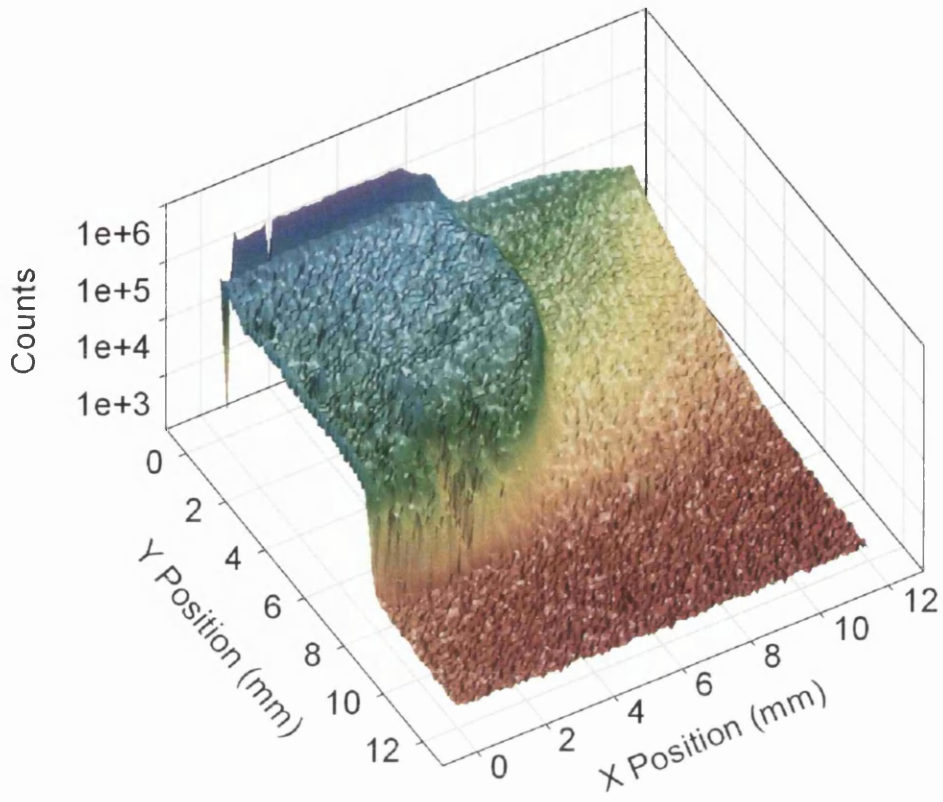

Figure 5.35: *Scan on 1 kGy irradiated feldspar after blackening of chamber*

In order to reduce scattering from the surface of the disc, the 1 kGy feldspar grains were dispensed onto a square glass substrate (10 mm by 10 mm) instead of a metal disc. The grains were dispensed after irradiation to ensure that the glass did not produce any luminescence signal. The sample holder and areas of the chamber were then covered in black foam material. These modifications were designed to ensure that as the laser illuminated the grains any laser light which was not absorbed by the grain would pass through the substrate and be absorbed by the black material which is a poor light reflector. The grains will still scatter the light through refraction and internal reflection but the reflection from the substrate should be reduced. The foam

material covering the reflecting surfaces in the chamber should also absorb any light reflecting around within the chamber. The effect of scatter is still clear in the results obtained with the equipment in this configuration (Figure 5.36). A large signal is obtained initially and the measured signal decreases throughout the measurement, as predicted by numerical modelling. This steep fall in the stimulated signal throughout the measurement is likely to be due to scatter. As the experiment was unsuccessful glass was not used as a substrate in any further experiments.

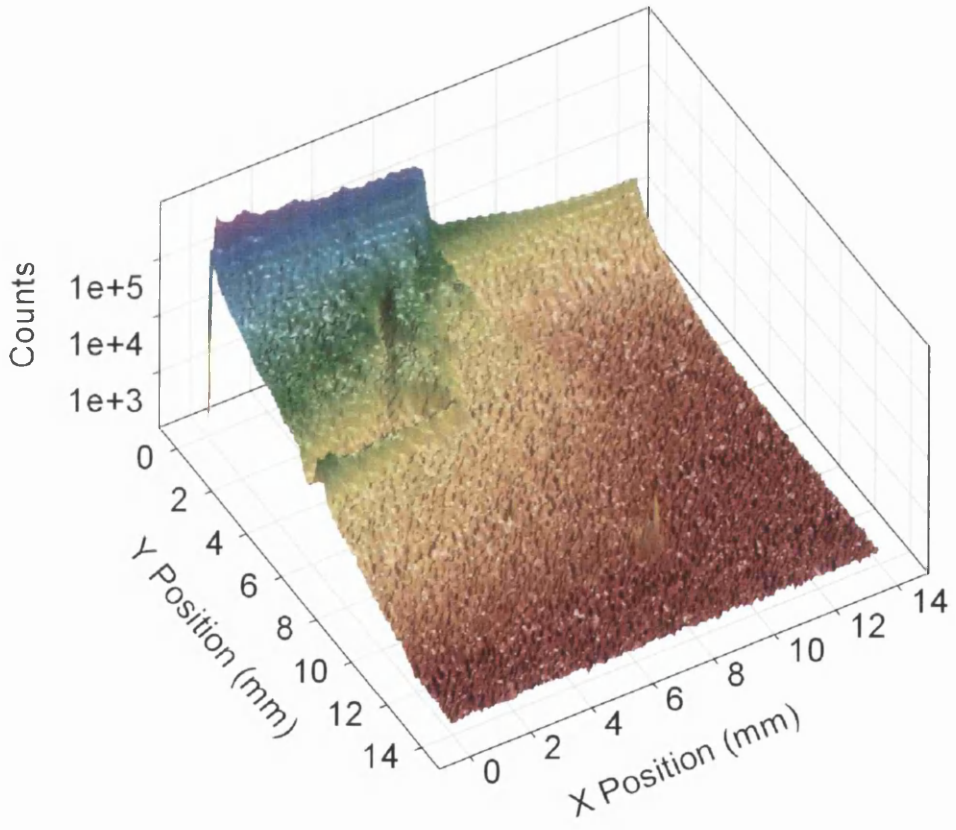

Figure 5.36: *Scan on 1 kGy irradiated feldspar on glass substrate*

An attempt was made to limit the effect of grain–to–grain scatter by covering the grains in silicone grease after they had been dispensed. The expectation was that the higher refractive index of the silicon grease when compared to air would reduce reflection and hence the amount of grain-to-grain scatter. The results show that scattering still occurs (Figure 5.37). The two features predicted by numerical modelling and observed earlier (Figures 5.33, 5.34, 5.35, 5.36) are still visible. Covering the grains in silicon grease has not reduced or eliminated grain-to-grain scatter.

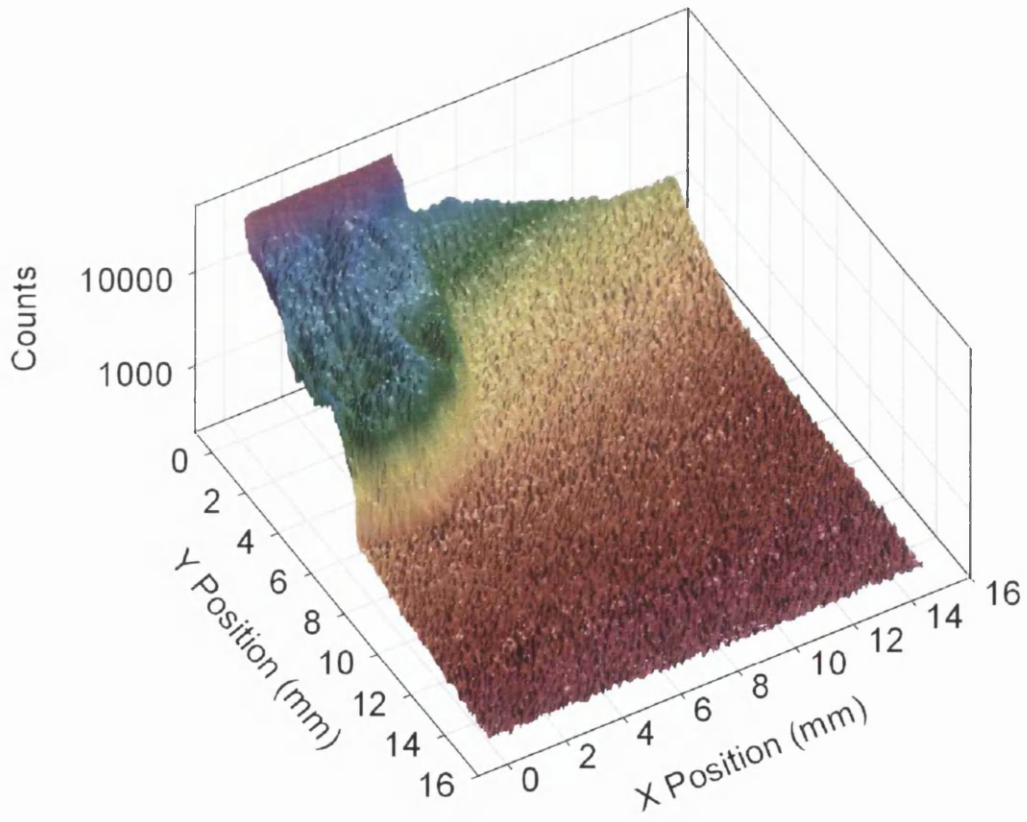

Figure 5.37: *Scan of 1kGy irradiated feldspar covered in silicon grease*

To assess the effectiveness of putting the grains into pits a disc with five pits was used (Figure 5.38). 1 kGy feldspar grains were dispensed into the pits and the disc was scanned using the IR laser (Figure 5.39). The purpose of the experiment was to conduct a qualitative investigation into scatter, and not to measure single grains, and so each pit contained several grains. In a routine experiment using this form of sample presentation a large number of pits would be used with one grain in each pit. Only four of the five pits were scanned. The fifth pit was not measured in order to provide a source of luminescence that had been stimulated by scattered light. The results do not show either of the features used to indicate the presence of scatter. The measured signal is not significantly higher in the initial stages of measurement and the signal does not decrease significantly as the measurement progresses. Although the signal from each pit seems to decrease with measurement this is due to the relative numbers of grains in each pit. There are no indications that scatter occurs.

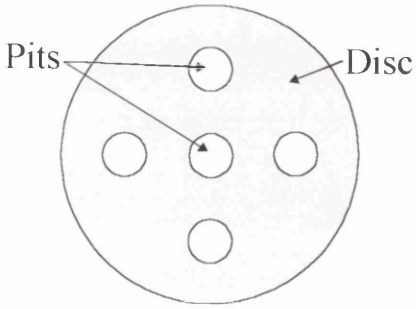

Figure 5.38: *Diagram of disc*

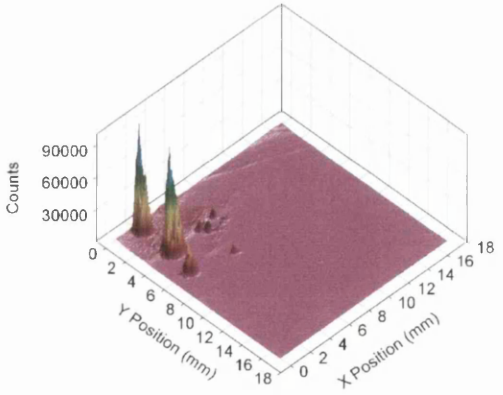

Figure 5.39: *Scan of 1 kGy irradiated feldspar dispensed onto disc with pits.*

5.4 Suggestions for further work to reduce scatter

Unfortunately it has not been possible to solve the problems presented by laser scatter while using evenly covered discs. It is likely that a change in the method of sample presentation will be necessary. Despite several attempts to counter the effect of laser scatter it seems the only remaining option is to present the grains within pits in the disc. In order to achieve this effectively consideration should be given to the size of the pits as dispensing grains into pits in the disc would be likely to present a new set of problems. Ideally the pits should be shallow enough to ensure that discs could be dispensed by wiping grains across their surface without the possibility that two grains could be found in the same pit. However, the pits should also be deep enough that the grain will be entirely contained within the pit, eliminating the possibility of laser scatter across the surface of the disc.

It should be possible to satisfy both of these conditions by machining a disc with shallow pits and, after the grains have been dispensed, using a mask to prevent scatter (Figures 5.40, 5.41).

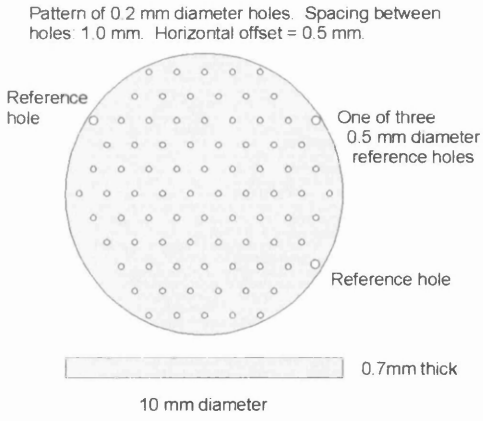

Figure 5.40: *Disc containing pits*

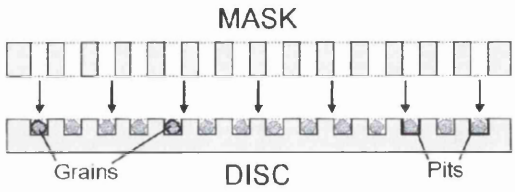

Figure 5.41: *Disc and mask*

This approach has never been used in this manner to overcome the problems of scattering and sample dispensing but should be achievable as long as the mask and disc can be aligned. By using different masks it may be possible to experiment with different grain spacings. For example, a mask which blocked off every second pit on the disc underneath would have the effect of doubling the grain spacing.

Illumination is provided from an angle and so the pits must be shallow enough to allow the laser to reach the bottom and illuminate the grain. However, it should also be noted that even if the grain is not directly illuminated by the laser it is possible that reflection from the walls of the pit may be sufficient to illuminate the grain. To reduce the effect of any limitation resulting from the depth of the pit illumination could be provided from directly above the sample, or at least from an angle closer to the vertical. The most obvious drawback with this approach would be the need to ensure that the laser assembly does not obstruct the photomultiplier tube and inhibit the measurement of the luminescence signal. One possible solution could be to use fibre optics. By focussing the laser beam into a fibre optic and positioning the end of

the fibre optic above each pit during illumination it may be possible to direct light onto each grain without obstructing the photomultiplier tube.

By using a fibre optic bundle it may also be possible to direct several lasers into the chamber. Using this configuration it may be possible to mount several lasers of different wavelengths far from the equipment, removing the need for mounting lasers and lenses directly onto the chamber. However, both approaches are worthy of further investigation. Connecting lasers and lenses directly onto the chamber could result in problems with vibration. Accurately maintaining the position of a 20 μm laser spot when the beam path is several centimetres long could present problems if the system is vulnerable to any kind of vibration. The fibre optic approach requires a solution to a different problem, that of coupling the laser efficiently to the fibre optic. This could be challenging, especially if the laser involved was not specifically designed for this kind of arrangement.

Whatever approach is employed it is important that the beam is well focussed as with a small laser spot it is very difficult to resolve grains which are not well separated. Even if the grains are contained within pits in the disc the laser spot should still be as small as possible to ensure that the laser beam only enters one pit at a time. The size of the laser spot could determine the smallest possible separation of pits on the disc which, in turn, will have implications for the number of samples that can be analysed by the system during each measurement. The size of the disc will also have implications for the number of samples that can be analysed. The single grain system

could measure discs far larger than the standard 10 mm diameter which have been used for all preliminary measurements. The number of grains (or pits) which can be presented on a single disc follows an r^2 dependence where r represents the radius of the disc. For this reason the use of larger discs would dramatically increase the throughput of the system. Consideration should also be given to making the discs square instead of circular. This would greatly simplify the cropping of the image during data analysis. The four corners of the square could also make it easier to compare images accurately.

5.5 Summary

The analysis using a disc with five pits is the only result which does not show evidence of scatter during measurement (Figure 5.39). Analyses conducted on evenly covered discs consistently show the effects of scatter. Blackening the interior of the sample chamber, modifying the substrate and using silicone grease to cover the grains do not significantly reduce the effect of scatter during measurement. The two features predicted by the numerical modelling, namely an initial peak followed by a gradient through the results, are observed in every analysis of an evenly covered disc. This suggests that it is not possible to analyse discs which are evenly covered in grains without encountering the problem of laser scatter.

In some cases the initial peak is more pronounced because the scan began when the laser spot was already on the disc (Figures 5.35-5.37). As the laser is switched on, the grain it strikes will be entirely surrounded by irradiated grains, which will respond strongly to stimulation. As the measurement progresses and the laser rasters across the disc, many of the grains will already have been bleached and so the signal will not be as large. This is why the distinctive peak appears at the beginning of the measurement, continuing throughout the first few raster lines of the scan.

Using pits to hold the grains during measurement will mean that the ability to image individual grains will become limited and dispensing samples may become more time consuming. For this reason the performance of the single grain instrument when applied to evenly covered discs should be evaluated.

In the next section mixtures of irradiated and unirradiated feldspar grains are used to simulate natural mixed systems. The mixtures are analysed to determine whether the single grain instrument is capable of identifying mixed populations of grains.

Chapter 6: Detection of mixed feldspars

6.1 Numerical modelling of mixed grain measurements

In order to better understand results obtained through the analysis of feldspar mixtures a program, Dwalen4, was written in POWER BASIC (Appendix C) to simulate the analyses and model the expected results. The program models the analysis of a mixed sample containing both irradiated and unirradiated grains by modelling one measurement on the mixed sample and a second measurement after the sample has been entirely bleached and reirradiated. The second measurement can then be used to normalise the result from the first. It is important that the effect of laser scatter on these results is understood as simple normalisation of two scans of the same disc would not account for the effect of laser scatter. If one scan was conducted on a sample in which some grains were unirradiated, laser scatter would produce a result which may not be effectively normalised by the result obtained after complete irradiation.

Dwalen4 uses the same principles as the program used to model the effect of laser scatter during measurement in section 5.2. Both programs generate matrices of numbers which represent the luminescence signal contained within each grain. In Dwalen4 two sets of matrices are used. The first set simulates the initial measurement. The second set simulates the measurement carried out to normalise the first reading. To represent real grain distributions the numbers in the matrices are randomly generated over a range from 100 to 1000000. In both the first and second sets the matrices are filled with the same numbers as they represent the same sample

in separate measurements. Unirradiated grains are represented by zeroing a proportion of the bins in the first matrix. This proportion is directly related to the number of unirradiated grains within the mixture. After "measurement" any bin in either set which contains a number less than 100 is emptied and filled with a randomly generated number with a range of 100 to 200. This is done to provide a realistic data set which accounts for background noise.

The effect of scatter is most apparent when using evenly covered discs and so measurements are simulated assuming evenly covered discs. However, it is also possible to simulate measurements involving up to five circular areas with different diameters. It is also assumed that scatter occurs from each point on the sample as it was shown in chapter 5 that this most accurately simulates the effect of scatter within the chamber.

The output of the program includes two "test" matrices which show the initial content of both matrices before measurement (Figures 6.1 and Figures 6.2) as well as the results of both simulated measurements (Figures 6.3 and Figure 6.4).

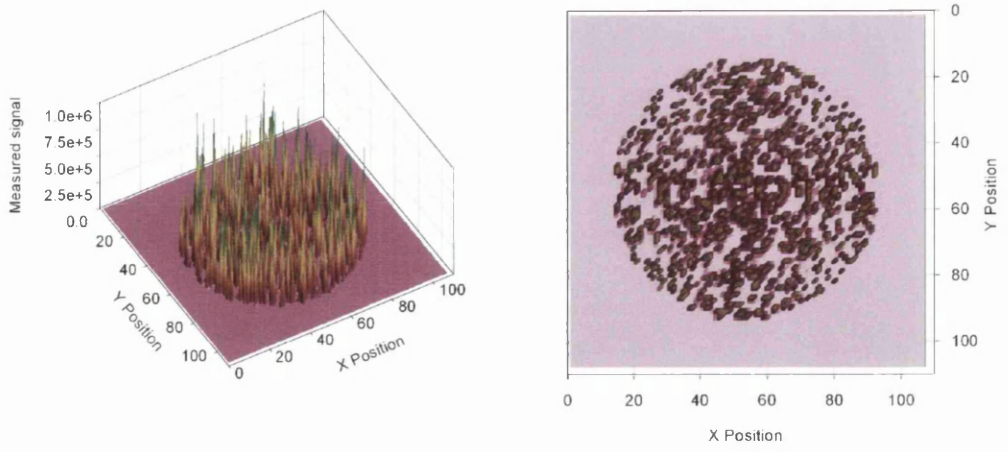

Figure 6.1: *Test matrix representing 20% irradiated mixture before first measurement*

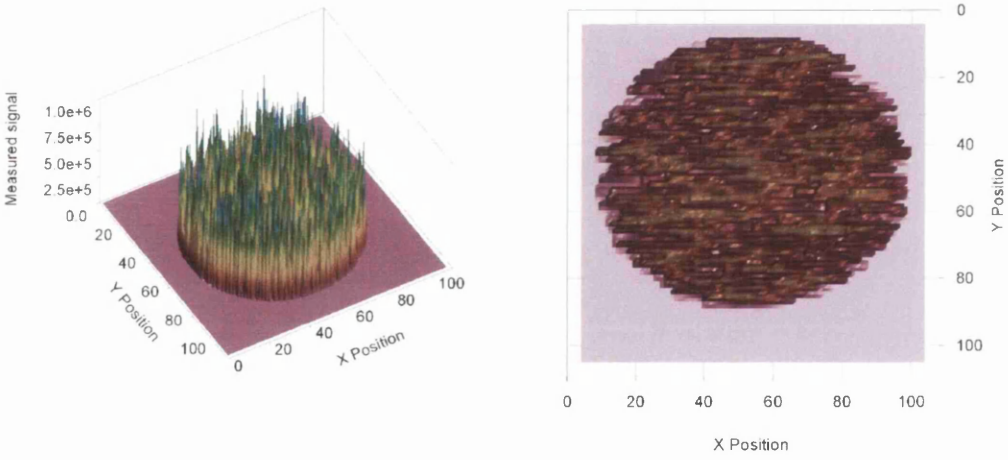

Figure 6.2: *Test matrix representing sample after 100% irradiation and before normalisation measurement*

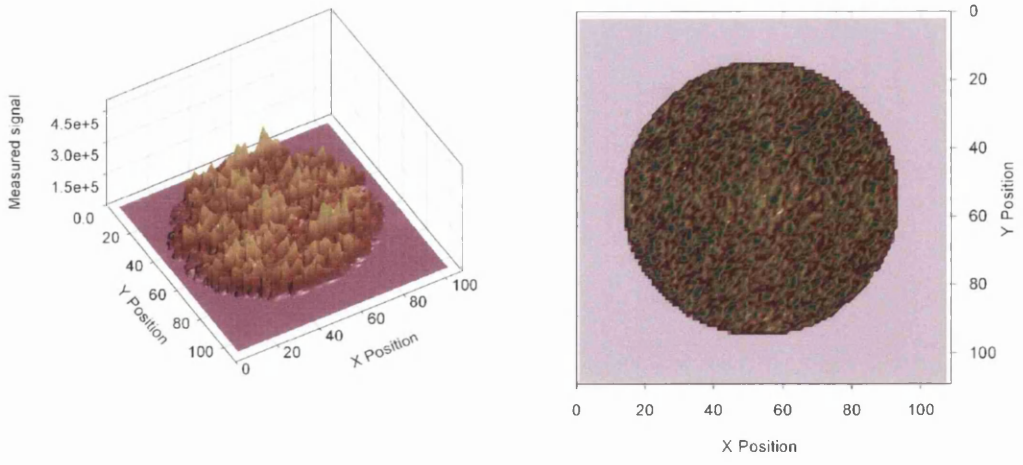

Figure 6.3: *Simulated results from first measurement of 20% irradiated mixture*

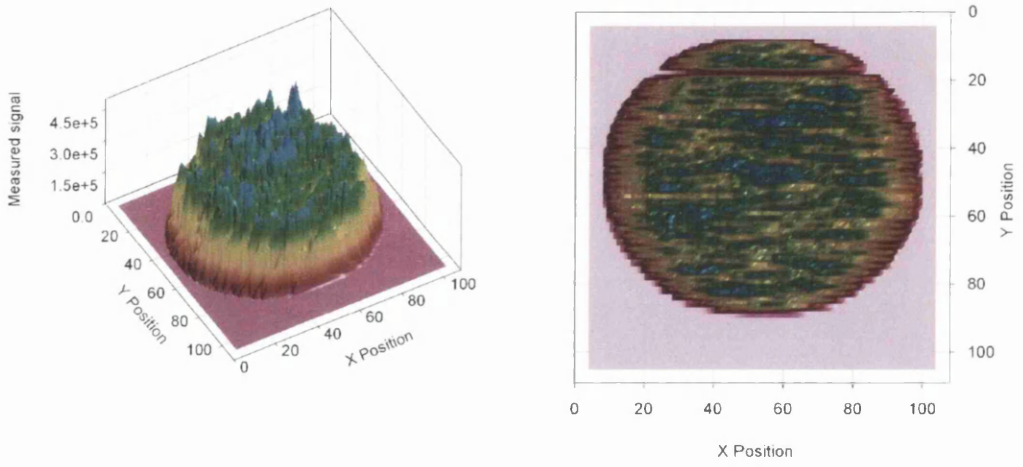

Figure 6.4: *Simulated results from normalisation measurement*

After the results have been generated the count from each point on the first measurement is plotted against the count from the same point on the second measurement (Figure 6.5). A mixture of irradiated and unirradiated grains should be indicated by two distinct linear scatters of data points. One linear scatter, with a gradient of one, corresponding to irradiated grains and the other, with a gradient of

zero, corresponding to unirradiated grains. The expected result is clearly shown using the test matrices for the measurements (Figure 6.6).

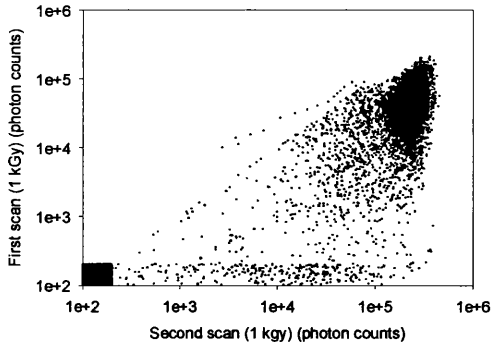

Figure 6.5: *Results from first simulated scan of 20% irradiated feldspar plotted against results from normalisation scan*

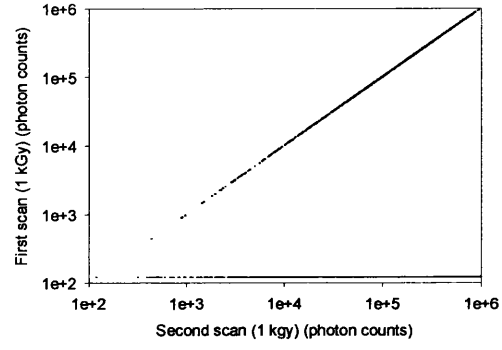

Figure 6.6: *Results from first test set plotted against results from second test set*

Results produced using the model are also plotted after normalising the initial measurement using the second measurement. A plot of the ratios of the first measurement divided by the second measurement against the brightness of the luminescence signal during the second measurement also provides information about the stored doses in the individual grains (Figure 6.7). A mixed sample where the irradiated grains have the same dose as the normalisation dose should produce a graph with two lines, or at least two clusters of points, corresponding to a ratio of one and a ratio of zero. However, because there is no luminescence signal in unirradiated grains during the initial measurement a line of negative gradient results when this constant is divided by the variable signal from the normalisation measurement and the ratio is plotted. This is clear from the normalised results produced using the test matrices (Figure 6.8).

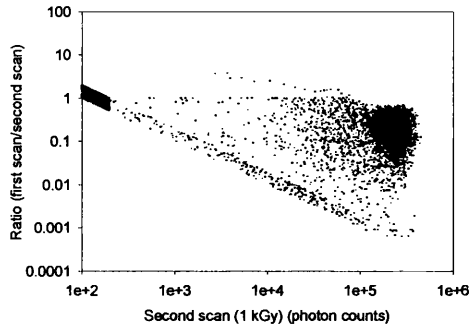

Figure 6.7: *Ratio of two results plotted against results from second scan*

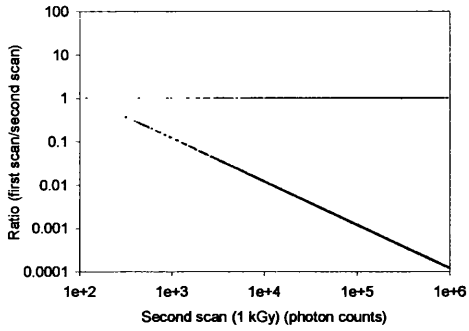

Figure 6.8: *Ratio of results from test sets plotted against results from second test set*

The distribution of stored doses present within the sample is shown using a histogram of the normalised results (Figure 6.9).

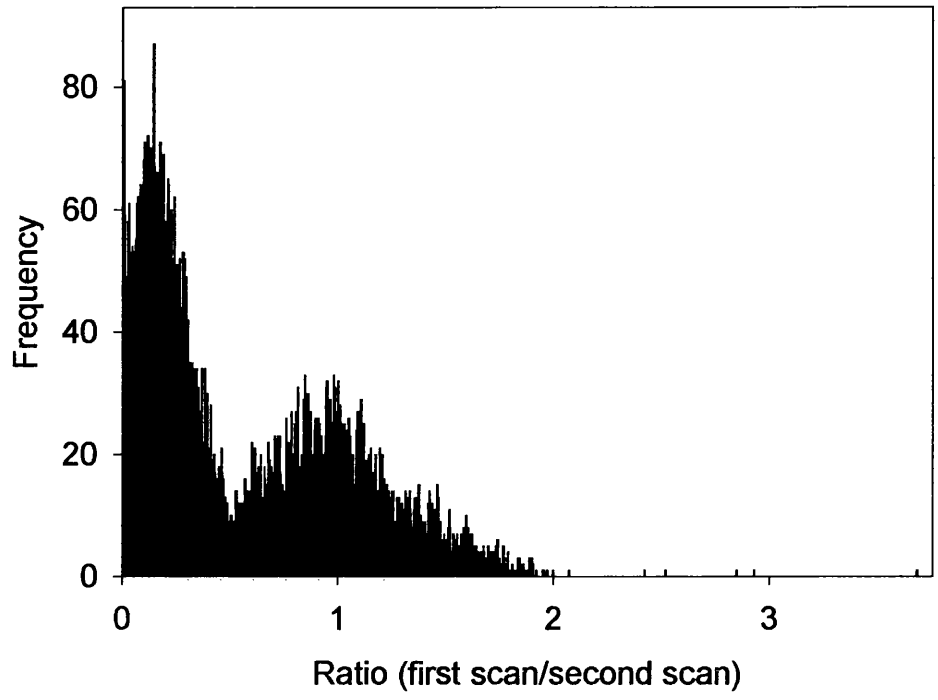

Figure 6.9: *Histogram of normalised simulated results from 20% irradiated mixture*

Modelling the analysis of samples containing 100%, 50%, 10% and 1% irradiated grains simulates the expected results and these results can be compared to those produced experimentally.

Plotting the two measurements against each other for an entirely irradiated sample produces a linear scatter with a gradient of one (Figure 6.10). As the concentration of irradiated grains is decreased a second linear scatter with a gradient of zero appears (Figure 6.13). When the concentration of irradiated grains is decreased to 10% the linear scatter with a gradient of one is no longer present (Figures 6.16, 6.19). The results show the scatter with a gradient of zero as well as a spread of data points

corresponding to a high signal on the second measurement. In an entirely unirradiated sample only the linear scatter with a gradient of zero is present (Figure 6.22). The same effect is observed when he ratio of the two measurements is plotted against the signal from the second measurement. In an entirely irradiated sample a scatter with a gradient of zero is produced which corresponds to irradiated grains (Figure 6.11). In a 50% irradiated sample a second linear scatter of data points with a negative gradient of one is present, corresponding to unirradiated grains (Figure 6.14). As the concentration is reduced to 10% or less the line no longer appears and a spread of data points is present (Figure 6.17, Figure 6.20). In an entirely unirradiated sample only the linear scatter with a gradient of negative one is present (Figure 6.23).

By plotting the results from the second graph in a histogram it should be possible to identify the populations of grains within the samples. Plotting the simulated results from the irradiated sample shows that most data points correspond to a ratio of one (Figure 6.12). As the concentration of irradiated grains is reduced to 50% the histogram broadens (Figure 6.16) and at lower concentrations splits to show two populations with ratios of zero and one. At lower concentrations of irradiated grains the number of data points which correspond to a ratio of zero increases (Figures 6.19 and 6.22). In the sample which is unirradiated the number of data points corresponding to a ratio of one is very small. These points result from areas containing no "grains" and occur as background signals in each measurement are divided by each other. In many of the results (Figures 6.10-11, 6.13-14, 6.16-17, 6.19-20) there are points which do not conform to the general trend. These few points are not significant as the total data set consists of 10000 such points.

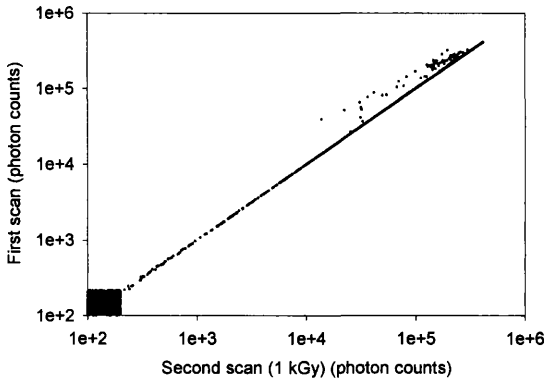

Figure 6.10: *Results from first simulated scan of irradiated feldspar plotted against results from second simulated scan*

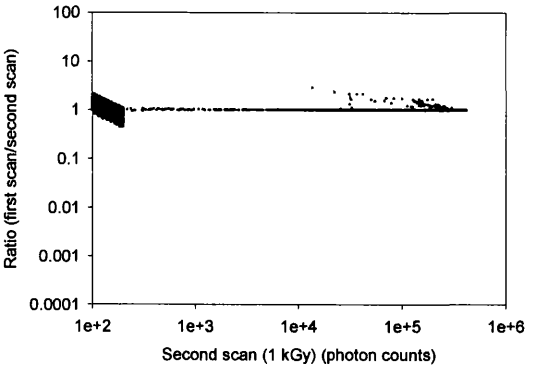

Figure 6.11: *Ratio of two simulated results plotted against results from second simulated scan*

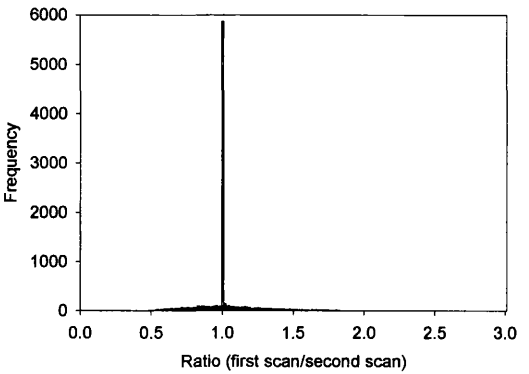

Figure 6.12: *Histogram of simulated normalised results from 1 kGy irradiated feldspar*

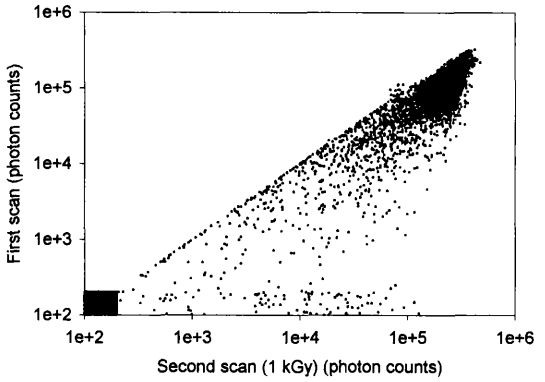

Figure 6.13: *Results from first simulated scan of 50% irradiated feldspar plotted against results from second simulated scan*

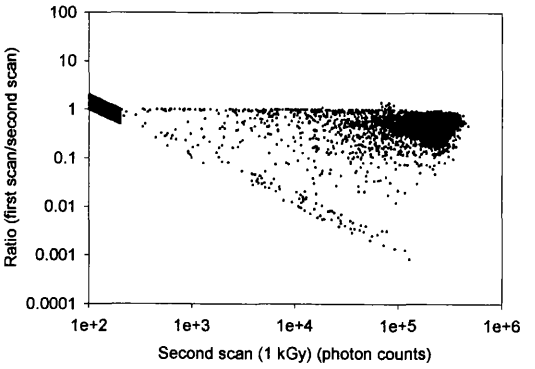

Figure 6.14: *Ratio of two simulated results plotted against results from second simulated scan*

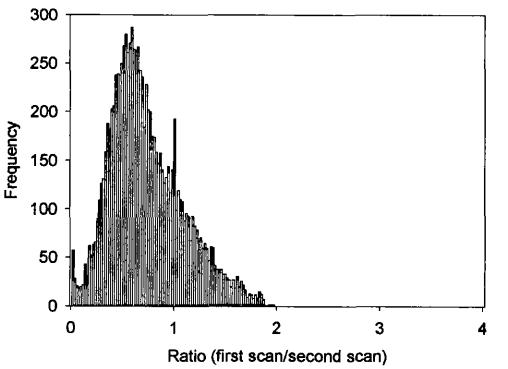

Figure 6.15: *Histogram of simulated normalised results from 50% irradiated feldspar*

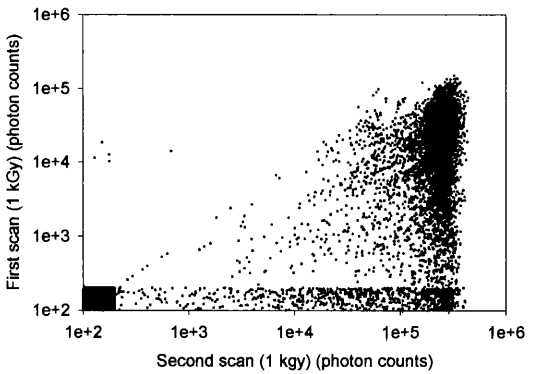

Figure 6.16: *Results from first simulated scan of 10% irradiated feldspar plotted against results from second simulated scan*

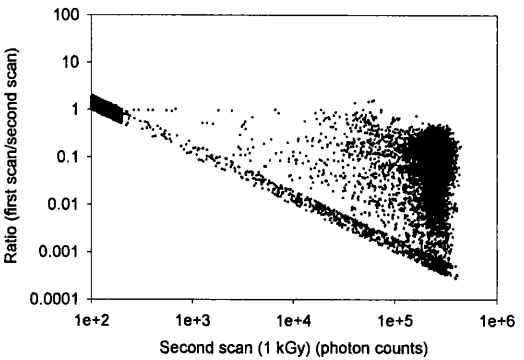

Figure 6.17: *Ratio of two simulated results plotted against results from second simulated scan*

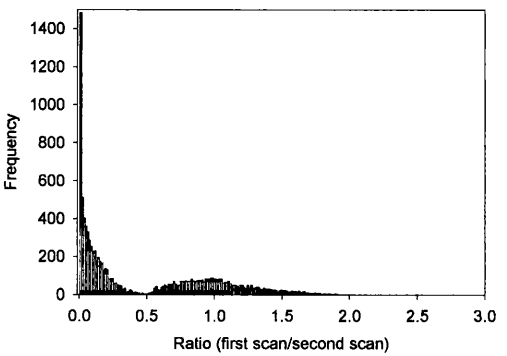

Figure 6.18: *Histogram of simulated normalised results from 10% irradiated feldspar*

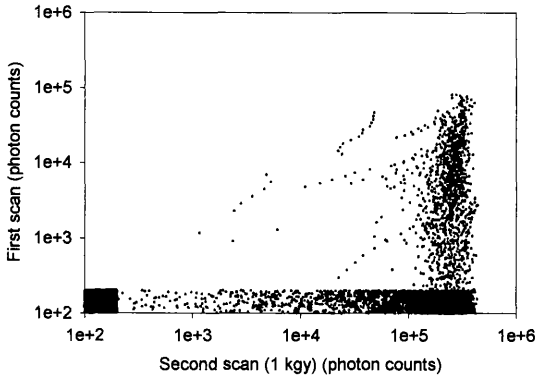

Figure 6.19: *Results from first simulated scan of 1% irradiated feldspar plotted against results from second simulated scan*

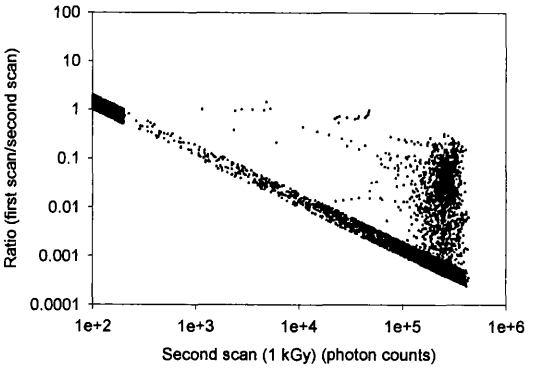

Figure 6.20: *Ratio of two simulated results plotted against results from second simulated scan*

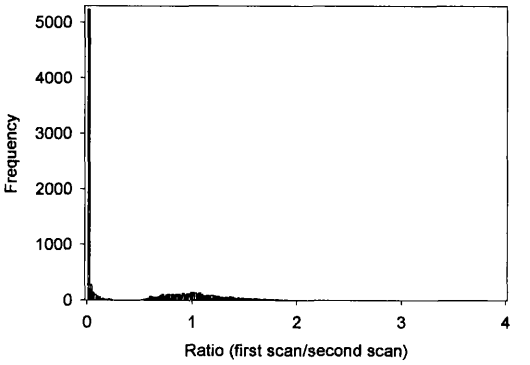

Figure 6.21: *Histogram of simulated normalised results from 1% irradiated feldspar*

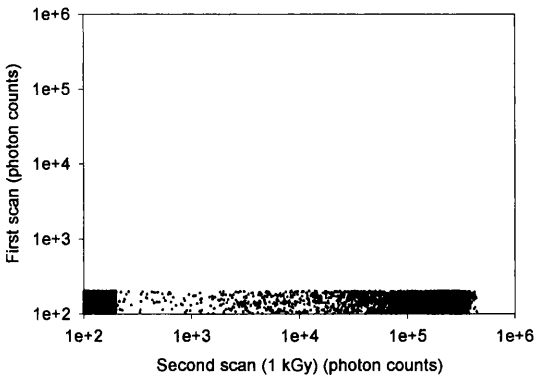

Figure 6.22: *Results from first simulated scan of unirradiated feldspar plotted against results from second simulated scan*

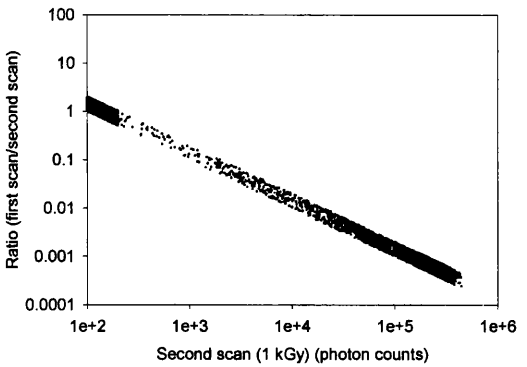

Figure 6.23: *Ratio of two simulated results plotted against results from second simulated scan*

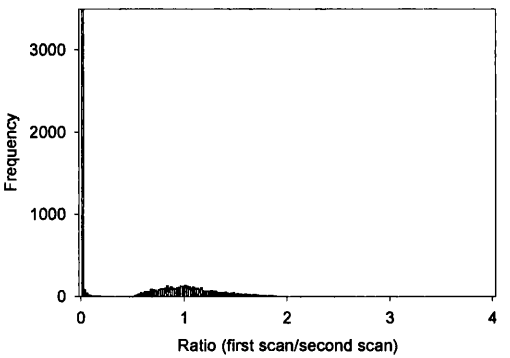

Figure 6.24: *Histogram of simulated normalised results from unirradiated feldspar*

The above graphs (Figures 6.10-6.24) show the types of results which can be expected when analysing irradiated, unirradiated and mixed samples. These simulated results show that it should be possible to distinguish between mixed samples and samples which are entirely irradiated or entirely unirradiated. However, areas without grains produce a background signal on both measurements, resulting in a normalised ratio of one. Unless an effort is made to exclude these areas from the analysis then even in entirely unirradiated samples a small number of data points will still produce a result which appears to indicate that irradiated grains are present.

In the next section the results produced using this model are compared with the results produced by analysing samples containing known concentrations of irradiated grains.

6.2 Analysis of mixed feldspars

In this section mixtures of irradiated and unirradiated grains of F1 feldspar are analysed in order to test whether the single grain system is capable of distinguishing between irradiated and unirradiated grains in a mixed system. The analysis of mixtures of 1 kGy irradiated F1 feldspar and unirradiated F1 feldspar simulates a natural mixed system. However, a natural system may contain a range of stored doses (all of which would probably be much lower than 1 kGy). Before the single grain system can be applied to samples from a natural environment where mixing or partial bleaching has occurred it should first be successfully applied to samples containing large, known doses mixed in known concentrations.

All analyses were carried out using the IR laser scanning over 15 mm by 15 mm squares. This results in over 25000 data points in each scan. Between measurements the discs were bleached for several hours in artificial daylight to remove any possible residual signal (although F1 feldspar is known to contain a small unbleachable residual signal). A preliminary scan (using irradiated grains sprinkled onto an disc entirely covered in unirradiated grains) illustrates the feasibility of measurements on mixed samples using the single grain system. Five different mixtures of different concentrations are analysed. 100%, 50%, 10%, and 1% irradiated mixtures were prepared as well as one mixture which contained no irradiated grains.

The discs of mixed feldspar were analysed before being bleached and reirradiated with a 1 kGy dose and reanalysed. The first measurement was then normalised through division by the second measurement. Any shift in the position of the disc was compensated for during analysis. Significant features (e.g. the edge of the disc or large peaks in the luminescence signal) on the two images were compared to determine the shift. The discs were observed to have shifted in position by between 0.1 and 2 mm between measurements. The x and y position data were then altered to compensate for this shift.

The count from each point on the first measurement was plotted against the count from the same point on the second measurement. A mixture of irradiated and unirradiated grains should be indicated by two distinct linear scatters of data points. One linear scatter, with a gradient of one, corresponding to irradiated grains and the other, with a gradient of zero, corresponding to unirradiated grains as shown in Figure 6.6. A plot of the ratios of the first measurement/second measurement against the brightness of the luminescence signal during the second measurement also provides information about the stored doses in the individual grains. A mixed sample should produce a graph with two lines, or at least two clusters of points, corresponding to a ratio of one and a ratio of zero as shown in Figure 6.8. The distribution of stored doses present within the sample is shown using a histogram of the results.

Scanning a disc covered in unirradiated feldspar grains with irradiated grains sprinkled onto it shows peaks. It is reasonable to assume that these peaks have resulted from irradiated grains (Figure 6.25). This shows that the system is capable of detecting irradiated grains among unirradiated grains.

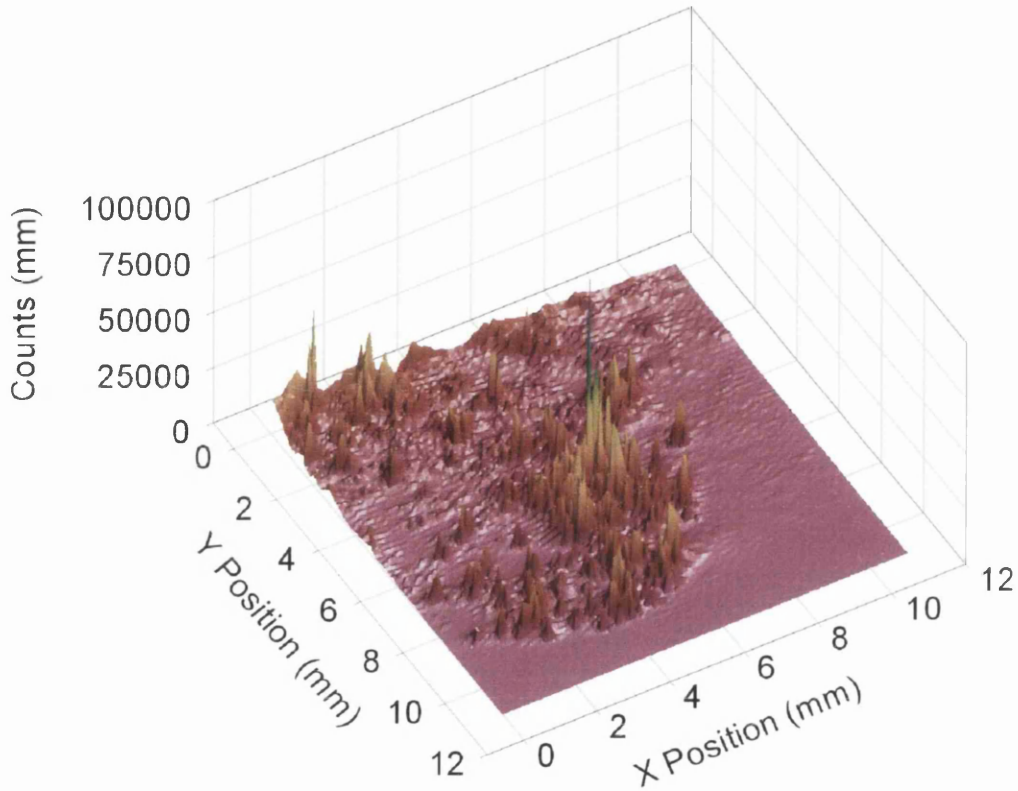

Figure 6.25: *Initial scan of disc with irradiated/unirradiated grains*

Various discs of F1 feldspar were used to establish whether the single grain instrument can detect inhomogeneous stored dose distributions. A disc of 1 kGy irradiated feldspar was analysed (Figure 6.26). The disc was then reirradiated with 1 kGy and the measurement procedure was repeated (Figure 6.27).

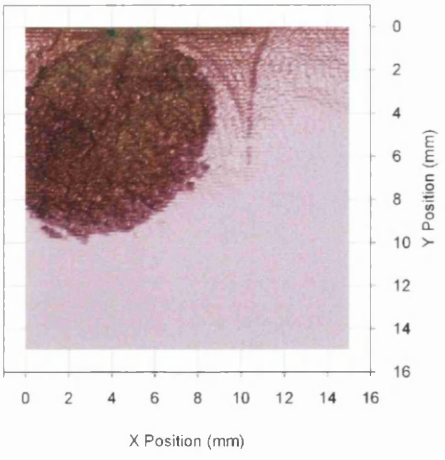

Figure 6.26: *Scan of 1 kGy irradiated feldspar*

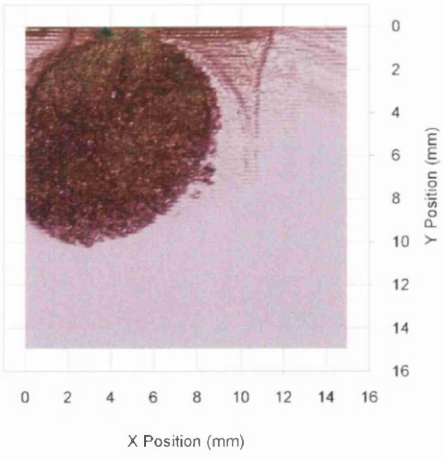

Figure 6.27: *Repeat scan of 1 kGy irradiated feldspar for normalisation*

The count from each point on the first measurement was plotted against the count from the same point on the second measurement (Figure 6.28). This graph shows a line with a gradient of one. This is consistent with the results obtained using numerical modelling (Figure 6.10). The expected result is confirmed when the ratio of the two measurements is plotted against the brightness of each point on the second scan (Figure 6.29). This is also consistent with the results from numerical modelling and shows that the ratio of the two results remains constant although the brightness varies by four orders of magnitude. The histogram shows that there is only one population of grains within the results (Figure 6.30). These exhibit a ratio of one when normalised, which corresponds to a dose of 1 kGy. In other words, these results are entirely in agreement with those produced using numerical modelling and show that the equipment produces the "correct" result when presented with an entirely homogeneous sample containing a high stored dose.

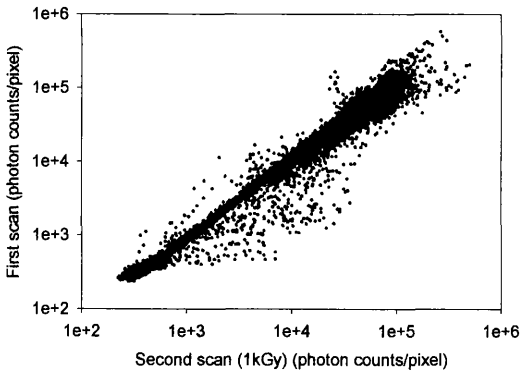

Figure 6.28: *Results from first scan plotted against results from second scan*

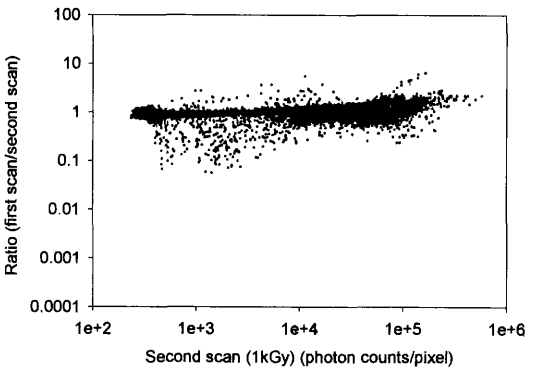

Figure 6.29: *Ratio of two results plotted against results from second scan*

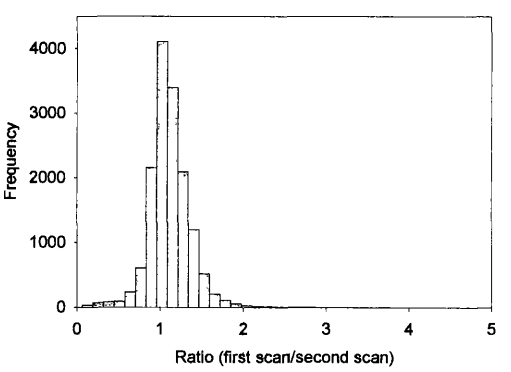

Figure 6.30: *Histogram of normalised results from 1 kGy irradiated feldspar*

The results from measurements of blends of irradiated and unirradiated feldspar, containing concentrations of 50%, 10% and 1% irradiated feldspar, as well as a sample containing only unirradiated grains, are shown in Figures 6.31–6.42.

In each case the results from the first reading are plotted against the results from the second reading, as described above. The results (Figures 6.31, 6.34, 6.37, 6.40) show that in the two extreme cases where the sample contains only irradiated or unirradiated grains the data points form lines with the expected gradients of one and zero respectively (Figures 6.28, 6.40). When the results from the 50% blend (Figure 6.31) are compared with the results from numerical modelling they are found to be in broad agreement. However, in the cases where 10% and 1% blends were used the results are not consistent with numerical modelling. A linear scatter with a gradient of zero is not observed on these results and instead the data are more suggestive of a linear scatter with a gradient of one. (Figures 6.34, 6.37)

Plotting the ratios of the first measurement and the second measurement against the brightness of the luminescence signal during the second measurement produces a linear scatter of negative gradient for samples containing 50%, 10% and 1% irradiated grains (Figures 6.32, 6.35, 6.38). This is broadly consistent with the results of numerical modelling (Figures 6.14, 6.17 and 6.20) but the results from real analyses are not as unambiguous as those from numerical modelling. However, the results from mixed samples do exhibit a far greater spread than those from entirely irradiated or unirradiated samples, as would be expected when more than one population of

grains is present. The results from the sample which was entirely unirradiated (Figure 6.41) show a decreasing ratio with brightness. This effect is predicted by modelling (Figure 6.23).

As the concentration of irradiated grains is reduced the frequency distributions of the ratio of the first scan to the second scan (Figures 6.33, 6.36, 6.39, 6.42) begin to show bimodality, indicating the presence of two populations within each sample. The population of irradiated grains, which correspond to the mode at a ratio of one, begins to reduce as the concentration of irradiated grains reduces. A second peak starts to become visible at zero, which corresponds to unirradiated grains. The unirradiated sample still shows a peak with a ratio of one, which seems to imply that irradiated grains are present. However, this peak is a result of scanning areas off the edge of the disc. As these areas were entirely blank the ratio is a result of the background signal being divided by itself. This anomaly could be removed by trimming the results more effectively. The results here behave entirely as predicted by numerical modelling, showing that these histograms of this type can be used to draw definite conclusions regarding the number of populations present within a sample.

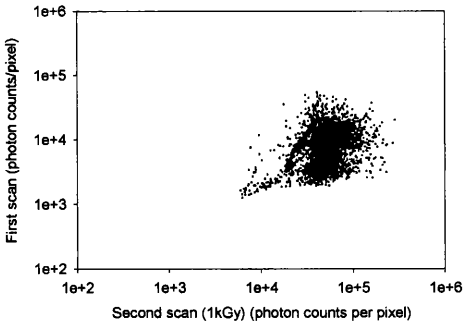

Figure 6.31: *Results from first scan of 50 % irradiated feldspar plotted against results from second scan*

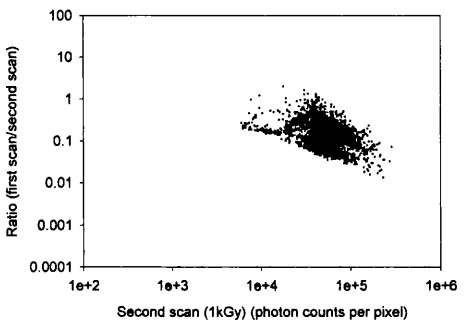

Figure 6.32: *Ratio of two results plotted against results from second scan*

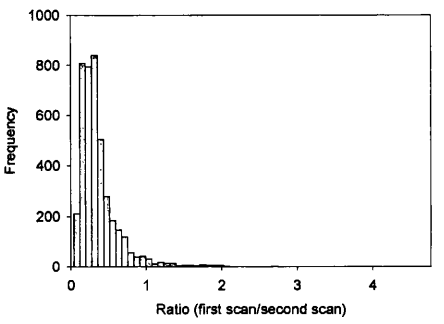

Figure 6.33: *Histogram of normalised results from 50 % irradiated feldspar*

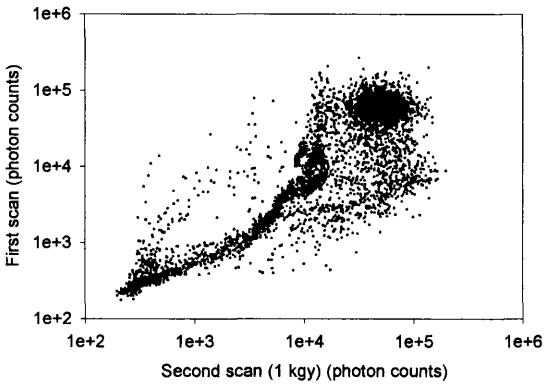

Figure 6.34: *Results from first scan of 10 % irradiated feldspar plotted against results from second scan*

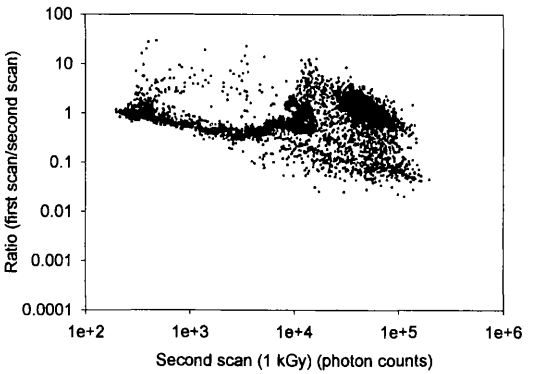

Figure 6.35: *Ratio of two results plotted against results from second scan*

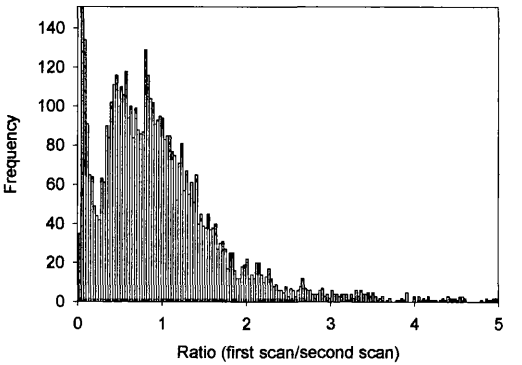

Figure 6.36: *Histogram of normalised results from 10 % irradiated feldspar*

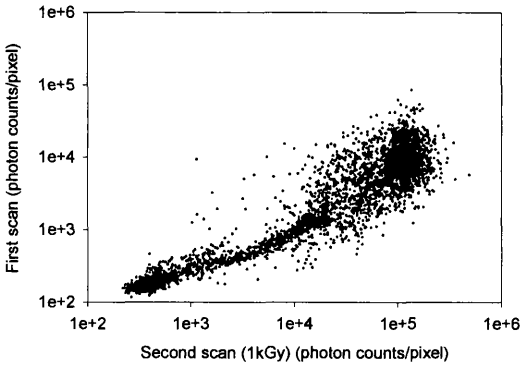

Figure 6.37: *Results from first scan of 1% irradiated feldspar plotted against results from second scan*

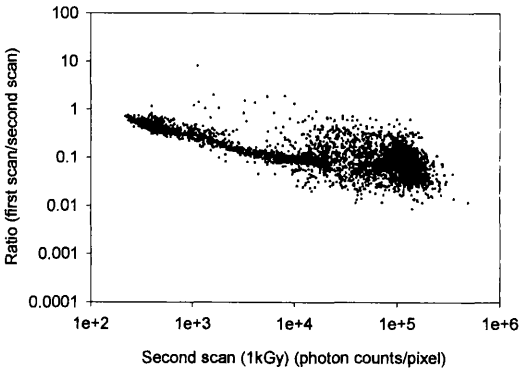

Figure 6.38: *Ratio of two results plotted against results from second scan*

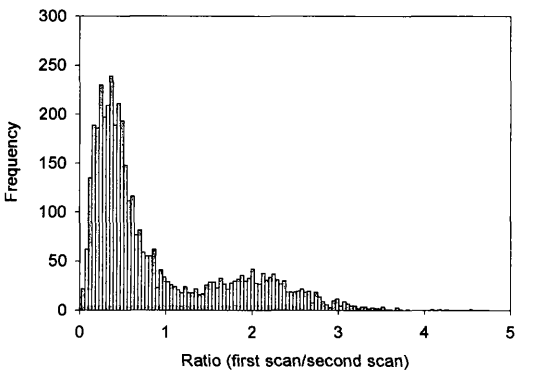

Figure 6.39: *Histogram of normalised results from 1 % irradiated feldspar*

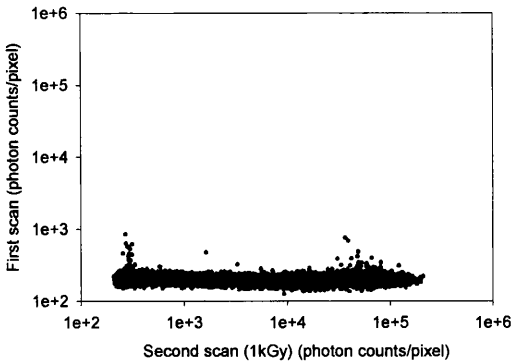

Figure 6.40: *Results from first scan of unirradiated feldspar plotted against results from second scan*

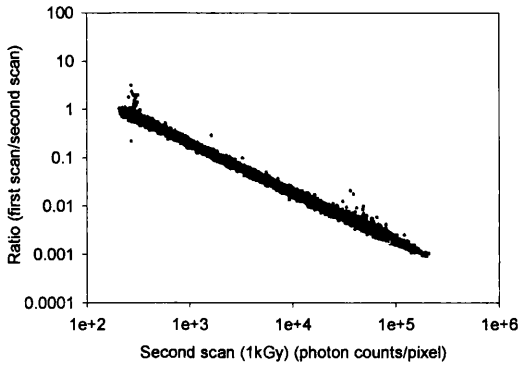

Figure 6.41: *Ratio of two results plotted against results from second scan*

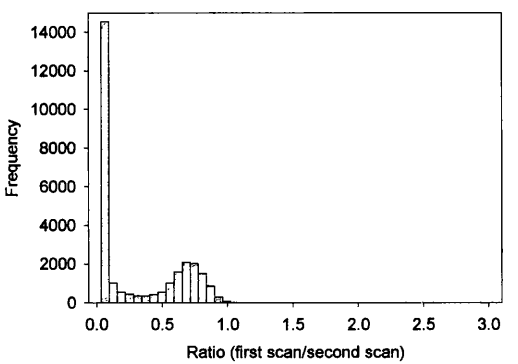

Figure 6.42: *Histogram of normalised results from unirradiated feldspar*

The foregoing results mean that the system may not yet capable of providing quantitative information about the number of grains of a particular population present within a sample. However, it may be capable of providing information about the number of populations which are present. One possible explanation for this shortcoming is slight misalignment of the two images which would account for some of the scatter in the data. Misalignment of images could be addressed by more rigorous procedures of sample analysis.

The results produced by the single grain system are in broad agreement with those predicted by numerical modelling and this suggests that the system is capable of distinguishing between mixed samples and samples that have a homogeneous dose. However, the concentration of irradiated grains in a sample cannot be determined by the system at present. By reducing the amount of scatter during measurement the results from the system would improve and the system should be capable of providing quantitative information about populations within mixed samples.

Chapter 7: Discussion and conclusions

In this thesis the potential of using scanning instrumentation coupled to focussed lasers has been explored. In the initial set-up an IR laser diode was used to produce images of feldspar grains on conventional discs to establish the basic capability of the instrument. The problem of laser scatter was investigated through numerical modelling and experiments were carried out using mixed grain populations to identify possible solutions to this problem.

The development of a scanning instrument capable of single grain measurements was initially prompted through measurements on samples from the NE Thailand "cover sands" for which competing aeolian and bioturbation origins have been proposed. Optically stimulated and thermally stimulated depth profiles for these cover sands are not in perfect agreement at shallow depths, which may be suggestive of bioturbation and heterogeneous bleaching of the "cover layer". If the mantle has indeed formed by bioturbation processes, the dose profiles can be viewed as artefacts of the mixing process. This presents a clear example of a system where single grain techniques would be valuable.

The issues raised by the Thai quartz show the need for a single grain measurement system. Preliminary measurements on the new SUERC system have shown that images of feldspar can be produced using an IR laser and that one scan removes the bulk of the measurable signal from the grains. It has also been shown that the system

is capable of detecting single grains and that the potential exists to measure doses as small as 2 Grays.

There are several issues regarding the instrumental set-up which must be addressed before the system can be routinely applied to single grain measurements. Clearly the spot size of the laser should be at least comparable to, and preferably considerably smaller than, the grains which are to be measured. At present the IR laser, which has been widely used for the single grain measurements, has a visible spot size of around 100 μm whereas grains are typically 90-150 μm in diameter.

The spot size is small enough to produce meaningful images and individual grains can be imaged if they are separated widely enough. However, ideally the system should be able to resolve individual grains which are close to each other. When the system is upgraded using a blue laser the first problem that must be resolved is the focussing of the beam. If the laser can be focussed to produce a smaller spot then this should dramatically increase the resolution of the system as well as the beam intensity. These two effects in combination should produce larger signals and clearer results.

Scattered light within the sample chamber was investigated. Although the laser is focussed on a single spot on the disc, the reflected beam may strike the walls of the chamber and be reflected back onto the disc. This means material on other areas of the disc will be stimulated by this laser light (no longer well focussed after reflection

from the disc and walls) and the signal from this material will be reduced before stimulation by the focussed laser spot. It is also possible that laser light is scattered by each grain during stimulation. This is likely to stimulate luminescence in neighbouring grains, resulting in signal depletion and loss of resolution. Numerical modelling showed that this effect will result in an initial peak in the results as well as a gradient throughout the measurement. This effect has been observed in some results. Numerical modelling also showed that on more sparsely covered discs the effect of laser scatter would not be as marked. Attempts were made, using several different approaches, to reduce the effect of scatter when measuring evenly covered discs without success. However, presenting the grains in pits within the discs eliminated the problem of laser scatter.

At present the samples are mounted on stainless steel discs. These discs could be adapted so that the grains are presented in a matrix of shallow pits. As well as solving the problem of laser scatter this may also reduce measurement time, as the system would not waste time scanning large empty spaces on the disc. This technique demands that the system has an accurate method of determining the orientation and position of the disc. One disadvantage of presenting grains within pits is that it may require greater sample preparation times which result in the samples spending more time under safelight with the associated risk of signal reduction. However, a technique could be developed which could present grains within pits in the disc without the need for long sample preparation times.

If pits were not used then the sample would be dispensed onto the disc as normal. It is likely that this would present fewer problems during sample preparation and would also mean that the problem of determining the orientation of the disc before measurement would no longer be relevant, as any change in the orientation of the disc could be compensated for during data analysis. If pits were not used, then a much smaller spot size would be required in order to resolve individual grains with confidence, and the problem of laser scatter would have to be resolved.

A further consideration related to sample presentation is that the single grain system at SUERC allows for a much larger disc size than is possible with other systems. As the number of grains that can be placed on the disc is dependent on the square of the radius, an increase in the radius of the disc would result in a large increase in the number of grains that can be measured in a single cycle, reducing the number of discs required.

Measurements on irradiated and unirradiated feldspar blends of known concentration have shown the potential of the system for measuring samples containing mixtures of grains with different luminescence characteristics. The results were broadly consistent with those produced using numerical modelling. However, it is clear that the performance of the system is not yet sufficient to allow the accurate measurement of samples from natural environments.

Almost all measurements conducted using the single grain system have been conducted using an IR laser. Feldspar responds to IR, green and blue stimulation but quartz does not respond well to stimulation by IR light and so a blue or green laser should be incorporated into the system. The IR laser could be replaced but there may be advantages to having different lasers working in parallel. It may be possible to scan initially with IR light, stimulating and bleaching any feldspar grains, and later with blue or green light which would stimulate quartz grains. This arrangement could be used to determine the quartz and feldspar content within a sample. However, there is no guarantee that bleaching feldspar with IR light would remove all the signal from the grains. The sample could be bleached with IR light and still respond to blue light afterwards. This effect has been investigated by Bannerjee et al. (2001) and the post-IR blue signal was found to be more stable than the signals obtained during both IR and blue stimulation.

At present the sample is positioned manually at the start of each measurement by aligning marks on the sample holder with the laser spot. Any variation in the start position has to be compensated for during image analysis. Ideally the sample would be reliably and reproducibly positioned before each measurement. In the present system notches on the discs are used to reproducibly position the discs before measurement.

In an improved system the disc containing the sample could be held in place using holes which would align with small pins on the sample holder. This could also provide a method of ensuring any mask used to cover the disc was aligned accurately. Three pins in a triangular configuration should be enough to ensure that the disc is reliably positioned on the sample holder. To ensure that the disc could not be placed on the holder in the wrong position or upside down the holes should not be placed in an equilateral triangular configuration. Placing the holes in a non-equilateral triangular configuration would provide only one possible position for the disc. If this system were used to position the disc on the sample holder there would also have to be a method of reproducibly positioning the sample holder under the laser. This could be done by using optical switches to cut the power to the motors as soon as they detect that the sample holder has been moved into position. Alternatively, registration holes could be used to detect the position of the disc. This is the technique used by the Risø laboratory in their single grain measurement equipment. When the laser spot shines down the registration hole reflection occurs which is measured by a photo-detector. In this way the equipment measures the position of the sample holder before measurement.

There are other possible methods of positioning the disc. Bright grains of a standard material such as CaF could be positioned on the disc. The laser could look for these grains before measurement or the signal from them could be used after measurement to register the image and account for any movement from the expected position.

One effect observed during measurements, which is certainly worthy of further investigation, is the distortion observed in the image of the disc. In some measurements the image of the circular disc is itself not circular (Figures 5.33, 5.34). This is a natural consequence of the method of illumination. As the laser shines onto the disc from an angle the laser spot on the disc surface will appear as an ellipse instead of a circle (the result of taking an angled section through a cylindrical beam). This effect could be more pronounced if the beam is not circular initially or if the disc is not horizontal on the sample holder. If the laser spot itself is an ellipse then the image will be distorted and the disc will appear to be elliptical. The images shown in Figures 4.2 and 4.3 also show some distortion. This may be because the slides which move the sample do not change direction instantly. It is likely that as the screws of the x-y stage change direction the first few turns of the motor do not actually turn the screw and move the sample. This small delay before the screw starts to move could be accounted for by sending extra pulses to the motor each time there is a change of direction. However, as this effect has not been observed during other measurements it is difficult to quantify it with confidence. When an improved laser is used in later measurements to produce clearer images, distortion may again be observed and modifications may have to be made to the program.

The distortion could be investigated and quantified to determine whether correction is possible, desirable or necessary. It is possible that as the images from all samples would be subject to this same distortion it would not present a problem during analysis. However, this would mean that discs would have to be measured in the

same position each time. If the distortion is consistent and quantifiable it may be relatively easy to correct using existing image processing software such as Idrisi32.

Focussing the laser to a small spot size is certain to result in the grain being subjected to very high intensity light. This may present problems as the response of the grain may vary according to the intensity of the incident light. Most luminescence measurements are carried out using light which is of significantly lower intensity than that of the focussed laser and so it may be necessary to model the internal behaviour of the material during illumination to ensure that assumptions about response and required measurement time are justified. It is possible that there may be practical limits on measurement time which are determined by the behaviour of single grains. It may also be necessary to construct models which take the different sizes and orientations of grains into account in order to predict the behaviour of single grains during illumination.

Incorporating an irradiator into the system would simplify many measurements. At present the sample has to be removed from the chamber for irradiation which increases the possibility of handling errors, which occur when discs are dropped or scratched during measurement. Also, as we are concerned with the measurement of single grains, it is far from ideal to move the sample between measurements as slight movement of the disc could result in grains on the disc being displaced from their initial position. By irradiating automatically, time could also be saved as the system could conduct measurements overnight. Individual measurements typically take a few

hours meaning that a run of measurements of the type required to conduct single aliquot regenerative analysis could take several days. An improved single grain instrument may also require another light source, in addition to any lasers used for stimulation, to bleach grains between measurements. If the lasers used bleach the samples effectively no such light source may be necessary but this requires further investigation.

Adding a heater plate to the sample holder would enable preheating within the chamber. This would reduce-handling and the probability of handling errors. Of greater interest is the opportunity this would provide for conducting luminescence measurements, or even irradiation, at elevated temperatures.

Heating could also be provided during measurement by coupling a CO_2 laser to the system and heating the grains individually as they are exposed to optical stimulation. CO_2 lasers emit light at 10.6 μm and this wavelength is not absorbed by impurities within grains. This would provide heating rates which are independent of impurity concentration. The use of a CO_2 laser to provide preheating prior to measurement or heating during OSL measurement has not yet been investigated and requires further investigation, particularly if a CO_2 laser is added to the system to conduct single grain TL measurements. However, there may be problems associated with illuminating a grain with visible light to induce luminescence while also using far infrared illumination to provide heating.

Although the system in its present form is not yet ready to be applied to the analysis of samples from natural environments where mixing or heterogeneous bleaching has occurred the single grain system should still be applied to problems of this type in the future. This would involve characterising the dose distributions within mixed or heterogeneously bleached samples. However, in some cases these measurements alone may not provide enough information to enable definite conclusion regarding the occurrence of mixing or heterogeneous bleaching. It may also be necessary to model mixing or bleaching processes to form expectations regarding the kind of dose distributions which would be found within the dose distributions if mixing or heterogeneous bleaching had occurred.

If the expected formation or deposition processes can be modelled effectively then an improved single grain system would be ideally suited to confirm the validity of these models. In the case of bioturbation, quantifying the degree of mixing in combination with the modelling of possible mixing processes could identify whether bioturbation has occurred. For example, by modelling the action of termites within soil as they transport sediment to build their mound, and the subsequent collapse of the mound, it may be possible to predict the distribution of grain sizes and stored doses at certain depths within a site and then test this prediction. Hence, the ability to measure the stored dose within individual grains would help to identify whether a particular sediment had been mixed.

Critique

The results presented in this thesis show the potential which exists for the measurement of luminescence from single grains of sediment. However, there are several areas which have been highlighted which could have been expanded or conducted differently. These are worthy of further investigation but in the time available for this study only a broad approach was possible.

Many of the experiments conducted in this thesis were intended to show the capability of the single grain instrument. For this reason F1 feldspar was used, as it is a standard material which is well suited to this purpose. However, it would also have been possible to use a natural sample of feldspar to test the capability of the instrument. The system could also have been fitted with a blue or green laser and used to analyse a sample of quartz from a natural environment. This would have shown how effective the instrument was when dealing with samples from natural environments. This would form a very profitable route for further research work.

One consideration throughout this research was that the system was not originally built to measure F1 feldspar. For this reason there was a reduced need to investigate the response and behaviour of F1 feldspar in as much depth as would have been required with natural samples of quartz or feldspar. However, if natural samples were chosen to test the instrument, much greater emphasis would have to be placed on establishing whether effects such as fading or recuperation present significant

problems when accurately determining dose. The effect of sensitivity changes between irradiations would also have to be considered and appropriate preheats would have to be used. These are likely to vary according to the type of material under investigation. In the determination of dose from natural samples practical considerations such as the treatment of errors and the most effective way of dealing with large datasets would also have to be taken into account.

In this investigation there were some experiments to quantify the performance of the instrumentation, and in particular the performance of the red laser. However there remain instrumental issues to be addressed regarding the current system. For example, the time taken for the laser to warm up and whether the laser spot drifts during warm up. In a larger experiment, it would have been possible to refine the design of the instrumentation and allow several different lasers to be tested to attain optimum performance.

In this thesis there has been a significant amount of modelling aimed at identifying the occurrence of scatter and minimising its effects. However, there are several possible approaches to the problem of scatter. In a more extended study it would also have been possible to model the laser scatter by examining the fundamental processes which give rise to scattering and predicting their effects. This could form the basis for a future research project.

Results were presented showing shine down curves from discs which were bleached by a stationary laser and these were used to show that scatter occurs. However, modelling could also have been used to simulate these results and this could have been very effectively combined with more detailed analysis of the shine down curves. These curves could have been deconvolved into their individual components allowing detailed comparison ad refinement. Hence, the explanation of the form of these graphs could have been more accurately and quantitatively determined and it should be possible to draw more definitive conclusions about the form of scatter through the shine down curves. An effective model of this type could have predicted the time required for the signal to reduce to background, and this has implications for measurement times. It could show the effect of any remaining signal on subsequent measurements. Again such work would provide a sound basis for future research.

The modelling conducted to predict the form of scatter should ideally have been conducted with greater reference to the physical characteristics of individual mineral grains. Material dependent information could have been incorporated which would have accounted for the different responses which quartz or feldspar grains of different dimensions would have to illumination. Models of this type may be able to predict the effect of grain spacing and the most effective way of presenting grains on a disc. This could also have been investigated in another way by using the models in this thesis to compare scattering from several different arrangements of grains. More attention could have been paid to the difference between results from evenly covered discs and the results from discs with several small patches of grains. Such questions of surface layer and grain geometries would require resolution in future work.

In this study, measurements were simulated on mixed samples containing irradiated and unirradiated grains to show that the system could recognise the presence of two populations. This could have been extended to include several populations of grains which had been subjected to various degrees of irradiation. This would more accurately represent and model the type of situation which may occur in natural situations. If this type of approach to modelling were taken then there are several complementary experiments which could have been profitably conducted. Samples containing more than two populations of grains, which were unirradiated and irradiated to varying degrees, could have been prepared and analysed and the results compared to the modelled results.

Experimental work could have been carried out to provide information about the mechanism by which scattering occurs. The effect of different scattering regimes on the total signal obtained could have been investigated in more detail had time allowed. Discs could have been subjected to visual inspection to ensure that a monolayer of grains was present on each disc. The effect of varying the length of the measurement times could have been investigated. Also, discs with several different configurations of grains and grain spacings could have been analysed to show the effect of scatter in different cases and the time taken for signals to reach background levels. Such experiments could easily form the basis of a future study.

Unfortunately it has not been possible to fully investigate all of the above areas in the course of this MSc research. However, the work conducted for this thesis has succeeded in establishing the performance of the single grain system by using one approach to conducting analyses and modelling the results. There remain many other possible approaches and many unresolved questions regarding the performance of the instrument and the feasibility of the single grain approach to luminescence analysis. The purpose of this critique has been to acknowledge these areas where extension work would be profitable and present these as areas for future research.

Bibliography

Aitken, M.J. (1985) *Thermoluminescence Dating.* Academic, London.

Aitken, M.J. (1998) *An Introduction to Optical Dating.* Oxford University Press, New York.

Bannerjee, D., Murray, A.S., Botter-Jensen, L., Lang, A. (2001) Equivalent dose estimation using a single aliquot of polymineral fine grains. *Radiation Measurements.* 33, 73-94.

Benko, L. (1983) *TL properties of individual quartz grains.* PACT 9. 175-182.

Berger, G.W. (1990) Effectiveness of natural zeroing of the thermoluminescence in sediments. *Journal of Geophysical Research.* 95. 12375-12397.

Berger, G.W. (1994) Thermoluminescence dating of sediments older than ~100ka. *Quaternary Geochronology (Quaternary Science Reviews).* 13, 445-456.

Clark, R. J. and Sanderson, D.C.W. (1994) Photostimulated luminescence excitation spectroscopy of feldspars and micas. *Radiation Measurements.* 23, 641-646.

Duller, G.A.T. (1997) A luminescence imaging system based on a charge-coupled device (CCD) camera. *Radiation Measurements.* 27, 91-99.

Duller, G.A.T., Botter-Jensen, L., Murray, A.S., Truscott, A.J. (1999) Single grain measurements using a novel automated reader. *Nuclear Instruments and Methods in Physics Research B.* 155, 506-514.

Godfrey-Smith, D.I., Huntley, D.J., and Chen, W.H. (1988) Optical dating studies of quartz and feldspar sediment extracts. *Quaternary Science Reviews.* 7, 373-380.

Grun, R., Packman, S., and Pye, K. (1989) *Problems involved in TL-dating of Danish Cover sands using K-feldspars.* Synopses from a workshop on long and short range limits in luminescence dating. The Research Laboratory for Archaeology and the History of Art, Oxford University, occasional publication no. 9. 13-18.

Hoang Ngoc Ky. (1989) The Thu Duc loess formation, a typical eolian deposit of tropical regions. In: *ESCAP Secretariat, Quaternary Stratigraphy of Asia and the Pacific.* IGCP 296 (1989). ESCAP Atlas of Stratigraphy X (Mineral Resources Development Series 60), 100-104.

Hoang Ngoc Ky. (1994) Stratigraphic correlation of Quaternary transgressional and regressional deposits in Vietnam and adjacent countries. In: *ESCAP Secretariat, Quaternary Stratigraphy of Asia and the Pacific.* IGCP 296. ESCAP, 215-214.

Houston, I. (1999) *The application of stimulated luminescence to the dating of South East Asian quartz.* BSc dissertation, Physics Department, University of Strathclyde.

Huntley, D.J., and Berger, G.W. (1995) Scatter in luminescence data for optical dating-some models. *Ancient TL.* 13, 5-9.

Huntley, D.J., Godfrey-Smith, D.I., Thewalt, M.L.W., and Berger, G.W. (1985) Optical dating of sediments. *Nature.* 313, 105-107.

Hutt, G., Jaek, I., and Tchonka, J. (1988) Optical dating: K-feldspars optical response stimulation spectra. *Quaternary Science Reviews.* 7, 318-386.

Jablonski, A. (1935) Uber den Mechanismus der Photolumineszenz von Farbstoffphosphoren. *Z. Phys.* 94, 38.

Lamothe,M., Balescu,S., Auclair,M. (1994) Natural IRSL intensities and apparent luminescence ages of single feldspar grains extracted from partially bleached sediments. *Radiation Measurements.* 23(2-3), 555-561.

Lamothe, M. (1996) Luminescence dating of feldspar in sedimentary environments: The problem of zeroing. *Geographie Physique et Quaternaire.* 50(3), 365-376.

Lamothe, M., Auclair, M. (1999) A solution to anomalous fading and age shortfalls in optical dating of feldspar minerals. *Earth and Planetary Science Letters.* 171, 319-323.

Loffler E.,and Kubiniok J. (1991) The age and origin of the Yasothon soils and associated gravel deposits. *Journal of the Geological Society of Thailand.* 1(1), 69-74.

Loffler E., and Kubiniok J. (1996) Landform development and bioturbation on the Khorat plateau, Northeast Thailand. *Natural History Bulletin of the Siam Society.* 44, 199-216.

McFee,C.J., Tite,M.S. (1994). Investigations into the thermoluminescence properties of single quartz grains using an imaging photon detector. *Radiation Measurements.* 23(2-3), 355-360.

McFee, C.J. (1998) The measurement of single grain IRSL EDs using an imaging photon detector. *Quaternary Science Reviews.* 17(11), 1001-1008.

Murray, A.S., and Roberts, R.G. (1997) Determining the burial time of single grains of quartz using optically stimulated luminescence. *Earth and Planetary Science Letters.* 152, 163-180.

Rhodes, E.J. (1990) *Optical dating of quartz from sediments.* Unpublished D.Phil. thesis. Oxford University.

Sanderson, D.C.W. and Clark, R. J. (1994) Pulsed photostimulated luminescence of alkali feldspars. *Radiation Measurements.* 23, 633-639.

Sanderson, D.C.W., Carmichael, L.A., and Naylor, J.D. (1995) Photostimulated luminescence and thermoluminescence techniques for the detection of irradiated food. *Food Science and Technology Today.* 9, 150-154.

Sanderson, D.C.W, P. Bishop, I. Houston, and M. Boonsener. (2000) Luminescence characterisation of quartz-rich cover sands from NE Thailand. *Quaternary Science Reviews*. (20)5-9, 893-900.

Šibrava, V. (1993) Quaternary sequences in Southeast Asia and their regional correlation. In: *ESCAP Secretariat, Quaternary Stratigraphy of Asia and the Pacific*. IGCP 296. ESCAP Atlas of Stratigraphy XIII (Mineral Resources Development Series 62), 1-29.

Smith, B.W., Aitken, M.J, Rhodes, E.J., Robinson, P.D, and Geldard, D.M. (1986) Optical dating: methodological aspects. *Radiation Protection Dosimetry*. 17, 229-233.

Spencer, J.Q. (1996) *The development of luminescence methods to measure thermal exposure in lithic and ceramic materials.* PhD thesis, University of Glasgow.

Spooner, N.A. (1994) On the optical dating signal from quartz. *Radiation Measurements*. 23, 593-600.

Templer, R., Walton, A. (1983) *Image intensifier studies of TL in zircons*. PACT. 9, 299-308.

Appendix A

```
‘Scan4  2/07/00
‘Scanning program
'CONTROL PROGRAM FOR THE SCANNING PSL METER
'AND THE PSL LOCK IN BOARD


'Initialisation
    defLNG a,b,i
    NO =100
    SP= 250
    x=NO * 0.0025
    y=NO * 0.0025
    dly = 1200 'DELAY FOR THE CONTROL WORD SENT TO X-Y STAGE
    dim a3(4096),A2(4096),F$(8)
    port = &h1b0
    port1a=port
    port1b=port+1
    port1c=port+2
    port2a=port+4
    port2b=port+5
    port2c=port+6
    cont1=port+3
    cont2=port+7
    width "lpt1:",80
    dl=100
    s=1
    DC%=300 'DARK COUNT
    TC=0   'DISK SAVE DEFAULT ON
    PR=0   'PRINTER DEFAULT OFF
    F$="TEST"
    out cont1,139  'configure for a3,b1,c1 o/p
```

```
    out cont2,155 'configure for A2 i/p B2 i/p C2 i/p
    CW=8
    GOSUB 55


SCREEN 12 ' 640x480 16 colour display
option base 1
DIM
R(6,8),S(5,5),C(16),XR(100),YR(100),B(6),H(511),A0(6),A1(6),X2(500),Y2(500)
DIM ZA(16383),Z(16383),X(16383),Y(16383),A(2730),red(16),green(16),blue(16)
DIM
X$(2),V$(2),A$(2),pal%(16),L1(16),L2(16),w(5,6),XA(10),XB(10),YA(10),YB(10)
DIM lookup%(175,175),IpX#(150),IpY#(150),Ipz#(150),ch$(50)
Y$="        " :PR=0

FOR I=1 TO 15:READ C(I):NEXT I :REM Colour codes
for i=1 to 15 :read pal%(i):next i:REM PALETTE
for i=1 to 16 :read red(i), green(i), blue(i):next i:REM colour table for export
26 DEF FNA(X)=INT(X+.5)
27 DEF FNB(X)=INT(10*X+.5)*.1
28 DEF FNC(X)=INT(X/5+1)*5
29 DEF FND(X)=INT(X/10+1)*10
30 DEF FNE(X)=INT(X/50+1)*50
31 DEF FNF(X)=INT(X/100+1)*100
32 DEF FNG(X)=INT(X*100+.5)/100
33 DEF FNH(X)=INT(X*1000+0.5)/1000
def fni(x)=int(log(x)/log(10)):rem exponent
def fnj(x)=x/(10^fni(x)):rem mantissa
MDL=0:N1=1:N2=1:N3=1:N4=1:N5=1:N6=400:REM initial values for mdl and
markers
bmapindex=1
```

```
40  'Main Menu
    cls
    gosub 55
    locate 1,20:print " 1 - Control "
    locate 2,20:print " 2 - Run "
    locate 3,20:print " 3 - File Results "
    locate 4,20:input "Option ";z
    on z gosub 50,99,500
    goto 40


50  'Control Menu
    cls
    locate 1,20:print " 1 - Clear counters "
    locate 2,20:print " 2 - Count down (led's off) "
    locate 3,20:print " 3 - Hold count (led's off) "
    locate 4,20:print " 4 - Up/down count "
    locate 5,20:print " 5 - Send Value "
    locate 6,20:print " 6 - Test "
    locate 7,20:print " 7 - Printer Default on/off "
    locate 8,20:print " 8 - Disk Save Default On/Off
    locate 9,20:print " 9 - Centre X-Y Stage "
    locate 10,20:input "Option (0 to end) ";z
    if z=0 then return
    on z gosub 55,60,65,70,75,80,85,90,1000
    goto 50

55  'Clear counters
    cw=12
    OUT port1a,cw
    FOR i=1 to 5000:NEXT i
    cw=8
    OUT PORT1A,CW
    for i=1 to 100:next i
```

```
    XF=0
    YF=0
    RETURN

60  'Count down (led's off)
    cw=0
    OUT PORT1A,CW
    RETURN

65  'Hold count (led's off)
    cw=8
    OUT port1a,cw
    RETURN

70  'Up/down count
    cw=2
    out port1a,cw
    RETURN

75  'Send Value
    INPUT "Control Value ";cw
    OUT port1a,cw
    RETURN

80  'Test counters
    GOSUB 55
    JAKSUM=16777215
    GOSUB 60
    N=1:gosub 101
    FOR J = 2 TO 11
    IF J = 2 THEN
    PRINT JAKSUM, JAK+16777215
    ELSE
    PRINT JAKSUM, JAK;" "
```

```
    END IF
    GOSUB 101
    NEXT J
    DC%=JAKSUM/10
    PRINT  "DARK COUNT RATE: ";DC%
    INPUT "Accept Dark Count Rate? (y/n)";D$
    IF UCASE$(D$)="N" THEN
    INPUT "Dark Count Rate";DC%
   END IF
    GOSUB 55
    RETURN

85  'Printer on/off
    if pr=0 then pr=1:print "Printer on  ":for i=1 to 500:next i:return
    if pr=1 then pr=0:print "Printer off ":for i=1 to 500:next i
    RETURN

90  'Disk Save Default On/Off
    if TC=0 then TC=1:print "Disk Save Default Off":delay 1:return
    if TC=1 then TC=0:print "Disk Save Default On":delay 1
    RETURN




95 REM simple linear scaling
        SCAL=0
        SCAL=CLNG(JAK)

IF LG=0 THEN GOSUB 97
        IF SCAL<MI THEN SCAL=MI
        IF SCAL>(MA-SINC) THEN SCAL=MA-SINC
        SCAL=INT((SCAL-MI)/SINC+1)
```

```
    xp=40:yp=40     'NO OF PIXELS/MM
      px=int(xp/10):py=int(yp/10)
      X0=INT((H)*XP+20):Y0=INT(20+(SAV)*YP)
      LINE (X0,Y0+PY)-(X0+PX,Y0),C(SCAL),BF
      RETURN



97 REM LOG BASE 10 SCALING
IF SCAL<1E-10 THEN SCAL=1E-10
SCAL=log(SCAL)/log(10)
RETURN



99 'Readout Cycle
   PRINT "CW= ";CW
   CLS
   GOSUB 55
   N=1
   INPUT "Filename (Including Path) ";F$
   INPUT "Sample Name              ";S$
   INPUT "Cycle Time (sec)         ";s
   INPUT "Step size (microns)      ";SP
   INPUT "Sample Size (x)mm.       ";sx
   INPUT "Sample Size (y)mm.       ";sy
   INPUT "Counting Mode? (1 = Count Up/down, 0 = Count Down ";CT
   IF CT=1 THEN
   PRINT "Up/down counting"
   ELSE
   CT=0
   PRINT "Down counting"
   END IF
CLS:LOCATE 1,20: input " Log(0)/linear(1) scale? ";LG
```

```
MI=1E2:MA=1E04:NI=14'DEFAULT VALUES FOR LOG SCALE
mi=log(mi)/log(10):ma=log(ma)/log(10)
SINC=((MA-MI)/NI)
        L1(1)=10^MI:L2(1)=(10^(MI+SINC))
        FOR I=2 TO NI
        L1(I)=10^(MI+(I-1)*SINC):L2(I)=10^(MI+i*SINC)
        NEXT I :REM LEVEL LIMITS
 IF LG=0 THEN 100
CLS:LOCATE 1,20: PRINT " Input min and max for scaling "
 LOCATE 2,20: INPUT " min, max, ";MI,MA
   NI=14
SINC=((MA-MI)/NI)
        L1(1)=MI:L2(1)=L1(1)+SINC
        FOR I=2 TO NI
        L1(I)=L2(I-1):L2(I)=L1(I)+SINC
        NEXT I :REM LEVEL LIMITS

100     NO = SP/2.5
    X=NO*0.0025
    Y=NO*0.0025
    gosub 1050 ' Move X-Y Stage to Start Position
    gosub 1065
    GOSUB 40

101  I=1:z=1
    GOSUB 300
    A3(I)=CLNG(B1+256*B2+65536*B3)
    ON TIMER(s) GOSUB 103
    TIMER ON
    WHILE NOT INSTAT
    IF I = (n+1) THEN EXIT LOOP
    WEND
    RETURN
```

```
103  I=I+1
     GOSUB 300
     A3(I)=CLNG(B1+256*B2+65536*B3)
     JAK= CLNG(A3(I)-A3(I-1))
     IF CT =1 THEN
       JAKSUM=CLNG(JAKSUM+JAK)
     ELSE
       JAK=-1*JAK
       IF JAK<0 THEN JAK=JAK+1677216
       JAKSUM=CLNG(JAKSUM+JAK)

     END IF
     TIME=CLNG(TIME+S)
     TIMER OFF
     RETURN

300 'Read Port 2
     b1 = inp (port2a) 'read byte 1
     b2 = inp (port2b) 'read byte 2
     b3 = inp (port2c) 'read byte 3
     RETURN

400  OUT PORT ,128 'disable o/p
     RETURN

500 'File Results
     IF TC=1 THEN RETURN
OPEN F$ for APPEND as #1
     IF H+SAV>0 THEN GOTO 510
      PRINT #1,"Filename: ";F$
      PRINT #1,"Sample ";S$
      PRINT #1,"Cycle Time (s): ";s
    IF CT = 1 THEN
      PRINT #1,"Counting mode: Up/down counting"
```

```
   ELSE
    PRINT #1,"Counting mode: Down counting"
   END IF
    PRINT #1,"Dark Count ";dc%
    PRINT #1,"X-Diameter of the sample";sx
    PRINT #1,"Y-Diameter of the sample";sy
    PRINT #1, time$,Date$
    PRINT #1,"   X CO-ORD       Y CO-ORD       COUNTS";CHR$(13)
510  PRINT #1,USING "  ###.###    ###.###       ########";H;SAV;JAK

    CLOSE #1

   IF PR=0 THEN RETURN  'Prints a hard copy of the results
   OPEN "LPT1:" FOR APPEND AS #1
   IF H+SAV>0 THEN GOTO 520
    PRINT #1, CHR$(13)
    PRINT #1, "Filename: ";F$
    PRINT #1, "Sample  : ";S$
    PRINT #1, "Cycle Time (s): ";s
    PRINT #1, "Dark Count    : ";dc%
    PRINT #1, "X-Diameter of the Sample :";sx
    PRINT #1, "Y-Diameter of the Sample :";sy
    PRINT #1, time$,Date$
        PRINT #1, " X CO-ORD       Y CO-ORD       COUNTS";CHR$(13)
520  PRINT #1,USING "  ###.###    ###.###       ########";H;SAV;JAK
    PRINT #1,CHR$(12)
   CLOSE #1
   RETURN

600 'X-Direction Change
   IF XF=0 THEN
       cw=cw+32
       XF=1
   ELSE
```

```
        CW=CW-32
        XF=0
    END IF

    OUT port1a,cw
    FOR ST = 1 TO DLY:NEXT ST
    RETURN

700 'Y-Direction Change
    IF YF=0 THEN
        cw=cw+128
        YF=1
    ELSE
        CW=CW-128
        YF=0
    END IF

    OUT port1a,cw
    FOR ST = 1 TO DLY:NEXT ST
    RETURN

800 'X-Pulse to Step

    FOR SP = 1 TO NO
      cw=cw+16
      OUT port1a,cw
      FOR ST = 1 to dly: NEXT ST
      cw=cw-16
      OUT port1a,cw
      FOR ST = 1 TO dly: NEXT ST
    NEXT SP
    RETURN

900 'Y-Pulse to Step
```

```
    FOR SP = 1 TO NO
      cw=cw+64
      OUT port1a,cw
      FOR ST = 1 to dly: NEXT ST
      cw=cw-64
      OUT port1a,cw
      FOR ST = 1 TO dly :NEXT ST
    NEXT SP
    RETURN

1000 'Centre X-Y Stage
    cls
    locate 1,20:print"1 - Change X-Direction"
    locate 2,20:print"2 - Change Y-Direction"
    locate 3,20:print"3 - Move in X-Direction"
    locate 4,20:print"4 - Move in Y-Direction"
    locate 5,20:print"5 - Change Step Size"
    locate 7,25:PRINT"PRESS RETURN TO END"

1010 LOCATE 12,20:PRINT"COMMAND ? ":Q$=INKEY$
    LOCATE 9,20 :PRINT "MOVING IN ";NO*2.5;" MICRON STEPS"
    IF Q$= CHR$(13) THEN GOSUB 55:NO =100 :RETURN
    IF Q$ =CHR$(49) THEN GOSUB 600:LOCATE 12,31:PRINT "CHANGE  X
DIRECTION"
    IF Q$ =CHR$(50) THEN GOSUB 700:LOCATE 12,31:PRINT "CHANGE  Y
DIRECTION"
    IF Q$ =CHR$(51) THEN GOSUB 800:LOCATE 12,31:PRINT "MOVE IN X
DIRECTION"
    IF Q$ =CHR$(52) THEN GOSUB 900:LOCATE 12,31:PRINT "MOVE IN Y
DIRECTION"
    IF Q$ =CHR$(53) THEN GOTO 1020
    goto 1010

1020 'SELECT STEP SIZE
```

```
    CLS
    LOCATE 1,20:PRINT "INPUT THE NO. OF STEPS PER KEY DEPRESSION"
    LOCATE 3,20:PRINT "EXAMPLE 400 = 1mm OF TRAVEL"
    LOCATE 5,20:INPUT "NO OF STEPS";NO
    x=NO * 0.0025
    y=NO * 0.0025
    CLS
    GOTO 1000


1050 'Move Stage to Start Position
'   PRINT "CW= ";CW
'   for L = 0 to sy/2 step y
'        GOSUB 900
'   next L
'   for H = 0 to sx/2 step x
'       GOSUB 800
'   next H
    GOSUB 55
    IF CT = 1 THEN
    GOSUB 70 'UP/DOWN COUNT
    ELSE
    GOSUB 60 'DOWN COUNT
    END IF
'   gosub 600 ' reverse x direction before start
'   GOSUB 600
    gosub 700 ' reverse y direction before start
    RETURN


  '                                    '

REM '    Plot Grid and Labels                    '
```

```
'                                    '

1065 for i=1 to 15:palette c(i),pal%(i):next i
PALETTE 0,0
color 15,63 ' change from 15,0
CLS
PSET  (0,0)
   X0=20:Y0=420
   FOR M=20  TO 420 STEP 80
    PSET (M,Y0)
    DRAW "U400;C15"
   NEXT M
rem  for M=420 to 580 step 80:pset (M,y0):draw "u120;":next M
   FOR P=420 TO 20 STEP-80
    PSET (X0,P)
    DRAW "R400;C15"
      NEXT P

   ' Boxes for Key '
   LOCATE 3,62:PRINT U$
    FOR I=NI TO 1 STEP -1
    J=NI-I
    LINE(600,64+J*16)-(620,48+J*16),C(I),BF
IF L2(NI)>999 THEN 1070
IF L2(NI)<1 THEN 1075 ELSE 1080

1070   IF I=1 THEN LOCATE J+4,62:PRINT USING "_<_ #######";L2(I):GOTO
1085
    IF I=NI THEN LOCATE J+4,62:PRINT USING "_>_ #######";L1(I):GOTO
1085
    LOCATE J+4,58: PRINT USING "#######_ _-#######";L1(I),L2(I):GOTO
1085
```

```
1075    IF I=1 THEN LOCATE J+4,64:PRINT USING "_<_ ##.###";L2(I):GOTO
1085
    IF I=NI THEN LOCATE J+4,64:PRINT USING "_>_ ##.###";L1(I):GOTO
1085
    LOCATE J+4,60: PRINT USING "###.##_ _-##.###";L1(I),L2(I):GOTO 1085

1080    IF I=1 THEN LOCATE J+4,64:PRINT USING "_<_ ###.##";L2(I):GOTO
1085
    IF I=NI THEN LOCATE J+4,64:PRINT USING "_>_ ###.##";L1(I):GOTO
1085
    LOCATE J+4,60: PRINT USING "###.##_ _-###.##";L1(I),L2(I)

1085  NEXT I
   LOCATE 1,10:PRINT L$:LOCATE 28,1:PRINT O1$+"  Cell : ";STR$(GR);" km
";:LOCATE 28,35:PRINT"File: "+F$;



1100 'Sample Scanning Subroutine
   'sx and sy are the sample size
   'x and y are the step sizes equal to the spot size
   JAKSUM=(CT-1)*(-16777215)
   T$=TIME$
   TIME=0
for L=0 to sy step y*2

        for H=0 to sx step x
              GOSUB 101
              SAV=L
                 GOSUB 95
          GOSUB 500 'FILE AND/OR PRINT RESULTS
              SAV=0
          IF H < sx THEN  GOSUB 800 ' MOVE STAGE
        next H
```

```
  GOSUB 900

    GOSUB 600
    for H=sx to 0 step -x
     IF (L+Y)>SY THEN
           IF H>0 THEN GOSUB 800
     ELSE
           GOSUB 101
           SAV=L+Y
             GOSUB 95
           GOSUB 500 'FILE AND/OR PRINT RESULTS
           SAV=0
           IF H > 0 THEN  GOSUB 800 'MOVE STAGE
        END IF
    next H
    IF L < SY THEN GOSUB 900
    GOSUB 600
next L
GOSUB 700
BACK=sy/y
FOR rety=0 to BACK
    GOSUB 900
NEXT rety
GOSUB 700
GOSUB 65 'LEDS OFF
PRINT "Initial time:  ";T$
PRINT "Final time:  ";TIME$
GOSUB 55 'CLEAR COUNTERS
PRINT "Measurement complete.  Press any key to continue."
WHILE NOT INSTAT
WEND
K$=INKEY$
RETURN
```

```
9000 REM
9090 DATA 1,2,3,4,5,6,7,8,9,10,11,12,13,14,15:REM Colour codes
9100 'DATA 8,49,17,9,25,10,23,19,55,54,38,52,36,44,63,15:rem old PALETTE
     DATA 8,49,17,9,25,10,23,19,55,54,38,52,36,44,0:rem new PALETTE
9120 'DATA 7,6,14,13,5,12,4,11,3,2,10,1,9,8,15,0:REM MONO PALETTE
     DATA 255,255,255:REM COLOUR TABLE - RED,GREEN,BLUE


     DATA 85,38,144
     DATA 37,30,177
     DATA 7,56,229
     DATA 1,129,180
     DATA 29,169,136
     DATA 68,213,130
     DATA 150,243,77
     DATA 200,249,4
     DATA 255,249,4
     DATA 252,202,16
     DATA 255,143,28
     DATA 255,79,2
     DATA 234,8,6
     DATA 204,5,56
     DATA 0,0,0
```

Appendix B

```
'Kring6
'Program for modelling laser scatter.
'Iain Houston 28/11/00


'initialisation

DIM B (115,115) 'RESULT ARRAY
DIM A (115,115) 'MASTER ARRAY
DIM C (115,115) 'TEST ARRAY
DIM D (115,115) 'CALCULATION ARRAY
L6=0.1
L5=0.2
L4=0.3
L3=0.4
L2=0.5
L1=0.6
L0=0.7
sc=0
LS=0
SET=0
cr1=54
cr2=54
cr3=54
cr4=29
cr5=54
cr6=79
cr7=29
cr8=54
cr9=79
cr10=54
```

```
100 'setup

INPUT "Should laser scatter when not on a grain? (1/0)", SC
INPUT "Customise laser spot? (1/0)",ls
IF LS=1 THEN GOSUB 110
INPUT "SINGLE CIRCLE (1) OR FIVE SMALL CIRCLES? (0)", SET
IF SET=1 THEN
INPUT "Radius of circle? 0-50", rad1
ELSE
INPUT "RADIUS OF CIRCLE 1? (0-25)", RAD1
INPUT "RADIUS OF CIRCLE 2? (0-25)", RAD2
INPUT "RADIUS OF CIRCLE 3? (0-25)", RAD3
INPUT "RADIUS OF CIRCLE 4? (0-25)", RAD4
INPUT "RADIUS OF CIRCLE 5? (0-25)", RAD5
INPUT "Change circle positions? (1/0)", ps
        IF PS =1 THEN
        INPUT "CENTRE OF CIRCLE 1 X,Y (BOUNDARIES: 14-94): ",CR1,CR2
INPUT "CENTRE OF CIRCLE 2 X,Y : ",CR3,CR4
INPUT "CENTRE OF CIRCLE 3 X,Y : ",CR5,CR6
INPUT "CENTRE OF CIRCLE 4 X,Y : ",CR7,CR8
INPUT "CENTRE OF CIRCLE 5 X,Y : ",CR9,CR10
ELSE
END IF

END IF
RAD1=RAD1*RAD1
RAD2=RAD2*RAD2
RAD3=RAD3*RAD3
RAD4=RAD4*RAD4
RAD5=RAD5*RAD5


105 ' SET BIN CONTENT
```

```
FOR K=14 to 94
FOR V=14 TO 94
C1=K
C2=V

A(K,V)=0
C(K,V)=0
B(K,V)=0
D(K,V)=0

IF SET=1 THEN
GOSUB 150
ELSE
gosub 150
gosub 160
gosub 170
gosub 180
gosub 190
END IF


CIRC1%=0
CIRC2%=0
CIRC3%=0
CIRC4%=0
CIRC5%=0

NEXT V
NEXT K
GOSUB 200

110' CUSTOMISE LASER SPOT
```

```
INPUT "% DEPLETION UNDER DIRECT ILLUMINATION?", L0
INPUT "% DEPLETION ONE STEP AWAY?",L1
INPUT "% DEPLETION TWO STEPS AWAY?",L2
INPUT "% DEPLETION THREE STEPS AWAY?",L3
INPUT "% DEPLETION FOUR STEPS AWAY?",L4
INPUT "% DEPLETION FIVE STEPS AWAY?",L5
INPUT "% DEPLETION SIX STEPS AWAY?",L6
L0=L0/100
L1=L1/100
L2=L2/100
L3=L3/100
L4=L4/100
L5=L5/100
L6=L6/100
RETURN


120 'CALCULATE REMAINING SIGNAL


FOR RM2=1 TO 108
FOR RM1=1 TO 108
PRINT ,RM1,RM2,A(RM1,RM2)
OPEN R$ FOR APPEND  AS #1
PRINT #1 ,RM1,RM2,A(RM1,RM2)
CLOSE #1
NEXT RM1
NEXT RM2
RETURN


130 'CLEAR CALCULATION MATRIX
FOR K2=0 to 108
FOR V2=0 TO 108
```

```
D(K2,V2)=0
NEXT V2
NEXT K2
RETURN

140'PRINT TEST MATRIX

FOR S=1 TO 108
FOR L=1 TO 108
PRINT ,L,S,C(L,S)
OPEN T$ FOR APPEND  AS #1
PRINT #1 ,L,S,c(L,S)
CLOSE #1
NEXT L
NEXT S
RETURN


150
CIRC1%=((C1-CR1)*(C1-CR1))+((C2-CR2)*(C2-CR2))
IF CIRC1%<rad1 THEN A(K,V)=100
IF CIRC1%<rad1 THEN C(K,V)=100
RETURN

160
CIRC2%=((C1-CR3)*(C1-CR3))+((C2-CR4)*(C2-CR4))
IF CIRC2%<RAD2 THEN A(K,V)=100
IF CIRC2%<RAD2 THEN C(K,V)=100
RETURN

170
CIRC3%=((C1-CR5)*(C1-CR5))+((C2-CR6)*(C2-CR6))
IF CIRC3%<RAD3 THEN A(K,V)=100
IF CIRC3%<RAD3 THEN C(K,V)=100
```

```
RETURN

180
CIRC4%=((C1-CR7)*(C1-CR7))+((C2-CR8)*(C2-CR8))
IF CIRC4%<RAD4 THEN A(K,V)=100
IF CIRC4%<RAD4 THEN C(K,V)=100
RETURN

190
CIRC5%=((C1-CR9)*(C1-CR9))+((C2-CR10)*(C2-CR10))
IF CIRC5%<RAD5 THEN A(K,V)=100
IF CIRC5%<RAD5 THEN C(K,V)=100
RETURN



200 'SIMULATE READING

INPUT "Generate test set? 1/0 ", t1
IF T1=1 THEN INPUT "Write to? ";T$
INPUT "CONDUCT MEASUREMENT? 1/0 ", S1
IF S1=1 THEN INPUT "SAVE AS? ";F$
INPUT "Calculate remaining signal in grains? (1/0)",rmg
IF RMG=1 THEN INPUT "WRITE TO? ";R$
IF T1=1 THEN GOSUB 140 ELSE

IF S1=0 THEN gosub 1000 else



FOR F = 4 to 104 step 2
```

```
FOR i = 4  TO 104

x=i
y=f

gosub 300  'calculate effect of readout
PRINT, X,Y,B(X,Y)
OPEN F$ FOR APPEND  AS #1
PRINT #1 ,X,Y,B(X,Y)
close #1

NEXT i

y=y+1


FOR j = 104 TO 4 STEP -1


x=j
y=f+1

gosub 300  'calculate
PRINT, X,Y,B(X,Y)
OPEN F$ FOR APPEND  AS #1
PRINT #1 ,X,Y,B(X,Y)
close #1

NEXT j

NEXT F
```

```
IF rmg=1 THEN GOSUB 120 ELSE
gosub 1000



300 'CALCULATE EFFECT OF READOUT
IF sc=0 AND C(X,Y)=0 THEN RETURN


'6 STEPS AWAY

FOR D1=1 TO 13

D(x-6,y-7+D1)=L6*A(X-6,Y-7+D1)
D(x+6,y-7+D1)=L6*A(X+6,Y-7+D1)

A(X-6,Y-7+D1)=A(X-6,Y-7+D1)-L6*A(X-6,Y-7+D1)
A(X+6,Y-7+D1)=A(X+6,Y-7+D1)-L6*A(X+6,Y-7+D1)

B(X,Y)=B(X,Y)+D(x-6,y-7+D1)+D(x+6,y-7+D1)

NEXT D1

FOR R1=1 TO 11

D(x-6+R1,y-6)=L6*A(X-6+R1,Y-6)
D(x-6+R1,y+6)=L6*A(X-6+R1,Y+6)

A(X-6+R1,Y-6)=A(X-6+R1,Y-6)-L6*A(X-6+R1,Y-6)
A(X-6+R1,Y+6)=A(X-6+R1,Y+6)-L6*A(X-6+R1,Y+6)

B(X,Y)=B(X,Y)+D(x-6+R1,y-6)+D(x-6+R1,y+6)
```

```
NEXT R1



'5 STEPS AWAY

FOR F1=1 TO 11

D(x-5,y-6+F1)=L5*A(X-5,Y-6+F1)
D(x+5,y-6+F1)=L5*A(X+5,Y-6+F1)

A(X-5,Y-6+F1)=A(X-5,Y-6+F1)-L5*A(X-5,Y-6+F1)
A(X+5,Y-6+F1)=A(X+5,Y-6+F1)-L5*A(X+5,Y-6+F1)

B(X,Y)=B(X,Y)+D(x-5,y-6+F1)+D(x+5,y-6+F1)


NEXT F1

FOR G1=1 TO 9

D(x-5+G1,y-5)=L5*A(X-5+G1,Y-5)
D(x-5+G1,y+5)=L5*A(X-5+G1,Y+5)

A(X-5+G1,Y-5)=A(X-5+G1,Y-5)-L5*A(X-5+G1,Y-5)
A(X-5+G1,Y+5)=A(X-5+G1,Y+5)-L5*A(X-5+G1,Y+5)

B(X,Y)=B(X,Y)+D(x-5+G1,y-5)+D(x-5+G1,y+5)

NEXT G1



'4 STEPS AWAY
```

```
FOR H1=1 TO 9

D(x-4,y-5+H1)=L4*A(X-4,Y-5+H1)
D(x+4,y-5+H1)=L4*A(X+4,Y-5+H1)

A(X-4,Y-5+H1)=A(X-4,Y-5+H1)-L4*A(X-4,Y-5+H1)
A(X+4,Y-5+H1)=A(X+4,Y-5+H1)-L4*A(X+4,Y-5+H1)

B(X,Y)=B(X,Y)+D(x-4,y-5+H1)+D(x+4,y-5+H1)

NEXT H1

FOR I1=1 TO 7

D(x-4+I1,y-4)=L4*A(X-4+I1,Y-4)
D(x-4+I1,y+4)=L4*A(X-4+I1,Y+4)

A(X-4+I1,Y-4)=A(X-4+I1,Y-4)-L4*A(X-4+I1,Y-4)
A(X-4+I1,Y+4)=A(X-4+I1,Y+4)-L4*A(X-4+I1,Y+4)

B(X,Y)=B(X,Y)+D(x-4+I1,y-4)+D(x-4+I1,y+4)

NEXT I1



'3 steps away

FOR M=1 TO 7

D(x-3,y-4+M)=L3*A(X-3,Y-4+M)
D(x+3,y-4+M)=L3*A(X+3,Y-4+M)
```

```
A(X-3,Y-4+M)=A(X-3,Y-4+M)-L3*A(X-3,Y-4+M)
A(X+3,Y-4+M)=A(X+3,Y-4+M)-L3*A(X+3,Y-4+M)

B(X,Y)=B(X,Y)+D(x-3,y-4+M)+D(x+3,y-4+M)

NEXT M

FOR N = 1 TO 5

D(x-3+N,y-3)=L3*A(X-3+N,Y-3)
D(x-3+N,y+3)=L3*A(X-3+N,Y+3)

A(X-3+N,Y-3)=A(X-3+N,Y-3)-L3*A(X-3+N,Y-3)
A(X-3+N,Y+3)=A(X-3+N,Y+3)-L3*A(X-3+N,Y+3)

B(X,Y)=B(X,Y)+D(x-3+N,y-3)+D(x-3+N,y+3)

NEXT N



'2 steps away

FOR O = 1 TO 5

D(x-2,y-3+O)=L2*A(X-2,Y-3+O)
D(x+2,y-3+O)=L2*A(X+2,Y-3+O)

A(X-2,Y-3+O)=A(X-2,Y-3+O)-L2*A(X-2,Y-3+O)
A(X+2,Y-3+O)=A(X+2,Y-3+O)-L2*A(X+2,Y-3+O)

B(X,Y)=B(X,Y)+D(x-2,y-3+O)+D(x+2,y-3+O)

NEXT O
```

```
FOR P = 1 TO 3

D(x-2+P,y-2)=L2*A(X-2+P,Y-2)
D(x-2+P,y+2)=L2*A(X-2+P,Y+2)

A(X-2+P,Y-2)=A(X-2+P,Y-2)-L2*A(X-2+P,Y-2)
A(X-2+P,Y+2)=A(X-2+P,Y+2)-L2*A(X-2+P,Y+2)

B(X,Y)=B(X,Y)+D(x-2+P,y-2)+D(x-2+P,y+2)

NEXT P


'1 step away

FOR Q=1 TO 3

D(x-1,y-2+Q)=L1*A(X-1,Y-2+Q)
D(x+1,y-2+Q)=L1*A(X+1,Y-2+Q)

A(X-1,Y-2+Q)=A(X-1,Y-2+Q)-L1*A(X-1,Y-2+Q)
A(X+1,Y-2+Q)=A(X+1,Y-2+Q)-L1*A(X+1,Y-2+Q)

B(X,Y)=B(X,Y)+D(x-1,y-2+Q)+D(x+1,y-2+Q)

NEXT Q

D(x-1,y)=L1*A(X-1,Y)
D(x+1,y)=L1*A(X+1,Y)

A(X-1,Y)=A(X-1,Y)-L1*A(X-1,Y)
A(X+1,Y)=A(X+1,Y)-L1*A(X+1,Y)
```

```
B(X,Y)=B(X,Y)+D(x-1,y)+D(x+1,y)

'on laser spot

D(X,Y)=L0*A(X,Y)

A(X,Y)=A(X,Y)-L0*A(X,Y)

B(X,Y)=B(X,Y)+D(x,y)


GOSUB 130
return


1000
end
```

Appendix C

```
'Dwalen4
'Program for modelling measurement using small steps.
'Iain Houston 12/12/00


'initialisation

DIM A (115,115) 'MASTER ARRAY
DIM B (115,115) 'RESULT ARRAY
DIM C (115,115) 'TEST ARRAY
DIM D (115,115) 'CALCULATION ARRAY
DIM E (115,115) 'MASTER ARRAY (NORM)
DIM F (115,115) 'RESULT ARRAY (NORM)
DIM G (115,115) 'TEST ARRAY (NORM)
DIM H (115,115) 'CALCULATION ARRAY (NORM)
RANDOMIZE TIMER
L6=0.1
L5=0.2
L4=0.3
L3=0.4
L2=0.5
L1=0.6
L0=0.7
sc=0
LS=0
SET=0
cr1=54
cr2=54
cr3=54
cr4=29
cr5=54
```

```
cr6=79
cr7=29
cr8=54
cr9=79
cr10=54

100 'setup

INPUT "Concentration of irradiated grains? ",conc1
INPUT "Should laser scatter when not on a grain? (1/0)", SC
INPUT "Customise laser spot? (1/0)",ls
IF LS=1 THEN GOSUB 110
INPUT "SINGLE CIRCLE (1) OR FIVE SMALL CIRCLES? (0)", SET
IF SET=1 THEN
INPUT "Radius of circle? 0-50", rad1
ELSE
INPUT "RADIUS OF CIRCLE 1? (0-25)", RAD1
INPUT "RADIUS OF CIRCLE 2? (0-25)", RAD2
INPUT "RADIUS OF CIRCLE 3? (0-25)", RAD3
INPUT "RADIUS OF CIRCLE 4? (0-25)", RAD4
INPUT "RADIUS OF CIRCLE 5? (0-25)", RAD5
INPUT "Change circle positions? (1/0)", ps
        IF PS =1 THEN
        INPUT "CENTRE OF CIRCLE 1 X,Y (BOUNDARIES: 14-94): ",CR1,CR2
INPUT "CENTRE OF CIRCLE 2 X,Y : ",CR3,CR4
INPUT "CENTRE OF CIRCLE 3 X,Y : ",CR5,CR6
INPUT "CENTRE OF CIRCLE 4 X,Y : ",CR7,CR8
INPUT "CENTRE OF CIRCLE 5 X,Y : ",CR9,CR10
ELSE
END IF

END IF
RAD1=RAD1*RAD1
RAD2=RAD2*RAD2
```

```
RAD3=RAD3*RAD3
RAD4=RAD4*RAD4
RAD5=RAD5*RAD5


105 ' SET BIN CONTENT


FOR K=14 to 94
FOR V=14 TO 94

C1=K
C2=V
A(K,V)=0
B(K,V)=0
C(K,V)=0
D(K,V)=0
E(K,V)=0
F(K,V)=0
G(K,V)=0
H(K,V)=0

IF SET=1 THEN
GOSUB 150
ELSE
gosub 150
gosub 160
gosub 170
gosub 180
gosub 190
END IF


CIRC1%=0
```

```
CIRC2%=0
CIRC3%=0
CIRC4%=0
CIRC5%=0

NEXT V
NEXT K
GOSUB 200

110' CUSTOMISE LASER SPOT
INPUT "% DEPLETION UNDER DIRECT ILLUMINATION?", L0
INPUT "% DEPLETION ONE STEP AWAY?",L1
INPUT "% DEPLETION TWO STEPS AWAY?",L2
INPUT "% DEPLETION THREE STEPS AWAY?",L3
INPUT "% DEPLETION FOUR STEPS AWAY?",L4
INPUT "% DEPLETION FIVE STEPS AWAY?",L5
INPUT "% DEPLETION SIX STEPS AWAY?",L6
L0=L0/100
L1=L1/100
L2=L2/100
L3=L3/100
L4=L4/100
L5=L5/100
L6=L6/100
RETURN


120 'CALCULATE REMAINING SIGNAL

FOR RM2=1 TO 108
FOR RM1=1 TO 108
PRINT ,RM1,RM2,A(RM1,RM2)
OPEN R$ FOR APPEND  AS #1
PRINT #1 ,RM1,RM2,A(RM1,RM2)
```

```
CLOSE #1
NEXT RM1
NEXT RM2
RETURN

125 'CALCULATE REMAINING SIGNAL (normalisation)

FOR RM2=1 TO 108
FOR RM1=1 TO 108
PRINT ,RM1,RM2,E(RM1,RM2)
OPEN RN$ FOR APPEND  AS #1
PRINT #1 ,RM1,RM2,E(RM1,RM2)
CLOSE #1
NEXT RM1
NEXT RM2
RETURN

130 'CLEAR CALCULATION MATRIX
FOR K2=0 to 108
FOR V2=0 TO 108
D(K2,V2)=0
NEXT V2
NEXT K2
RETURN

135 'CLEAR CALCULATION MATRIX (normalisation)
FOR K=0 to 108
FOR V=0 TO 108
H(K,V)=0
NEXT V
NEXT K
RETURN

140'PRINT TEST MATRIX
```

```
FOR S=1 TO 108
FOR L=1 TO 108
PRINT ,L,S,C(L,S)
OPEN T$ FOR APPEND  AS #1
PRINT #1 ,L,S,c(L,S)
CLOSE #1
NEXT L
NEXT S
RETURN

145'PRINT TEST MATRIX (normalisation)

FOR S=1 TO 108
FOR L=1 TO 108
PRINT ,L,S,G(L,S)
OPEN TN$ FOR APPEND  AS #1
PRINT #1 ,L,S,G(L,S)
CLOSE #1
NEXT L
NEXT S
RETURN

150
CIRC1%=((C1-CR1)*(C1-CR1))+((C2-CR2)*(C2-CR2))
IF CIRC1%<rad1 THEN
CONT1=RND*1000
CONT2=RND*1000
CONT=CONT1*CONT2
CONT=CONT+200
E(K,V)=CONT
G(K,V)=E(K,V)
A(K,V)=E(K,V)
C(K,V)=A(K,V)
CONC=RND*100
```

```
IF CONC>CONC1 THEN A(K,V)=0
C(K,V)=A(K,V)
ELSE
END IF
RETURN

160
CIRC2%=((C1-CR3)*(C1-CR3))+((C2-CR4)*(C2-CR4))
IF CIRC2%<RAD2 THEN
CONT1=RND*1000
CONT2=RND*1000
CONT=CONT1*CONT2
CONT=CONT+200
E(K,V)=CONT
G(K,V)=E(K,V)
A(K,V)=E(K,V)
C(K,V)=A(K,V)
CONC=RND*100
IF CONC1>CONC THEN A(K,V)=0
C(K,V)=A(K,V)
ELSE
END IF
RETURN

170
CIRC3%=((C1-CR5)*(C1-CR5))+((C2-CR6)*(C2-CR6))
IF CIRC3%<RAD3 THEN
CONT1=RND*1000
CONT2=RND*1000
CONT=CONT1*CONT2
CONT=CONT+200
E(K,V)=CONT
G(K,V)=E(K,V)
A(K,V)=E(K,V)
```

```
C(K,V)=A(K,V)
CONC=RND*100
IF CONC1>CONC THEN A(K,V)=0
C(K,V)=A(K,V)
ELSE
END IF
RETURN

180
CIRC4%=((C1-CR7)*(C1-CR7))+((C2-CR8)*(C2-CR8))
IF CIRC4%<RAD4 THEN
CONT1=RND*1000
CONT2=RND*1000
CONT=CONT1*CONT2
CONT=CONT+200
E(K,V)=CONT
G(K,V)=E(K,V)
A(K,V)=E(K,V)
C(K,V)=A(K,V)
CONC=RND*100
IF CONC1>CONC THEN A(K,V)=0
C(K,V)=A(K,V)
ELSE
END IF
RETURN

190
CIRC5%=((C1-CR9)*(C1-CR9))+((C2-CR10)*(C2-CR10))
IF CIRC5%<RAD5 THEN
CONT1=RND*1000
CONT2=RND*1000
CONT=CONT1*CONT2
CONT=CONT+200
E(K,V)=CONT
```

```
G(K,V)=E(K,V)
A(K,V)=E(K,V)
C(K,V)=A(K,V)
CONC=RND*100
IF CONC1>CONC THEN A(K,V)=0
C(K,V)=A(K,V)
ELSE
END IF
RETURN



200 'SIMULATE READING

INPUT "Generate test set? 1/0 ", t1
IF T1=1 THEN INPUT "Write to? ";T$
INPUT "Generate normalisation test set? 1/0 ", tn1
IF TN1=1 THEN INPUT "Write to? ";TN$
INPUT "CONDUCT MEASUREMENT? 1/0 ", S1
IF S1=1 THEN INPUT "SAVE AS? ";F$
INPUT "Conduct normalisation measurement? 1/0 ", SN1
IF SN1=1 THEN INPUT "SAVE AS? ";N$
INPUT "Calculate remaining signal in grains? (1/0)",rmg
IF RMG=1 THEN INPUT "WRITE TO? ";R$
INPUT "Calculate remaining signal in normalisation set? (1/0)",rmg2
IF RMG2=1 THEN INPUT "WRITE TO? ";RN$



IF T1=1 THEN GOSUB 140 ELSE

IF S1=0 THEN gosub 600 else



FOR F = 4 to 104 step 2
```

```
FOR i = 4  TO 104
x=i
y=f

gosub 300  'calculate effect of readout
BACK=RND*200
IF BACK<100 THEN BACK=BACK+100
IF B(X,Y)<150 THEN B(X,Y)=BACK
PRINT, X,Y,B(X,Y)
OPEN F$ FOR APPEND  AS #1
PRINT #1 ,X,Y,B(X,Y)
close #1

NEXT i

y=y+1


FOR j = 104 TO 4 STEP -1


x=j
y=f+1

gosub 300  'calculate
BACK=RND*200
IF BACK<100 THEN BACK=BACK+100
IF B(X,Y)<150 THEN B(X,Y)=BACK
PRINT, X,Y,B(X,Y)
OPEN F$ FOR APPEND  AS #1
PRINT #1 ,X,Y,B(X,Y)
close #1
```

```
NEXT j

NEXT F


IF rmg=1 THEN GOSUB 120 ELSE
gosub 600



300 'CALCULATE EFFECT OF READOUT
IF sc=0 AND C(X,Y)=0 THEN RETURN


'6 STEPS AWAY

FOR D1=1 TO 13

D(x-6,y-7+D1)=L6*A(X-6,Y-7+D1)
D(x+6,y-7+D1)=L6*A(X+6,Y-7+D1)

A(X-6,Y-7+D1)=A(X-6,Y-7+D1)-L6*A(X-6,Y-7+D1)
A(X+6,Y-7+D1)=A(X+6,Y-7+D1)-L6*A(X+6,Y-7+D1)

B(X,Y)=B(X,Y)+D(x-6,y-7+D1)+D(x+6,y-7+D1)

NEXT D1

FOR R1=1 TO 11

D(x-6+R1,y-6)=L6*A(X-6+R1,Y-6)
D(x-6+R1,y+6)=L6*A(X-6+R1,Y+6)
```

```
A(X-6+R1,Y-6)=A(X-6+R1,Y-6)-L6*A(X-6+R1,Y-6)
A(X-6+R1,Y+6)=A(X-6+R1,Y+6)-L6*A(X-6+R1,Y+6)

B(X,Y)=B(X,Y)+D(x-6+R1,y-6)+D(x-6+R1,y+6)

NEXT R1



'5 STEPS AWAY

FOR F1=1 TO 11

D(x-5,y-6+F1)=L5*A(X-5,Y-6+F1)
D(x+5,y-6+F1)=L5*A(X+5,Y-6+F1)

A(X-5,Y-6+F1)=A(X-5,Y-6+F1)-L5*A(X-5,Y-6+F1)
A(X+5,Y-6+F1)=A(X+5,Y-6+F1)-L5*A(X+5,Y-6+F1)

B(X,Y)=B(X,Y)+D(x-5,y-6+F1)+D(x+5,y-6+F1)



NEXT F1

FOR G1=1 TO 9

D(x-5+G1,y-5)=L5*A(X-5+G1,Y-5)
D(x-5+G1,y+5)=L5*A(X-5+G1,Y+5)

A(X-5+G1,Y-5)=A(X-5+G1,Y-5)-L5*A(X-5+G1,Y-5)
A(X-5+G1,Y+5)=A(X-5+G1,Y+5)-L5*A(X-5+G1,Y+5)

B(X,Y)=B(X,Y)+D(x-5+G1,y-5)+D(x-5+G1,y+5)
```

```
NEXT G1



'4 STEPS AWAY

FOR H1=1 TO 9

D(x-4,y-5+H1)=L4*A(X-4,Y-5+H1)
D(x+4,y-5+H1)=L4*A(X+4,Y-5+H1)

A(X-4,Y-5+H1)=A(X-4,Y-5+H1)-L4*A(X-4,Y-5+H1)
A(X+4,Y-5+H1)=A(X+4,Y-5+H1)-L4*A(X+4,Y-5+H1)

B(X,Y)=B(X,Y)+D(x-4,y-5+H1)+D(x+4,y-5+H1)

NEXT H1

FOR I1=1 TO 7

D(x-4+I1,y-4)=L4*A(X-4+I1,Y-4)
D(x-4+I1,y+4)=L4*A(X-4+I1,Y+4)

A(X-4+I1,Y-4)=A(X-4+I1,Y-4)-L4*A(X-4+I1,Y-4)
A(X-4+I1,Y+4)=A(X-4+I1,Y+4)-L4*A(X-4+I1,Y+4)

B(X,Y)=B(X,Y)+D(x-4+I1,y-4)+D(x-4+I1,y+4)

NEXT I1



'3 steps away
```

```
FOR M=1 TO 7

D(x-3,y-4+M)=L3*A(X-3,Y-4+M)
D(x+3,y-4+M)=L3*A(X+3,Y-4+M)

A(X-3,Y-4+M)=A(X-3,Y-4+M)-L3*A(X-3,Y-4+M)
A(X+3,Y-4+M)=A(X+3,Y-4+M)-L3*A(X+3,Y-4+M)

B(X,Y)=B(X,Y)+D(x-3,y-4+M)+D(x+3,y-4+M)

NEXT M

FOR N = 1 TO 5

D(x-3+N,y-3)=L3*A(X-3+N,Y-3)
D(x-3+N,y+3)=L3*A(X-3+N,Y+3)

A(X-3+N,Y-3)=A(X-3+N,Y-3)-L3*A(X-3+N,Y-3)
A(X-3+N,Y+3)=A(X-3+N,Y+3)-L3*A(X-3+N,Y+3)

B(X,Y)=B(X,Y)+D(x-3+N,y-3)+D(x-3+N,y+3)

NEXT N



'2 steps away

FOR O = 1 TO 5

D(x-2,y-3+O)=L2*A(X-2,Y-3+O)
D(x+2,y-3+O)=L2*A(X+2,Y-3+O)

A(X-2,Y-3+O)=A(X-2,Y-3+O)-L2*A(X-2,Y-3+O)
```

```
A(X+2,Y-3+O)=A(X+2,Y-3+O)-L2*A(X+2,Y-3+O)

B(X,Y)=B(X,Y)+D(x-2,y-3+O)+D(x+2,y-3+O)

NEXT O

FOR P = 1 TO 3

D(x-2+P,y-2)=L2*A(X-2+P,Y-2)
D(x-2+P,y+2)=L2*A(X-2+P,Y+2)

A(X-2+P,Y-2)=A(X-2+P,Y-2)-L2*A(X-2+P,Y-2)
A(X-2+P,Y+2)=A(X-2+P,Y+2)-L2*A(X-2+P,Y+2)

B(X,Y)=B(X,Y)+D(x-2+P,y-2)+D(x-2+P,y+2)

NEXT P


'1 step away

FOR Q=1 TO 3

D(x-1,y-2+Q)=L1*A(X-1,Y-2+Q)
D(x+1,y-2+Q)=L1*A(X+1,Y-2+Q)

A(X-1,Y-2+Q)=A(X-1,Y-2+Q)-L1*A(X-1,Y-2+Q)
A(X+1,Y-2+Q)=A(X+1,Y-2+Q)-L1*A(X+1,Y-2+Q)

B(X,Y)=B(X,Y)+D(x-1,y-2+Q)+D(x+1,y-2+Q)

NEXT Q

D(x-1,y)=L1*A(X-1,Y)
```

```
D(x+1,y)=L1*A(X+1,Y)

A(X-1,Y)=A(X-1,Y)-L1*A(X-1,Y)
A(X+1,Y)=A(X+1,Y)-L1*A(X+1,Y)

B(X,Y)=B(X,Y)+D(x-1,y)+D(x+1,y)

'on laser spot

D(X,Y)=L0*A(X,Y)

A(X,Y)=A(X,Y)-L0*A(X,Y)

B(X,Y)=B(X,Y)+D(x,y)


GOSUB 130
return




600 'SIMULATE READING

IF TN1=1 THEN GOSUB 145 ELSE

IF SN1=0 THEN gosub 1000 else

FOR F = 4 to 104 step 2

FOR i = 4  TO 104
x=i
y=f
```

```
gosub 700  'calculate effect of readout
BACK=RND*200
IF BACK<100 THEN BACK=BACK+100
IF F(X,Y)<150 THEN F(X,Y)=BACK
PRINT, X,Y,F(X,Y)
OPEN N$ FOR APPEND  AS #1
PRINT #1 ,X,Y,F(X,Y)
close #1

NEXT i

y=y+1


FOR j = 104 TO 4 STEP -1


x=j
y=f+1

gosub 700  'calculate
BACK=RND*200
IF BACK<100 THEN BACK=BACK+100
IF F(X,Y)<150 THEN F(X,Y)=BACK
PRINT, X,Y,F(X,Y)
OPEN N$ FOR APPEND  AS #1
PRINT #1 ,X,Y,F(X,Y)
close #1

NEXT j

NEXT F
```

```
IF rmg2=1 THEN GOSUB 125 ELSE
gosub 1000



700 'CALCULATE EFFECT OF READOUT
IF sc=0 AND G(X,Y)=0 THEN RETURN


'6 STEPS AWAY

FOR D1=1 TO 13

H(x-6,y-7+D1)=L6*E(X-6,Y-7+D1)
H(x+6,y-7+D1)=L6*E(X+6,Y-7+D1)

E(X-6,Y-7+D1)=E(X-6,Y-7+D1)-L6*E(X-6,Y-7+D1)
E(X+6,Y-7+D1)=E(X+6,Y-7+D1)-L6*E(X+6,Y-7+D1)

F(X,Y)=F(X,Y)+H(x-6,y-7+D1)+H(x+6,y-7+D1)

NEXT D1

FOR R1=1 TO 11

H(x-6+R1,y-6)=L6*E(X-6+R1,Y-6)
H(x-6+R1,y+6)=L6*E(X-6+R1,Y+6)

E(X-6+R1,Y-6)=E(X-6+R1,Y-6)-L6*E(X-6+R1,Y-6)
E(X-6+R1,Y+6)=E(X-6+R1,Y+6)-L6*E(X-6+R1,Y+6)

F(X,Y)=F(X,Y)+H(x-6+R1,y-6)+H(x-6+R1,y+6)
```

```
NEXT R1



'5 STEPS AWAY

FOR F1=1 TO 11

H(x-5,y-6+F1)=L5*E(X-5,Y-6+F1)
H(x+5,y-6+F1)=L5*E(X+5,Y-6+F1)

E(X-5,Y-6+F1)=E(X-5,Y-6+F1)-L5*E(X-5,Y-6+F1)
E(X+5,Y-6+F1)=E(X+5,Y-6+F1)-L5*E(X+5,Y-6+F1)

F(X,Y)=F(X,Y)+H(x-5,y-6+F1)+H(x+5,y-6+F1)


NEXT F1

FOR G1=1 TO 9

H(x-5+G1,y-5)=L5*E(X-5+G1,Y-5)
H(x-5+G1,y+5)=L5*E(X-5+G1,Y+5)

E(X-5+G1,Y-5)=E(X-5+G1,Y-5)-L5*E(X-5+G1,Y-5)
E(X-5+G1,Y+5)=E(X-5+G1,Y+5)-L5*E(X-5+G1,Y+5)

F(X,Y)=F(X,Y)+H(x-5+G1,y-5)+H(x-5+G1,y+5)

NEXT G1



'4 STEPS AWAY
```

```
FOR H1=1 TO 9

H(x-4,y-5+H1)=L4*E(X-4,Y-5+H1)
H(x+4,y-5+H1)=L4*E(X+4,Y-5+H1)

E(X-4,Y-5+H1)=E(X-4,Y-5+H1)-L4*E(X-4,Y-5+H1)
E(X+4,Y-5+H1)=E(X+4,Y-5+H1)-L4*E(X+4,Y-5+H1)

F(X,Y)=F(X,Y)+H(x-4,y-5+H1)+H(x+4,y-5+H1)

NEXT H1

FOR I1=1 TO 7

H(x-4+I1,y-4)=L4*E(X-4+I1,Y-4)
H(x-4+I1,y+4)=L4*E(X-4+I1,Y+4)

E(X-4+I1,Y-4)=E(X-4+I1,Y-4)-L4*E(X-4+I1,Y-4)
E(X-4+I1,Y+4)=E(X-4+I1,Y+4)-L4*E(X-4+I1,Y+4)

F(X,Y)=F(X,Y)+H(x-4+I1,y-4)+H(x-4+I1,y+4)

NEXT I1



'3 steps away

FOR M=1 TO 7

H(x-3,y-4+M)=L3*E(X-3,Y-4+M)
H(x+3,y-4+M)=L3*E(X+3,Y-4+M)
```

```
E(X-3,Y-4+M)=E(X-3,Y-4+M)-L3*E(X-3,Y-4+M)
E(X+3,Y-4+M)=E(X+3,Y-4+M)-L3*E(X+3,Y-4+M)

F(X,Y)=F(X,Y)+H(x-3,y-4+M)+H(x+3,y-4+M)

NEXT M

FOR N = 1 TO 5

H(x-3+N,y-3)=L3*E(X-3+N,Y-3)
H(x-3+N,y+3)=L3*E(X-3+N,Y+3)

E(X-3+N,Y-3)=E(X-3+N,Y-3)-L3*E(X-3+N,Y-3)
E(X-3+N,Y+3)=E(X-3+N,Y+3)-L3*E(X-3+N,Y+3)

F(X,Y)=F(X,Y)+H(x-3+N,y-3)+H(x-3+N,y+3)

NEXT N



'2 steps away

FOR O = 1 TO 5

H(x-2,y-3+O)=L2*E(X-2,Y-3+O)
H(x+2,y-3+O)=L2*E(X+2,Y-3+O)

E(X-2,Y-3+O)=E(X-2,Y-3+O)-L2*E(X-2,Y-3+O)
E(X+2,Y-3+O)=E(X+2,Y-3+O)-L2*E(X+2,Y-3+O)

F(X,Y)=F(X,Y)+H(x-2,y-3+O)+H(x+2,y-3+O)

NEXT O
```

```
FOR P = 1 TO 3

H(x-2+P,y-2)=L2*E(X-2+P,Y-2)
H(x-2+P,y+2)=L2*E(X-2+P,Y+2)

E(X-2+P,Y-2)=E(X-2+P,Y-2)-L2*E(X-2+P,Y-2)
E(X-2+P,Y+2)=E(X-2+P,Y+2)-L2*E(X-2+P,Y+2)

F(X,Y)=F(X,Y)+H(x-2+P,y-2)+H(x-2+P,y+2)

NEXT P


'1 step away

FOR Q=1 TO 3

H(x-1,y-2+Q)=L1*E(X-1,Y-2+Q)
H(x+1,y-2+Q)=L1*E(X+1,Y-2+Q)

E(X-1,Y-2+Q)=E(X-1,Y-2+Q)-L1*E(X-1,Y-2+Q)
E(X+1,Y-2+Q)=E(X+1,Y-2+Q)-L1*E(X+1,Y-2+Q)

F(X,Y)=F(X,Y)+H(x-1,y-2+Q)+H(x+1,y-2+Q)

NEXT Q

H(x-1,y)=L1*E(X-1,Y)
H(x+1,y)=L1*E(X+1,Y)

E(X-1,Y)=E(X-1,Y)-L1*E(X-1,Y)
E(X+1,Y)=E(X+1,Y)-L1*E(X+1,Y)
```

```
F(X,Y)=F(X,Y)+H(x-1,y)+H(x+1,y)

'on laser spot

H(X,Y)=L0*E(X,Y)

E(X,Y)=E(X,Y)-L0*E(X,Y)

F(X,Y)=F(X,Y)+H(x,y)


GOSUB 135
return

1000
end
```